above are conservative in consideration of the following:

- Conservatisms associated with the deterministic PMH inputs, as previously discussed;
- Conservatism added through SLOSH assessment to establish appropriate reference and sensitivity storm sets for use with JPM-OS; and
- Conservatism added through consideration of applicable uncertainty, error and SLR.

2.4.3 Conclusions

Deterministic Probable Maximum Storm Surge

The ADCIRC simulation representing this combination of parameters (i.e., STORMID 1097) resulted in maximum stillwater elevations of 21.3 and 20.9 ft NAVD88 (i.e., reflecting linear adjustment to the AWL) at the SPS intake and discharge locations, respectively. These elevations translate to 22.74 and 22.34 ft MSL; the former value is nearly identical to the existing design basis stillwater elevation of 22.7 ft MSL at the SPS intake location (Dominion, 2014).

Probabilistic Storm Surge

At an AEP level of approximately 1E-6, stillwater elevation at the SPS intake and discharge locations are calculated to be 17.5 ft NAVD88 and 17.0 ft NAVD88, respectively. These elevations translate to 18.9 ft MSL and 18.4 ft MSL, respectively.

2.4.4 References

2.4.4-1 **ANS 1992**. "ANS/ANS-2.8-1992 – Determining Design Basis Flooding at Power Reactor Sites", American National Standards Institute/American Nuclear Society, 1992

2.4.4-2 **Blake et al. 2011**. "The Deadliest, Costliest, and Most Intense United States Tropical Cyclones from 1851 to 2010 (and Other Frequently Requested Hurricane Facts)", Blake, E.S., Landsea, C.W. and Gibney, E.J., National Hurricane Center, National Oceanic and Atmospheric Administration Technical Report NWS NHC-6, August 2011.

2.4.4-3 **Dominion 2014**. Surry Power Station Updated Final Safety Analysis Report (SPS UFSAR), Revision 46.02.

2.4.4-4 **Emanuel et al. 2004**. "Environmental Control of Tropical Cyclone Intensity", Emanuel, K., Des Autels, C., Holloway, C. and Korty, R., Journal of the Atmospheric Sciences, Vol. 61, 843-858, April 2004.

2.4.4-5 **Emanuel et al. 2006**. "A statistical-deterministic approach to hurricane risk assessment", Bull. Amer. Meteor. Soc., 19, 299-314, K. Emanuel, A., S. Ravela, E. Vivant, and C. Risi, 2006.

2.4.4-6 **ESSA 1970**. "Joint probability of tide frequency analysis applied to Atlantic City and Long Beach Island, NJ", U.S.Department of Commerce, Environmental Science Service Administration, Weather Bureau, Myers, V.A., April 1970.

2.4.4-7 **FEMA 2012**. "Operating Guidance No. 8-12, Joint Probability – Optimal Sampling Method for Tropical Storm Surge Frequency Analysis", U.S. Department of Homeland Security, Federal Emergency Management Agency, March, 2012.

2.4.4-8 NOAA 1979. "Meteorological Criteria for Standard Project Hurricane and Probable Maximum Hurricane Wind Fields, Gulf and East Coast of the United States", National Oceanic and Atmospheric Administration Technical Report NWS 23, September 1979.

2.4.4-9 NOAA 2013. "Revised Atlantic Hurricane Database (HURDAT 2)", National Oceanic and Atmospheric Administration, National Hurricane Center, http://www.aoml.noaa.gov/hrd/hurdat/2011.html, Date accessed December and January, 2013, Date updated June 10, 2013.

2.4.4-10 NOAA 2012a. "SLOSH Display Program (1.65b)", National Oceanic and Atmospheric Administration, Evaluation Branch, Meteorological Development Lab, National Weather Service, January 2012.

2.4.4-11 NOAA 2012b. "SLOSH Model v3.97" National Oceanic and Atmospheric Administration, Evaluation Branch, Meteorological Development Lab, National Weather Service, January 2012.

2.4.4-12 NRC 2011. "NUREG / CR–7046: Design Basis Flood Estimation for Site Characterization at Nuclear Power Plants", U.S. Nuclear Regulatory Commission, November 2011.

2.4.4-13 NRC 2012. "NUREG/CR-7134 - The Estimation of Very-Low Probability Hurricane Storm Surges for Design and Licensing of Nuclear Power Plants in Coastal Areas", U.S. Nuclear Regulatory Commission, October 2012.

2.4.4-14 NRC 2013. "JLD-ISG-2012-06: Guidance for Performing a Tsunami, Surge, or Seiche Hazard Assessment", U.S. Nuclear Regulatory Commission, Revision 0, January 2013.

2.4.4-15 USACE 1994. "ADCIRC: an advanced three-dimensional circulation model for shelves coasts and estuaries, report 2: user's manual for ADCIRC-2DDI", Westerink, J.J., C.A. Blain, R.A. Luettich, Jr. and N.W. Scheffner, 1994, Dredging Research Program Technical Report DRP-92-6, U.S. Army Engineers Waterways Experiment Station, Vicksburg, MS., 156p.

2.4.4-16 WRT 2013. Synthetic Hurricane Event Set, WindRiskTech, LLC, Chesapeake_ncep_renanalcal.csv, Chesapeake _ncep_reanalcal2.csv and Chesapeake _ncep_reanalcal_freq.csv, September, 2013.

Table 2.4-1: Top 10 Extreme Water Levels.

(a) Sewells Point (Station 8638610)

Rank	Year	Date	Highest WL (feet, NAVD88)	Event Type	Event Name
1	1933	8/23/1933	6.41	H1	1933 Chesapeake-Potomac Hurricane
2	2003	9/18/2003	6.28	H1/TS	Isabel 2003
3	2009	11/12/2009	6.12	TS	"Nor'Ida" 2009
4	2011	8/28/2011	5.95	H1	Irene 2011
5	1962	3/7/1962	5.61	ET	Ash Wednesday Storm of 1962
6	2012	10/29/2012	5.19	H1/ET	Sandy 2012
7	1936	9/18/1936	5.11	H2	Not Named
8	2006	11/22/2006	5.02	ET	Late November 2006 Nor'Easter
9	1998	2/5/1998	4.97	ET	Not Named
10	2006	10/7/2006	4.91	N/A	Not Named

(b) Chesapeake Bay Bride Tunnel (Station 8638863)

Rank	Year	Date	Highest WL (feet, MSL)	Event Type	Event Name
1	2009	11/12/2009	6.15	TS	"Nor'Ida" 2009
2	2003	9/18/2003	6.13	H1/TS	Isabel 2003
3	2011	8/28/2011	5.95	H1	Irene 2011
4	2012	10/29/2012	5.62	H1/ET	Sandy 2012
5	2006	11/22/2006	5.24	ET	Late November 2006 Nor'Easter
6	1998	2/5/1998	5.17	ET	Not Named
7	2006	10/7/2006	4.93	N/A	Not Named
8	2009	12/19/2009	4.78	N/A	Not Named
9	1998	1/28/1998	4.72	N/A	Not Named
10	1978	4/27/1978	4.55	N/A	Not Named

(c) Kiptopeke (Station 8632200)

Rank	Year	Date	Highest WL (feet, NAVD88)	Event Type	Event Name
1	1962	3/7/1962	5.16	ET	Not Named
2	2009	11/13/2009	5.01	H1	"Nor'Ida" 2009
3	2012	10/29/2012	4.88	H1/TS	Sandy 2012
4	2003	9/18/2003	4.61	TS	Isabel 2003
5	2011	8/28/2011	4.57	H1	Irene 2011
6	2009	12/19/2009	4.07	N/A	Not Named
7	1998	2/5/1998	4.05	ET	Not Named
8	2011	10/29/2011	3.94	N/A	Not Named
9	2006	10/7/2006	3.89	N/A	Not Named
10	1977	10/14/1977	3.86	N/A	Not Named

Notes: **1. H1, H2 indicate Category 1 and Category 2 Hurricane, respectively.**
2. TS indicates Tropical Storm; ET indicates Extra-tropical Storm.

Table 2.4-2: NOAA SLOSH MOM Water Levels at Selected Gage Locations.

NOAA CO-OP Station (No.)	SLOSH Grid Cell (hor3)	CAT 1	CAT 2	CAT 3	CAT 4
		(feet, NAVD88)			
Sewells Point (8638610)	142 - 194	4.6	8.2	11.6	14.8
CBBT (8638863)	167 - 198	4.6	7.9	11.1	14.5
Kiptopeke (8632200)	180 - 222	4.1	7.2	10.4	13.9

Note: 1. CAT reflects Saffir-Simpson storm intensity category.

Table 2.4-3: Numbers of WRT storms and storm segments within the OIR, including classifications by Saffir-Simpson category.

OIR Region	storms	storm segments
All Qualifying	6874	24185
>= Cat 3 (96 kt)	247	534
>= Cat 4 (113 kts)	48	85
>= Cat 5 (137 kts)	5	8

Table 2.4-4: Recommended PMH-level parameters and parameter ranges

Storm Bearing	Maximum Wind Speed, vm	Forward Speed, fspd	Radius of Maximum Winds, rmw
-120°	100.3 kt	4.4 – 29.0 kt	8.3 – 41.7 nm
-110°	102.0 kt	4.9 – 30.7 kt	8.4 – 41.2 nm
-100°	104.4 kt	5.6 – 32.4 kt	8.6 – 40.5 nm
-90°	107.3 kt	6.6 – 34.1 kt	8.8 – 39.7 nm
-80°	110.9 kt	7.7 – 35.8 kt	9.1 – 38.6 nm
-70°	115.1 kt	9.0 – 37.5 kt	9.4 – 37.4 nm
-60°	119.9 kt	10.5 – 39.2 kt	9.8 – 35.9 nm
-50°	125.3 kt	12.2 – 40.9 kt	10.2 – 34.3 nm
-40°	131.3 kt	14.1 – 42.6 kt	10.6 – 32.5 nm
-30°	138.0 kt	16.2 – 41.1 kt	11.1 – 30.6 nm
-20°	145.3 kt	18.5 – 39.2 kt	11.6 – 28.4 nm

Table 2.4-5: Refinement Storm Set parameters. Vm is maximum sustained wind speed; CPD is central pressure deficit; Rmax is radius of maximum wind.

STORMID	Vm (kt)	CPD (mb)	Bearing (deg. from N)	Forward Speed (kt)	Rmax (nm)	Landfall Mile Post (via NWS 23)	Landfall Latitude (Dec. Degrees)	Landfall Longitude (Dec. Degrees)
948	115	90	-70	15	35	2250	36.30	-75.80
1093	120	91	-60	15	30	2250	36.30	-75.80
1097	120	98	-60	15	35	2225	35.91	-75.60
1098	120	98	-60	15	35	2250	36.30	-75.80
1127	120	94	-60	20	35	2225	35.91	-75.60
1128	120	94	-60	20	35	2250	36.30	-75.80
1237	125	99	-50	15	30	2225	35.91	-75.60
1257	125	95	-50	20	30	2225	35.91	-75.60
1351	131	101	-40	15	25	2200	35.48	-75.47
1356	131	109	-40	15	30	2200	35.48	-75.47
1357	131	109	-40	15	30	2225	35.91	-75.60
1376	131	104	-40	20	30	2200	35.48	-75.47
1377	131	104	-40	20	30	2225	35.91	-75.60
1396	131	101	-40	25	30	2200	35.48	-75.47
1476	138	116	-30	20	30	2200	35.48	-75.47

Table 2.4-6: Maximum simulated stillwater surge elevations associated with the OS Storm Set – reference set at the SPS intake and discharge locations (SLOSH and ADCIRC results shown).

STORMID	SLOSH - SPS discharge (ft NAVD88)	SLOSH - SPS intake (ft NAVD88)	ADCIRC - SPS discharge (ft NAVD88)	ADCIRC - SPS intake (ft NAVD88)
5131	6.0	6.3	5.4	5.8
5132	9.5	9.7	7.8	8.6
5133	14.0	14.1	10.3	11.4
5134	14.0	14.1	9.1	10.3
6346	7.4	7.6	6.1	6.7
6347	11.4	11.5	8.6	9.6
6348	15.5	15.5	10.2	11.3
6349	12.8	12.8	8.4	9.0
7701	9.7	9.8	7.2	8.1
7702	14.1	14.0	9.1	10.1
7703	15.6	15.1	9.8	10.1
7704	10.8	11.1	7.2	7.5
9161	13.6	13.2	8.3	9.1
9162	14.6	14.1	9.3	9.2
9163	12.7	12.7	8.0	8.0
9164	8.8	9.3	6.2	5.7
10706	12.2	12.2	6.8	6.4
10707	10.4	10.7	6.7	6.1
10708	9.4	9.9	6.7	5.9
10709	7.1	7.9	4.8	4.2

Table 2.4-7: Maximum simulated stillwater surge elevations associated with the OS Storm Set – sensitivity set at the SPS intake and discharge locations (SLOSH and ADCIRC results shown). Note that STORMID = 6348 is used to evaluate parameter sensitivities (i.e., results associated with STORMID = 6348 are highlighted)

STORMID	SLOSH - SPS discharge (ft NAVD88)	SLOSH - SPS intake (ft NAVD88)	ADCIRC - SPS discharge (ft NAVD88)	ADCIRC - SPS intake (ft NAVD88)
6173	5.3	5.8	4.2	4.7
6213	7.0	7.5	5.4	6.1
6253	8.7	9.0	6.5	7.3
6288	10.7	11.0	7.7	8.7
6318	12.8	13.0	8.9	10.0
6373	18.6	18.1	11.5	12.8
6388	22.1	21.5	12.9	14.2
6343	16.0	15.7	11.6	12.8
6353	14.9	14.7	9.1	10.2
6358	13.6	13.4	8.1	9.1
6363	12.2	12.3	7.5	8.3
6143	12.4	12.6	7.6	8.8
6578	17.7	17.2	12.4	13.3
6803	19.0	18.7	14.2	15.0
7008	19.7	19.6	15.7	16.3
7178	20.0	19.9	16.8	17.2
6348	15.5	15.5	10.2	11.3

Figure 2.4-1: Site locus and NOAA tide gage locations.

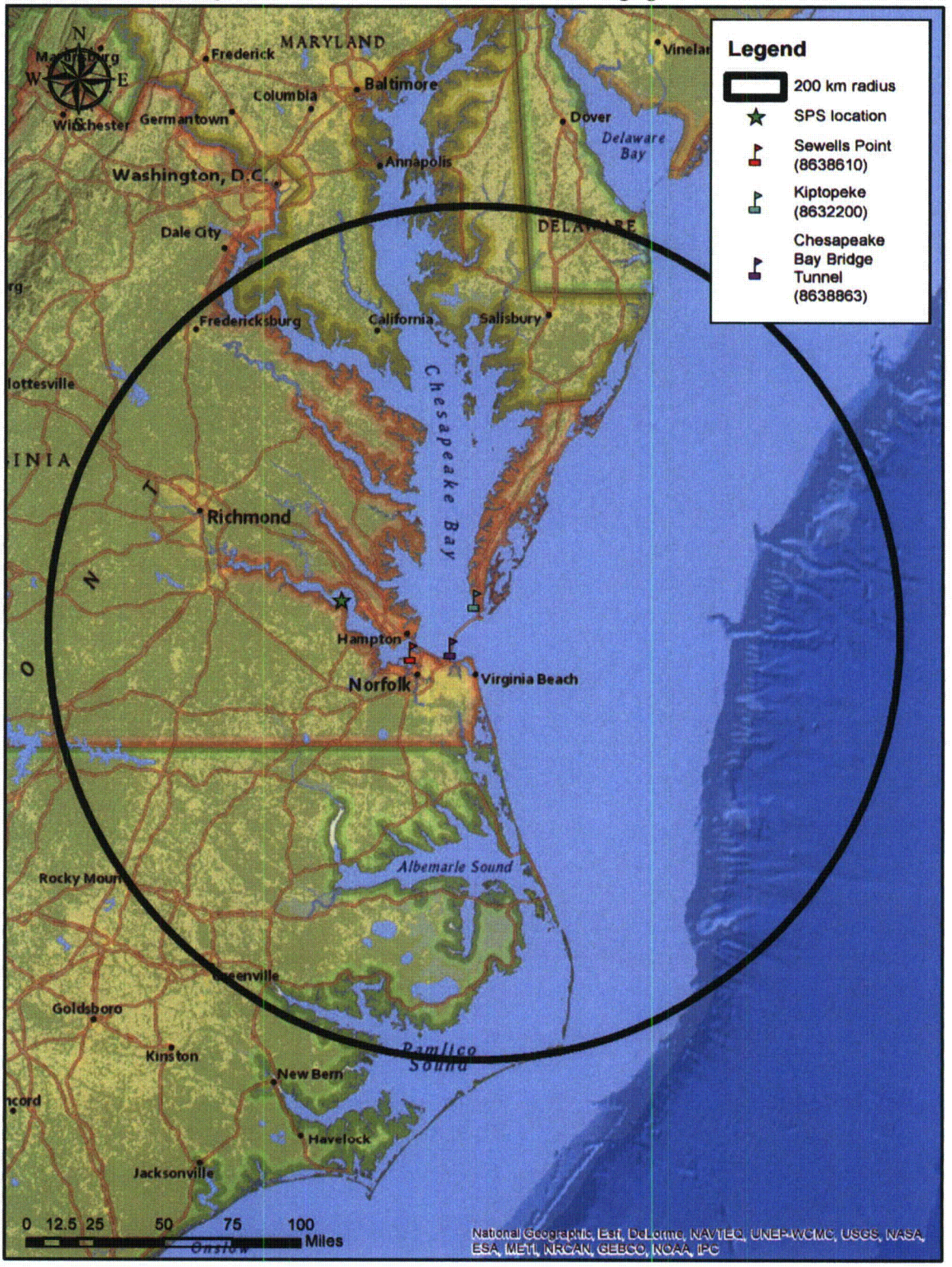

Figure 2.4-2: Illustration of several key PMH parameters.

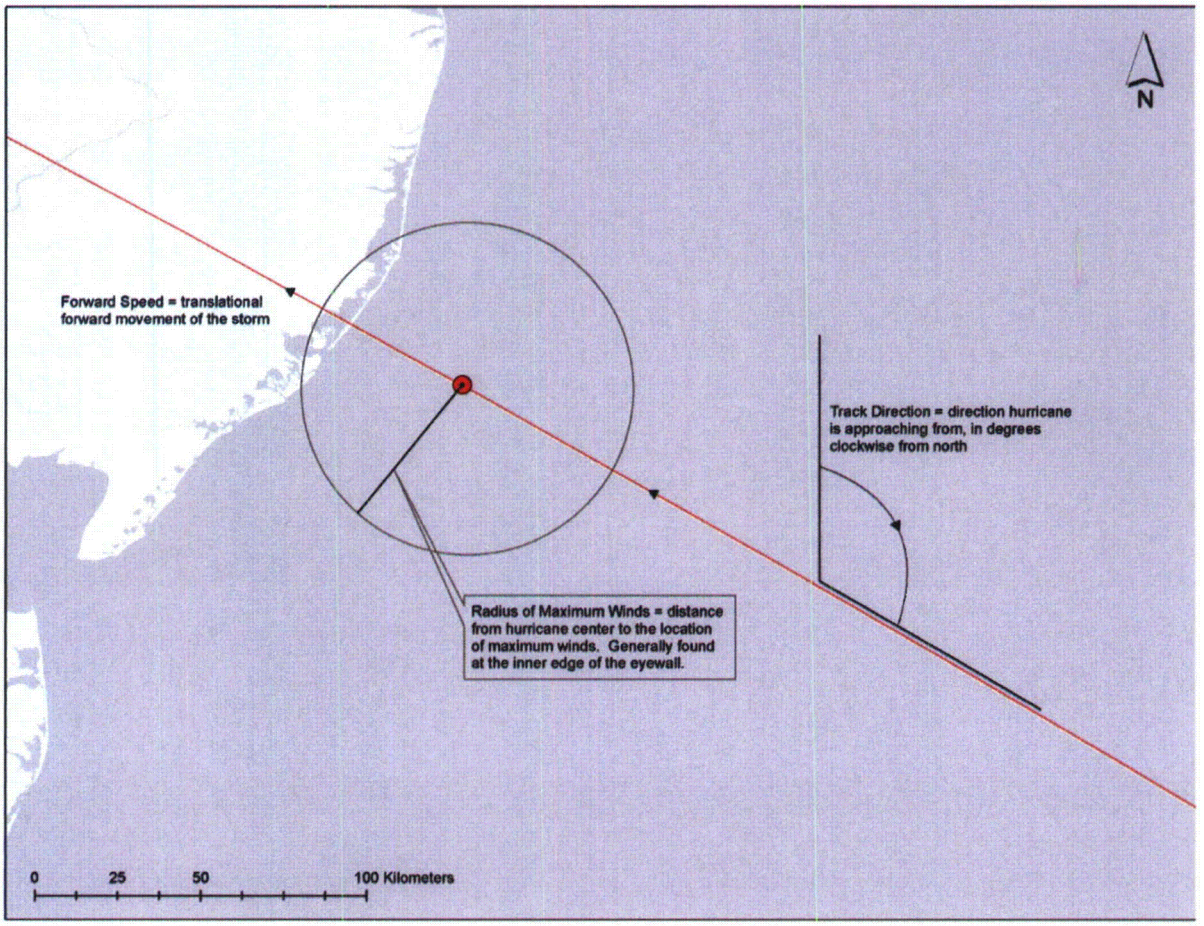

Figure 2.4-3: Historical hurricane tracks intersecting the study area (200 km radius from Chesapeake Bay).

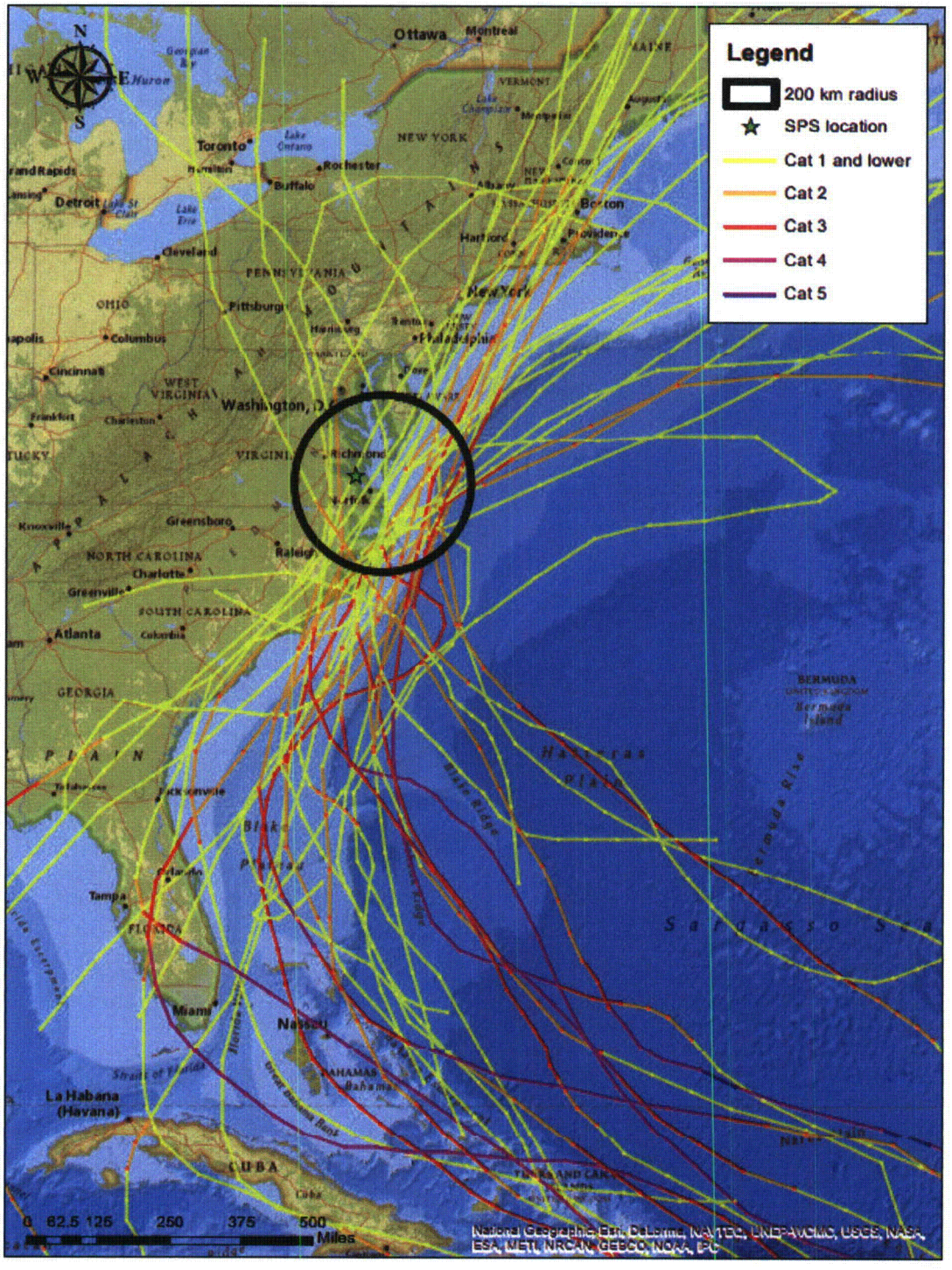

Figure 2.4-4: Selected historical hurricane tracks impacting the SPS vicinity.

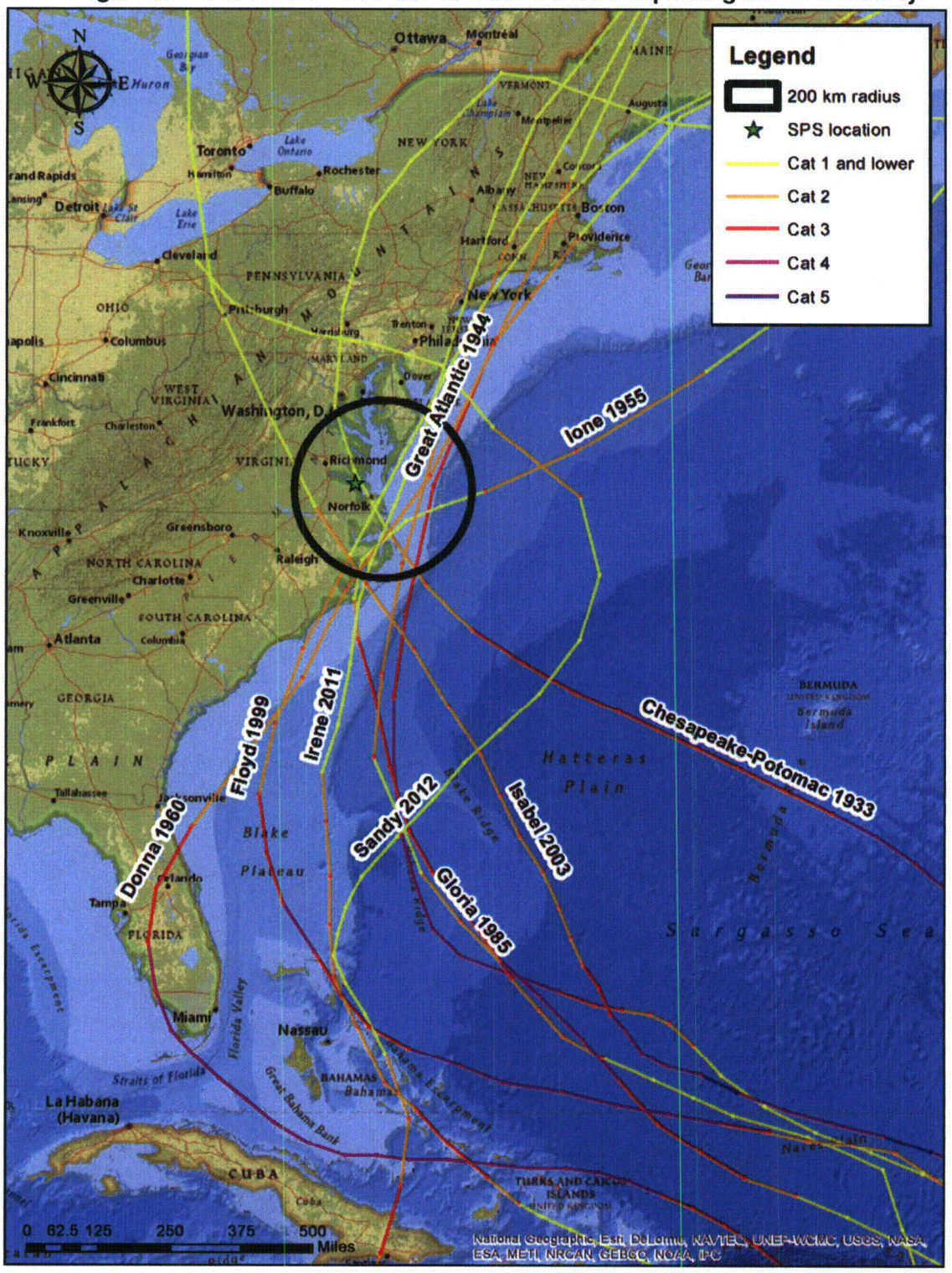

Figure 2.4-5: SPS mile post location (NWS 23, Figure 1.1). Adapted from NOAA 1979 (NOAA 1979).

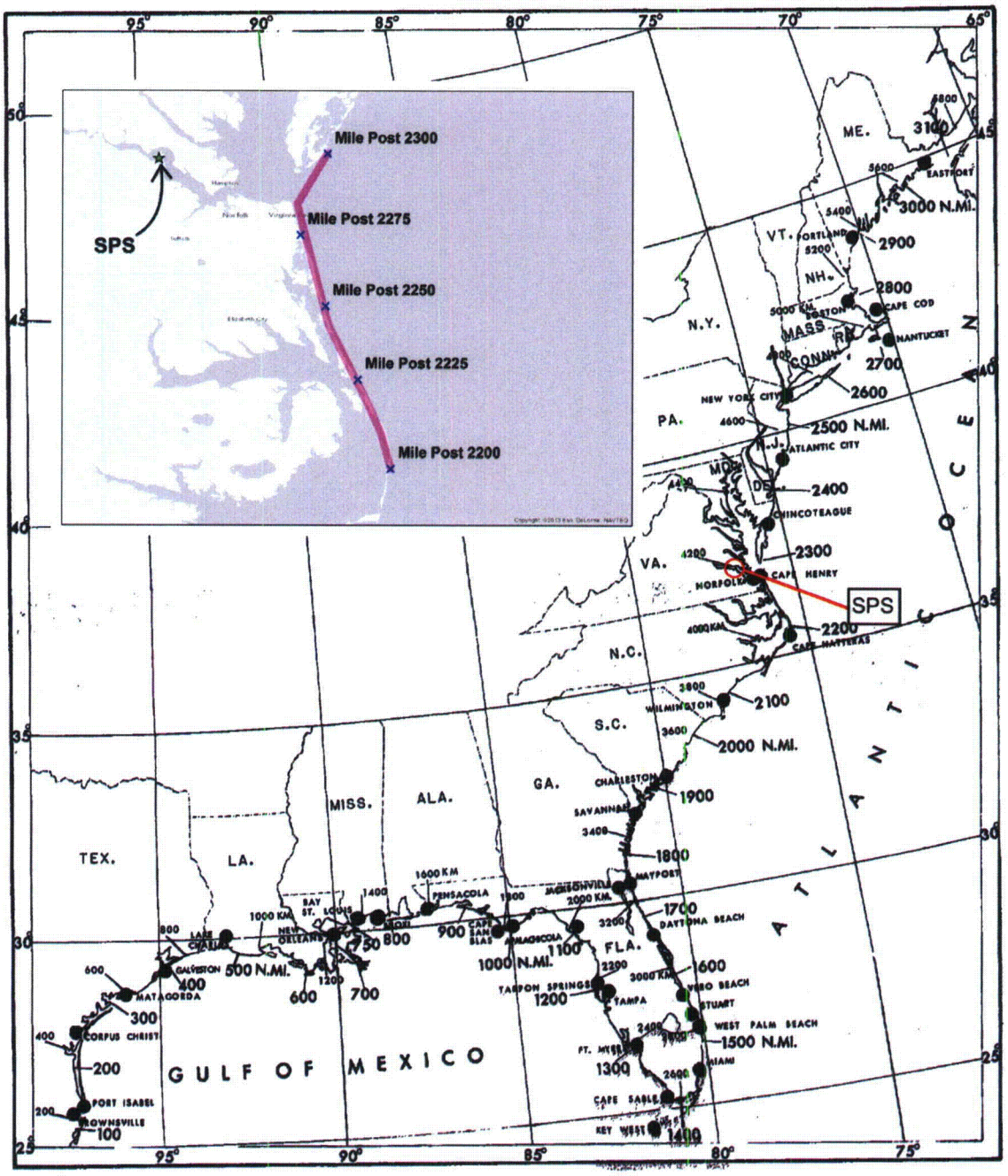

Figure 1.1.--Locator map with coastal distance intervals marked in nautical miles and kilometers.

Figure 2.4-11: A Probability Density Histogram (PDH) and non-parametric Probability Density Function (PDF) for maximum sustained winds (mxw) within the IR. The inset shows the Gaussian kernel function.

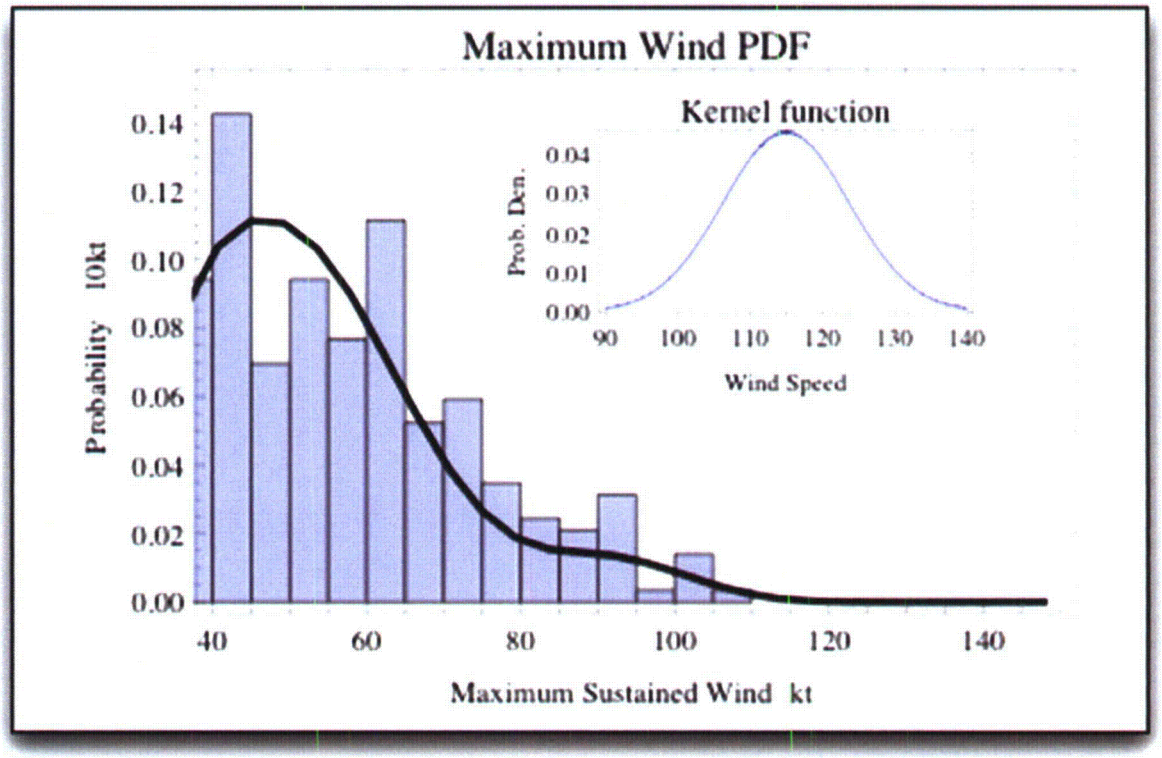

Figure 2.4-12: Hurricane parameter (i.e, mxw, fspd, fdir and dmxw) cross-correlations for the three analytical regions (IR, OR and RR) based on HURDAT2 dataset. Shading indicates statistical significance at the 95% level.

Cross-Correlation (Top=IR; Mid=OR; Bottom=RR)

	mxw	fspd	fdir	dmxw
mxw	1. 1. 1.	0.1 0.09 0.06	−0.22 −0.15 −0.14	−0.19 −0.08 −0.05
fspd	0.1 0.09 0.06	1. 1. 1.	0.12 0.14 0.2	0.15 0.07 −0.02
fdir	−0.22 −0.15 −0.14	0.12 0.14 0.2	1. 1. 1.	0.32 0.11 0.02
dmxw	−0.19 −0.08 −0.05	0.15 0.07 −0.02	0.32 0.11 0.02	1. 1. 1.

Figure 2.4-13: Scatter plots of fdir versus fspd data within the three analytical regions for the 162-year HURDAT2 record.

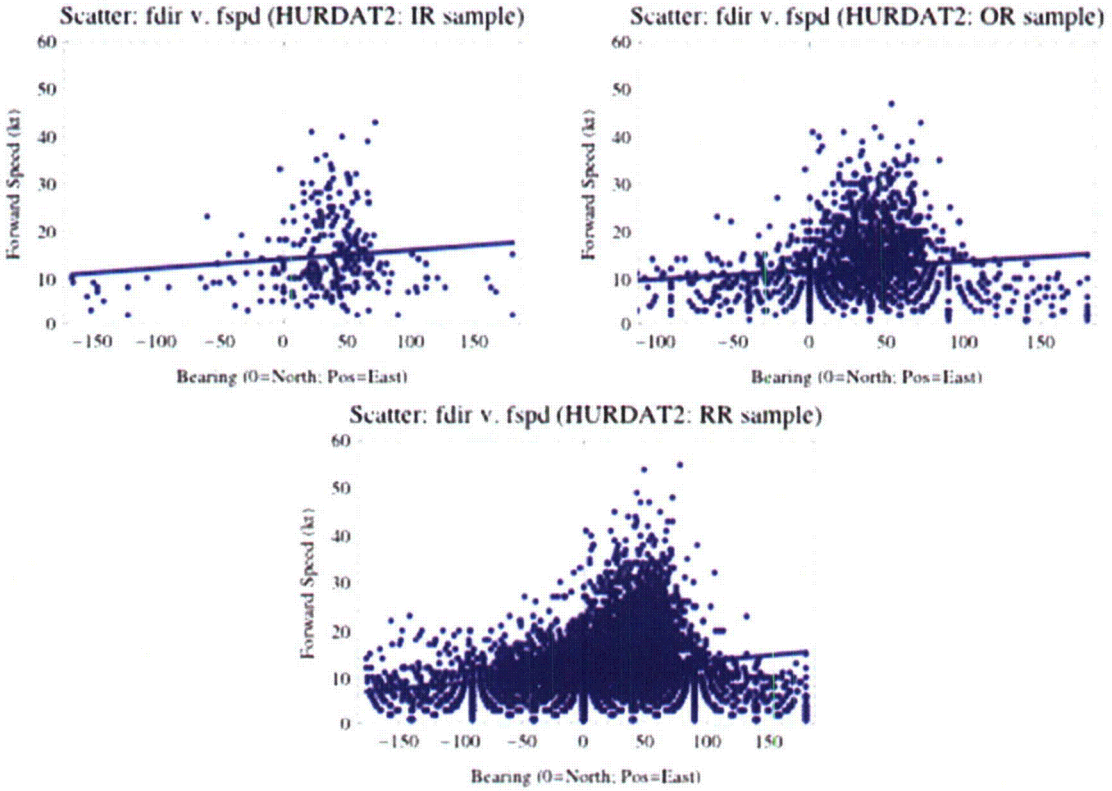

Figure 2.4-14: Scatter plots of fdir versus mxw data within the three analytical regions for the 162-year HURDAT2 record.

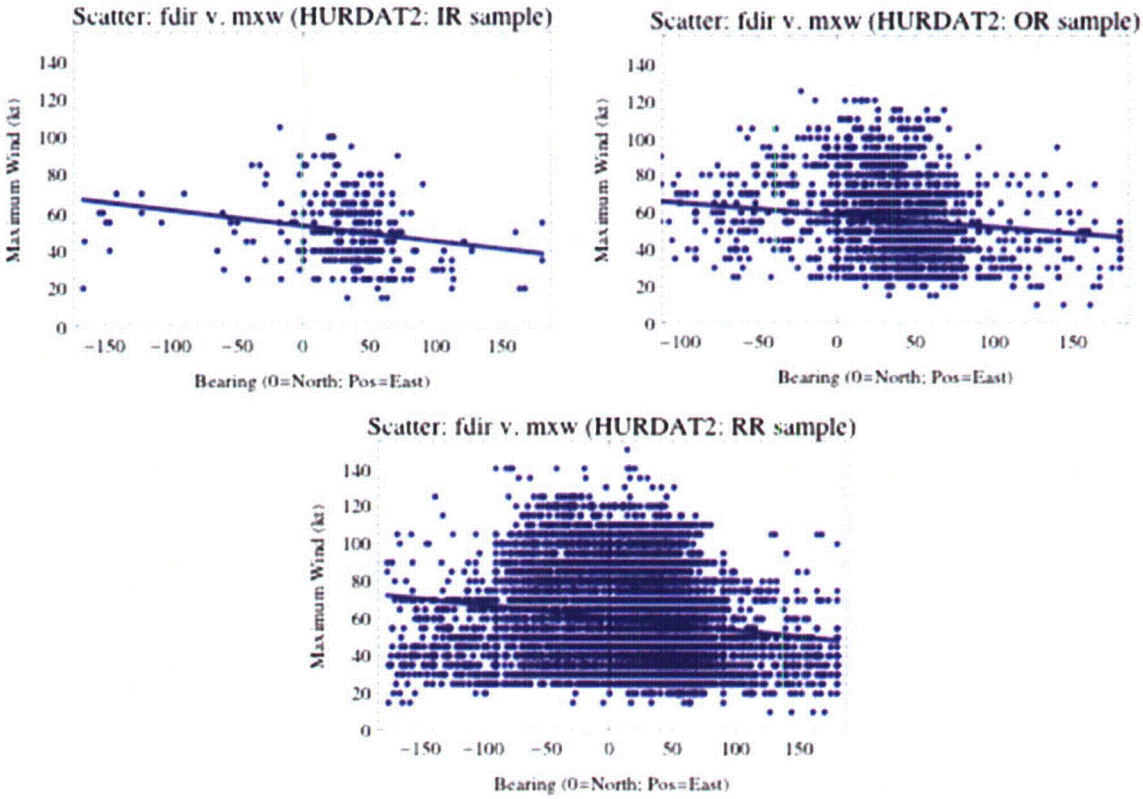

Figure 2.4-15: Scatter plots of mxw versus fspd data within the three analytical regions for the 162-year HURDAT2 record.

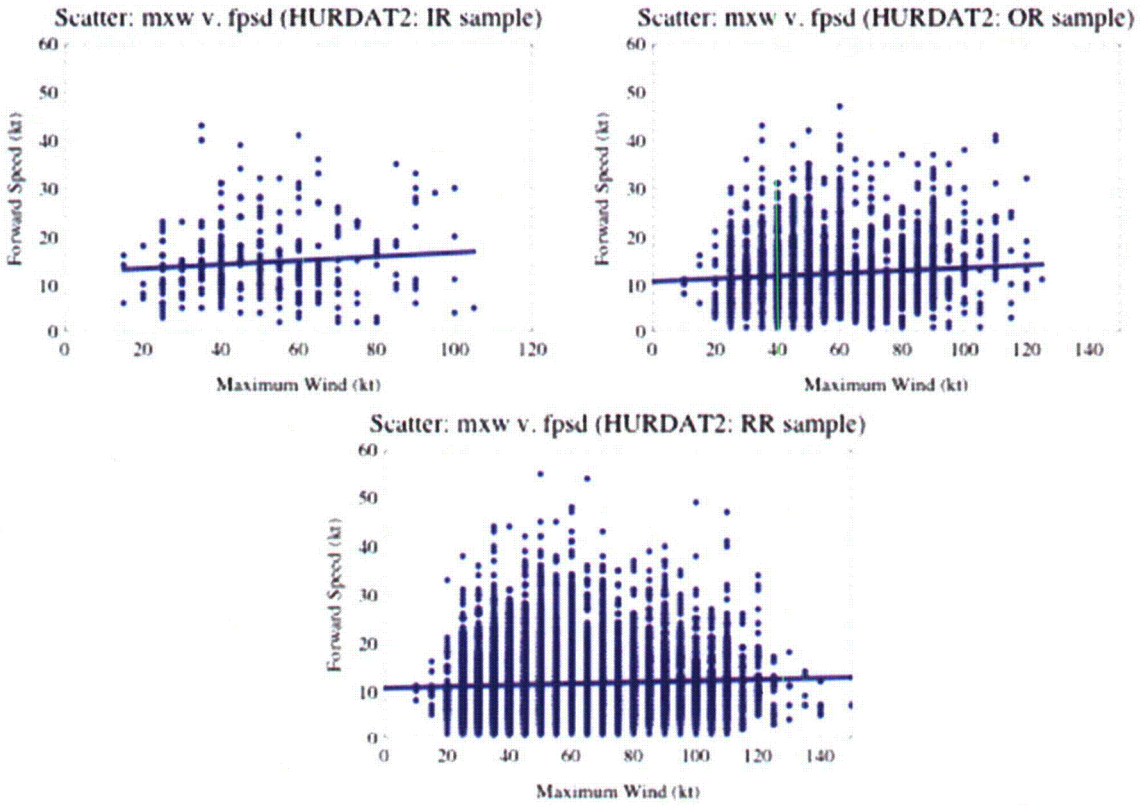

Figure 2.4-16: Scatter plots of fdir versus dmxw data within the three analytical regions for the 162-year HURDAT2 record.

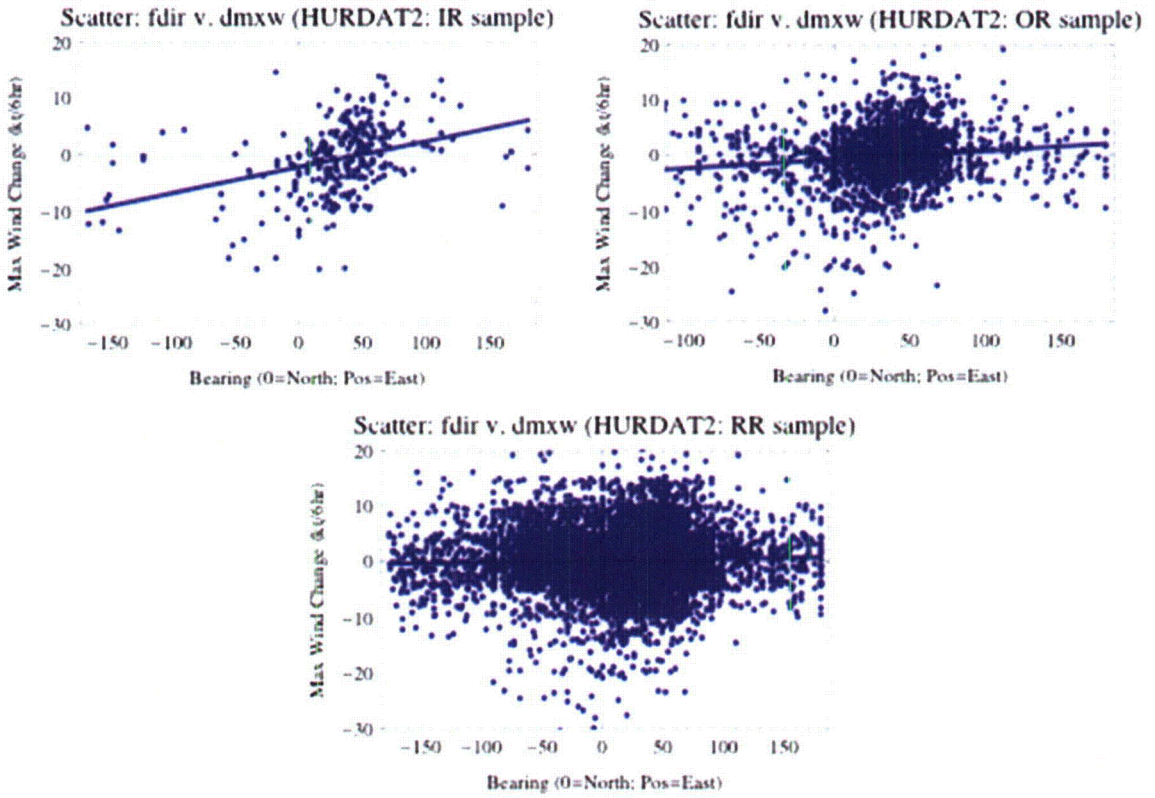

Figure 2.4-17: Scatter plots of mxw versus dmxw data within the three analytical regions for the 162-year HURDAT2 record.

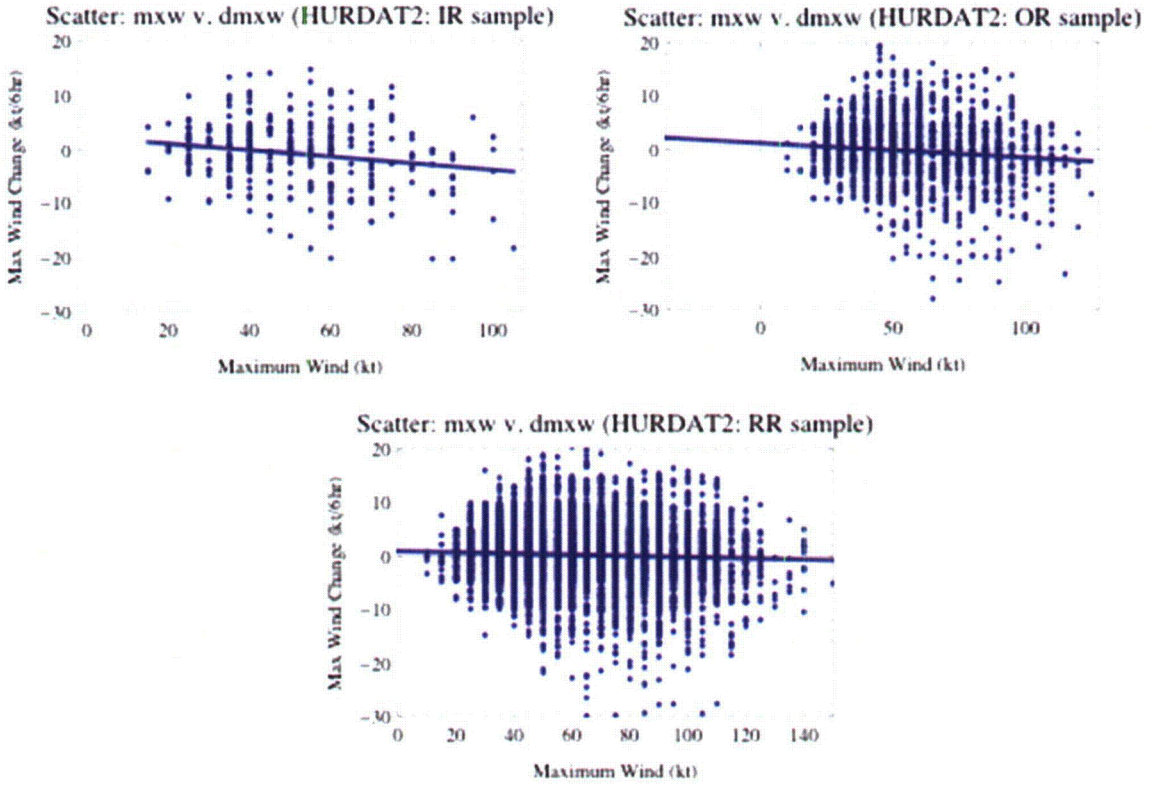

Figure 2.4-18: Scatter plots of fspd versus dmxw data within the three analytical regions for the 162-year HURDAT2 record.

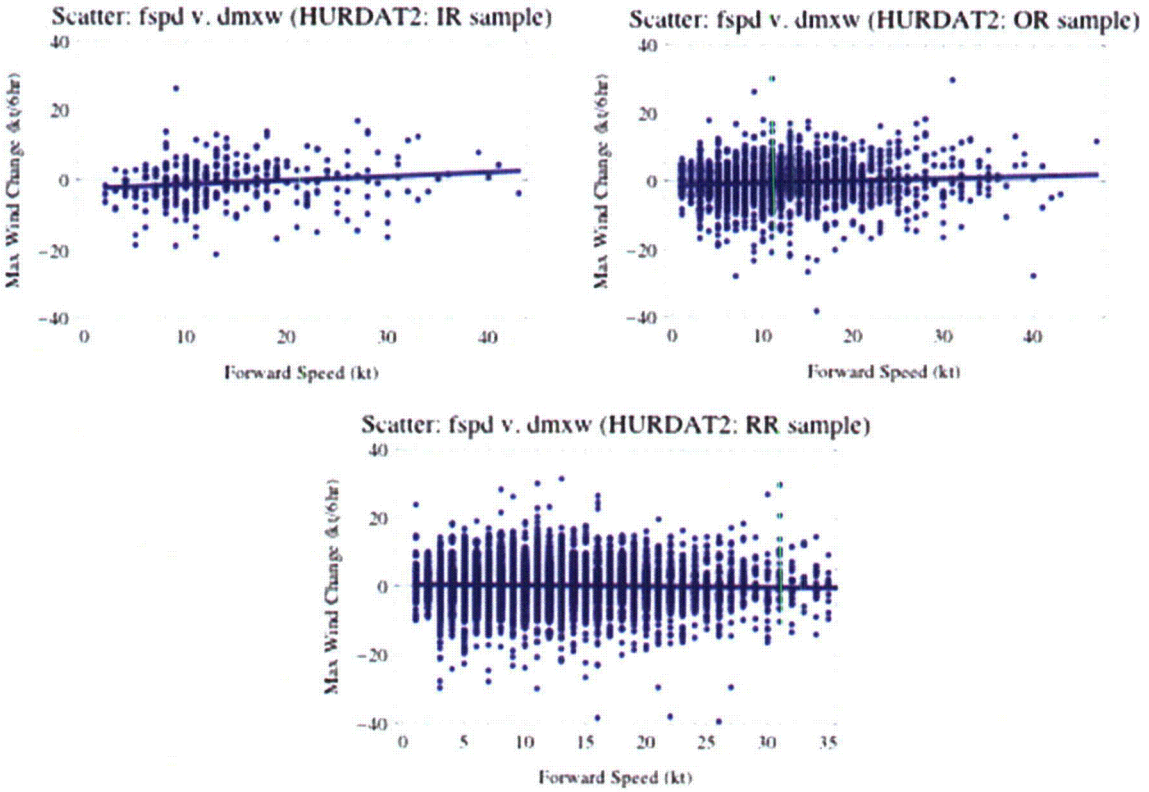

Figure 2.4-19: Comparisons between HURDAT2 distributions of storm bearing (fdir), shown by multiple lines, and the WRT population estimate, shown by gray line surrounded by central 98% uncertainty bounds. See text for explanation of the calculation procedure.

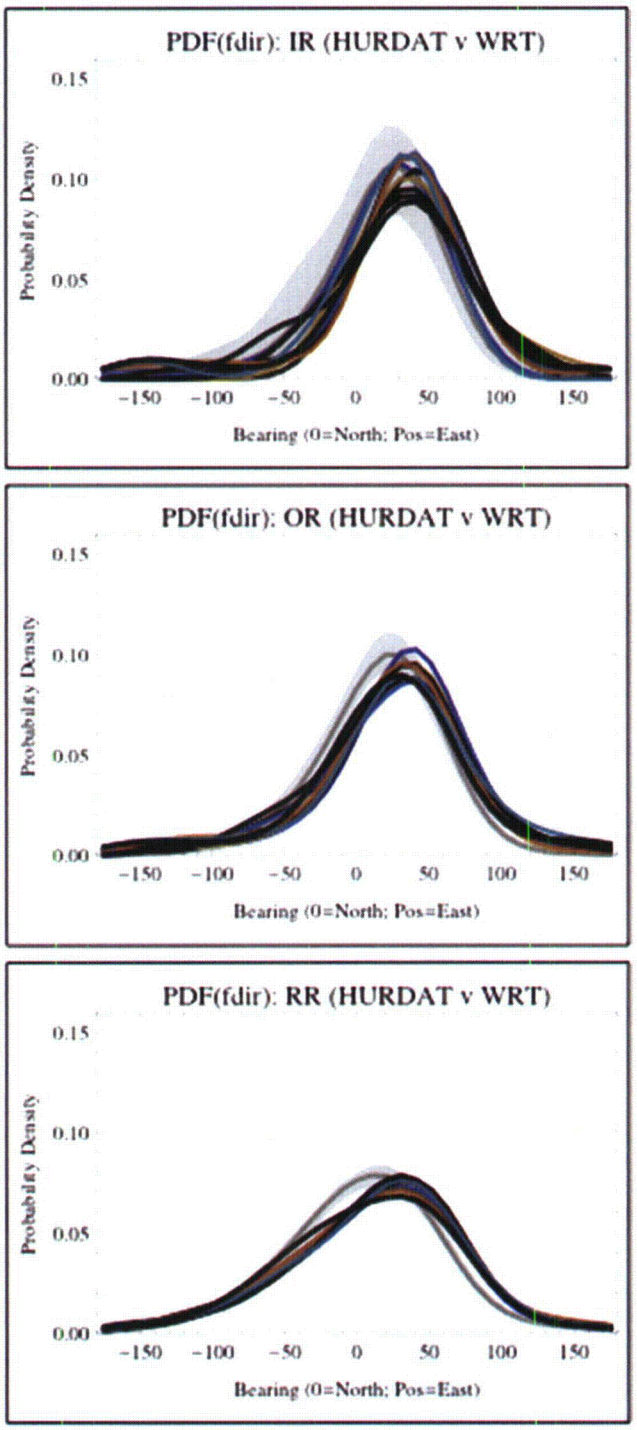

Figure 2.4-20: As in Figure 2.4-19 except pertaining to the storms' translation speed (fspd).

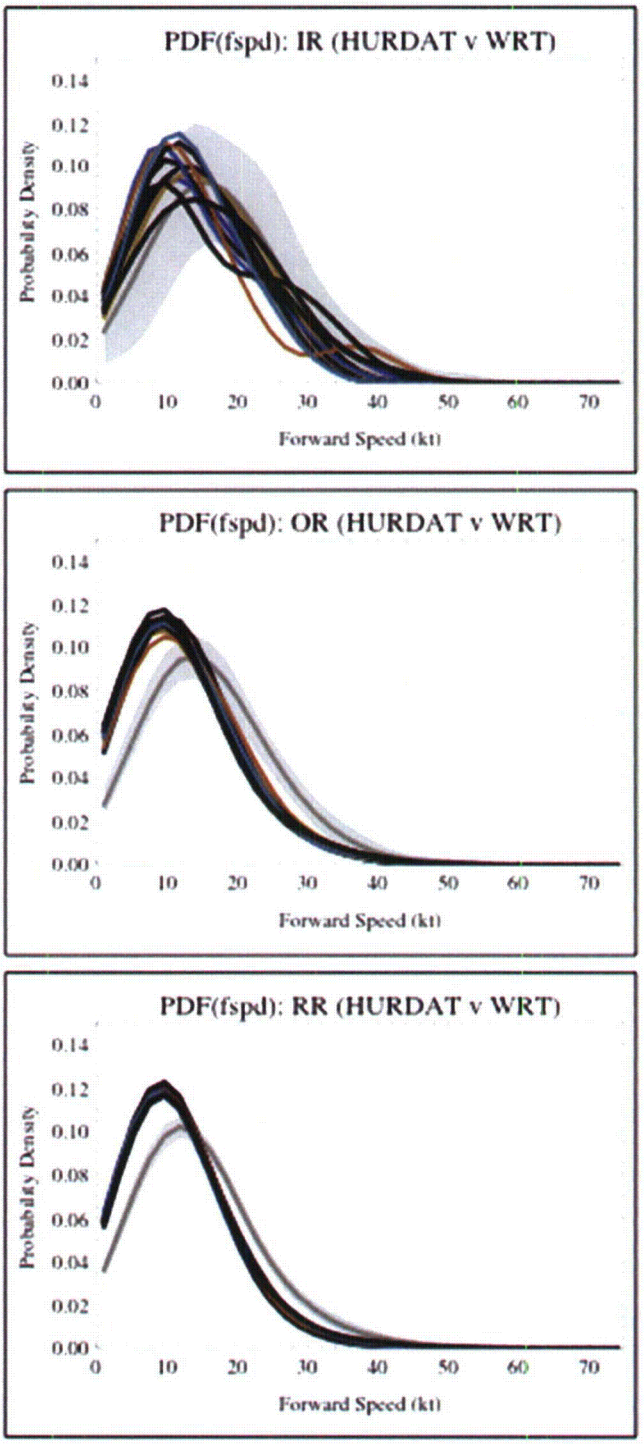

Figure 2.4-21: As in Figure 2.4-19 except pertaining to the storms' change in intensity, as indicated by the 6-hourly change in 1-min maximum sustained winds (dmxw).

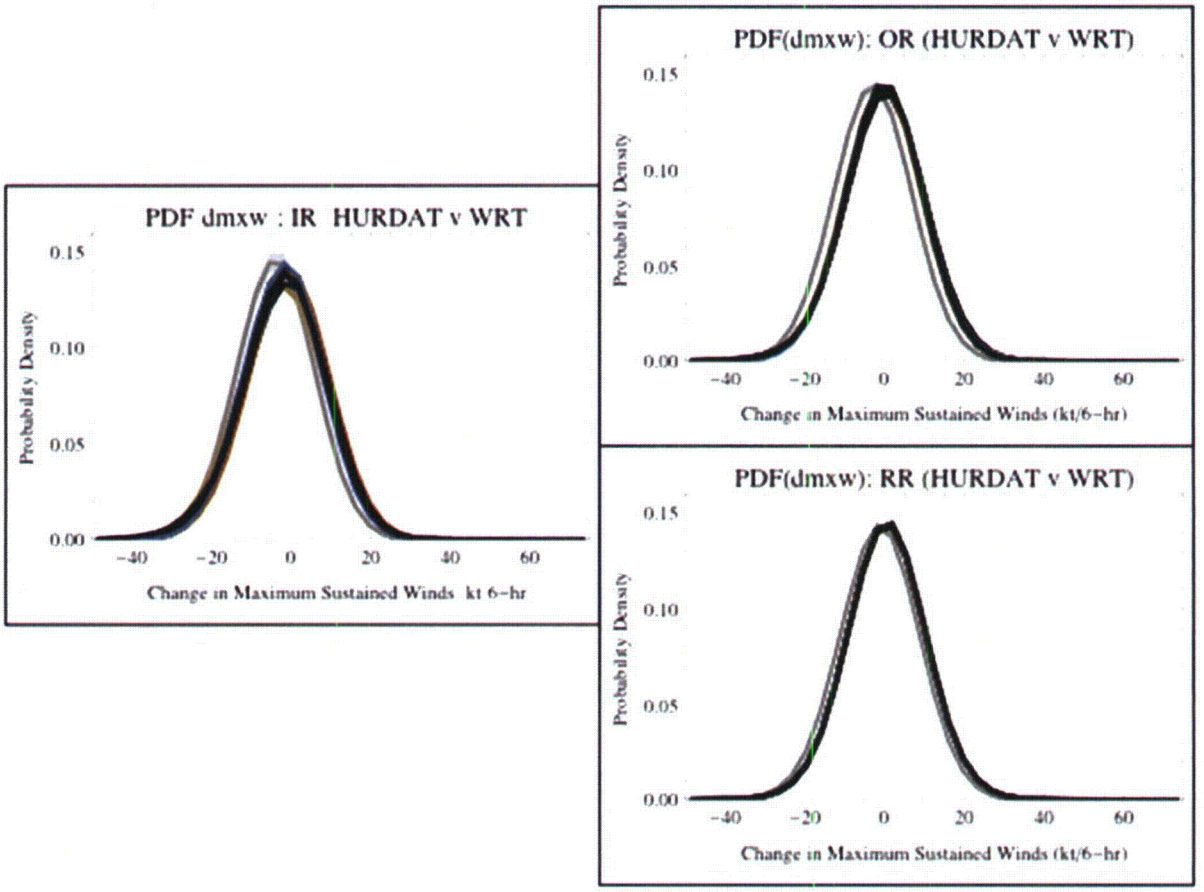

Figure 2.4-22: As in Figure 2.4-19 except pertaining to the 1-minute maximum sustained winds. (as indicated by vm in the WRT data set). The right panels show magnifications of Category 1 at higher hurricanes (upper) and Category 3 and higher hurricanes (lower).

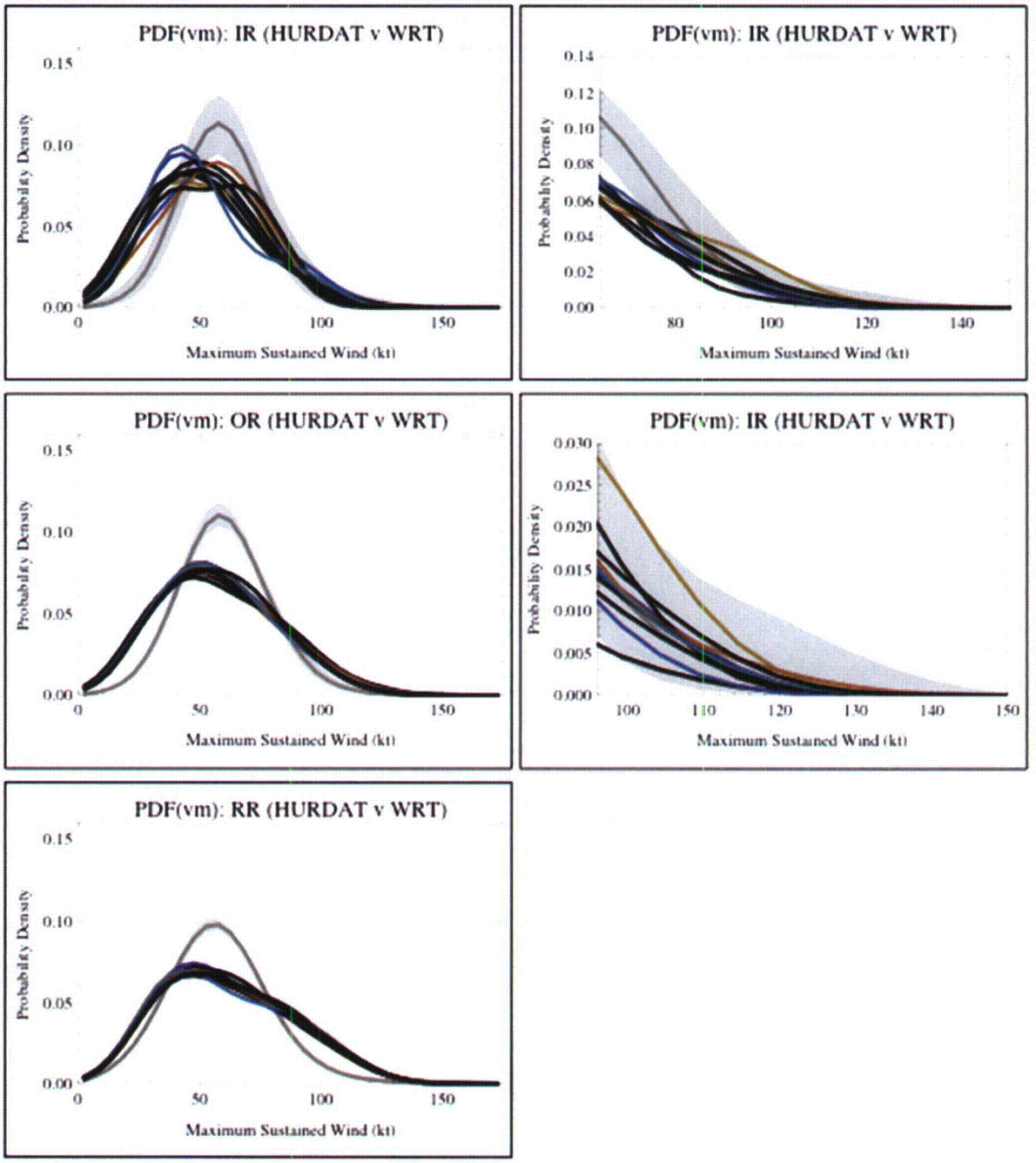

Figure 2.4-23: SPS Circular Region (IR), Offshore Portion (OIR) and Storm Segment Data

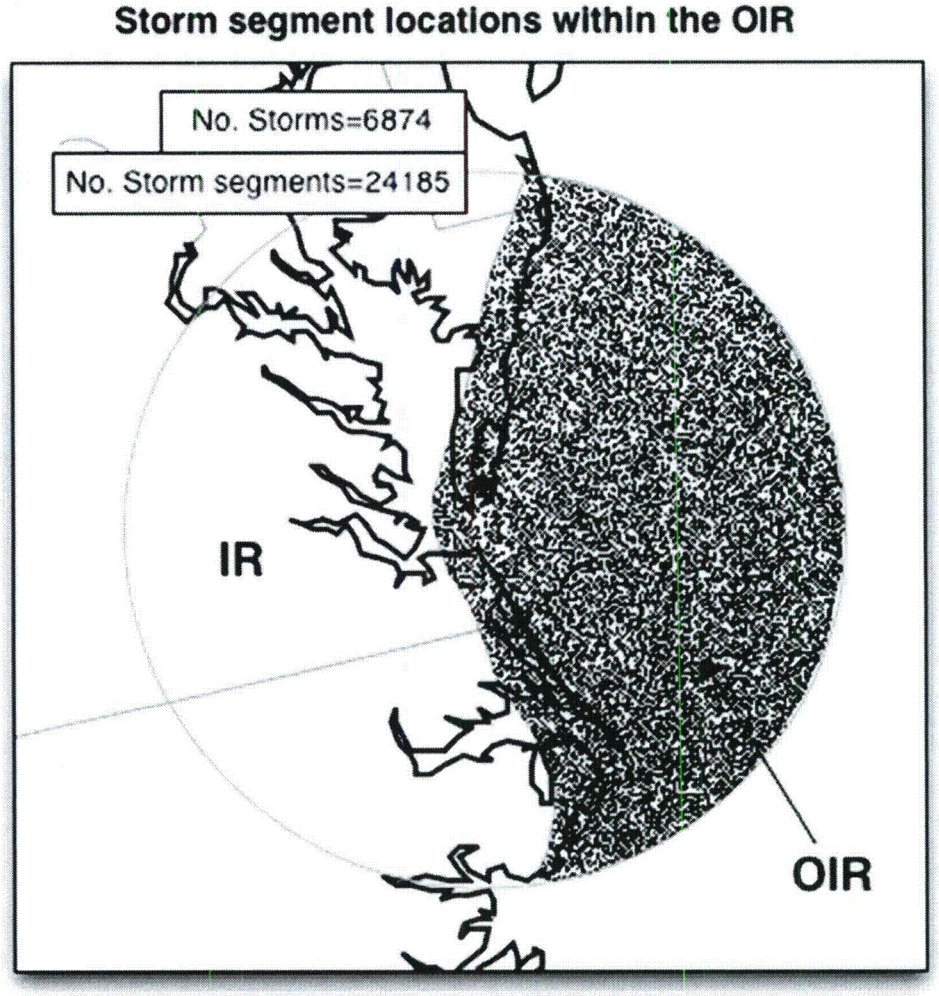

Figure 2.4-24: Annual Frequency of Synthetic Storms by Year and 31-year Averages.

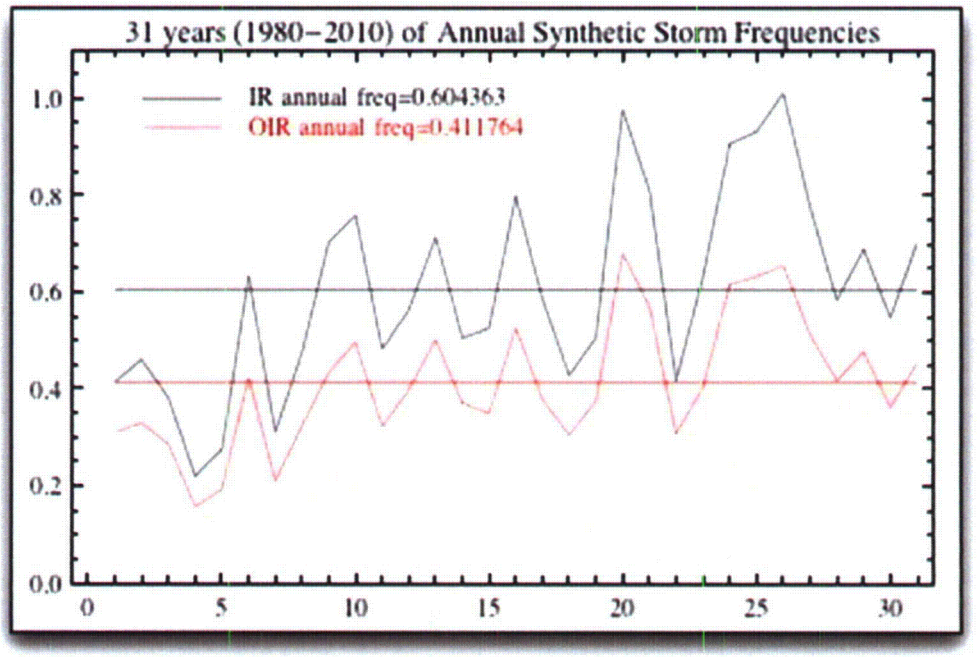

Figure 2.4-25: The PDF, CDF, tabulated probabilities and annual frequencies for the vm parameter within the OIR based on the WRT dataset.

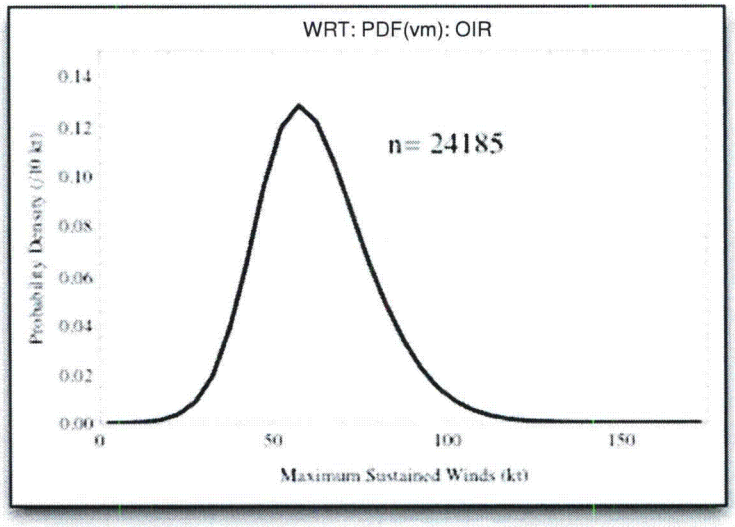

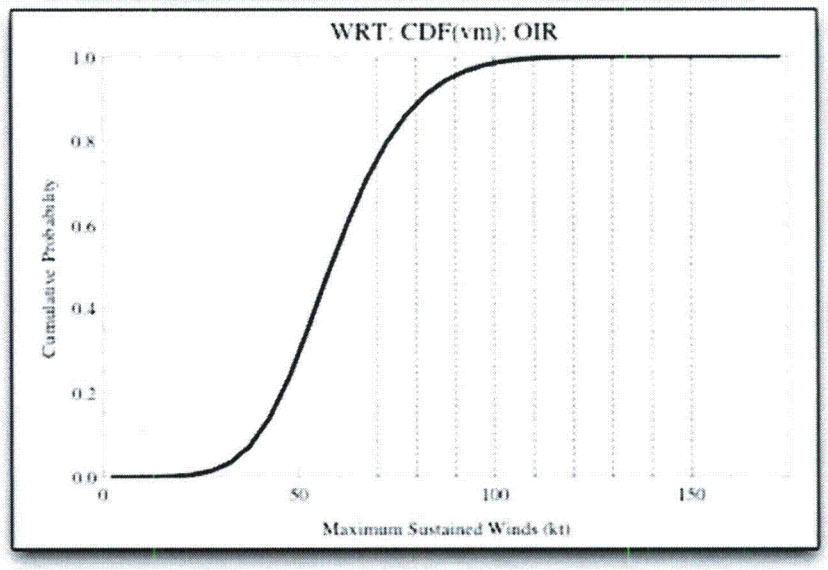

Probability of vm (per interval of 10 kt)

vm	70	80	90	100	110	120	130	140	150
Pr(vm)	0.17126	0.09655	0.04551	0.01829	0.00632	0.0021	0.00078	0.00029	0.00011
An_Freq(vm)	0.07052	0.03975	0.01874	0.00753	0.0026	0.00087	0.00032	0.00012	0.00004

Figure 2.4-26: The PDF, CDF, tabulated probabilities and annual frequencies for the fdir parameter within the OIR based on the WRT dataset.

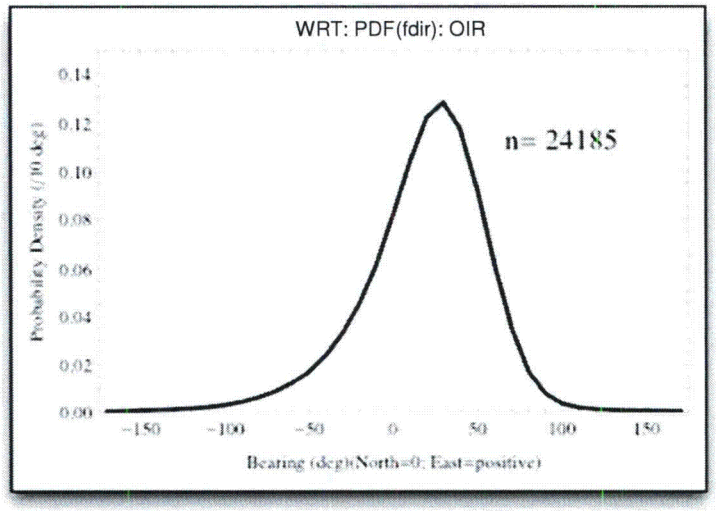

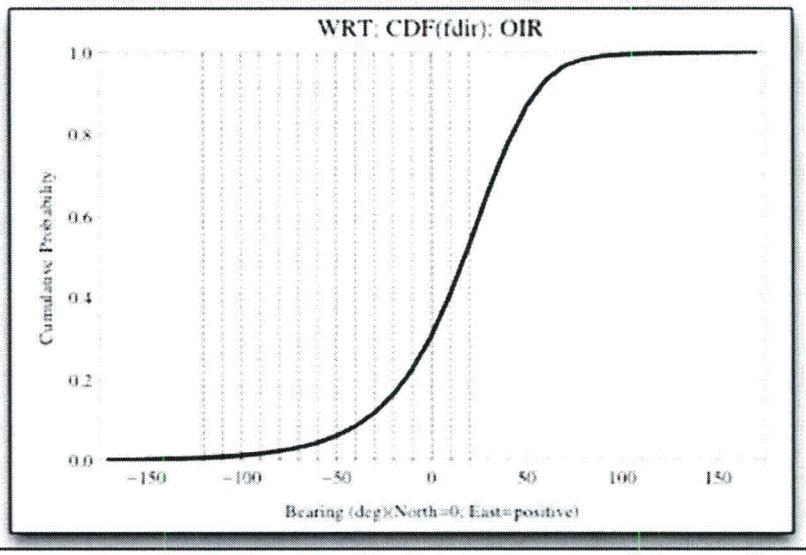

Probability of fdir (per interval of 10 deg)

fdir	-120	-110	-100	-90	-80	-70	-60	-50	-40	-30	-20	-10	0	10	20
Pr(fdir)	0.002	0.003	0.004	0.005	0.007	0.01	0.015	0.02	0.028	0.039	0.053	0.071	0.093	0.114	0.127
An. Freq(fdir)	0.001	0.001	0.002	0.002	0.003	0.004	0.006	0.008	0.012	0.016	0.022	0.029	0.038	0.047	0.052

Figure 2.4-27: The PDF, CDF, tabulated probabilities and annual frequencies for the fspd parameter within the OIR based on the WRT dataset.

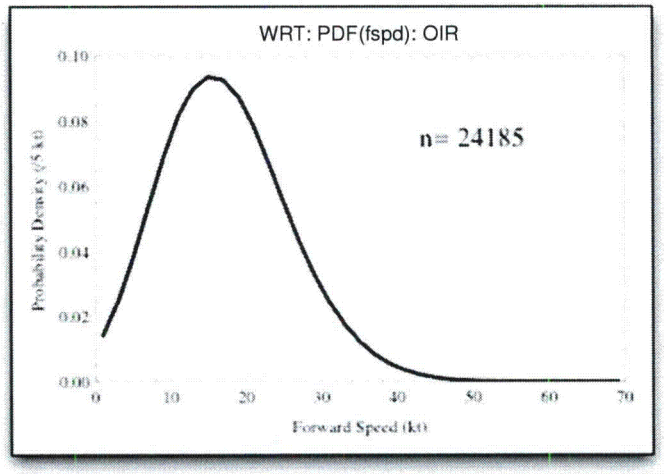

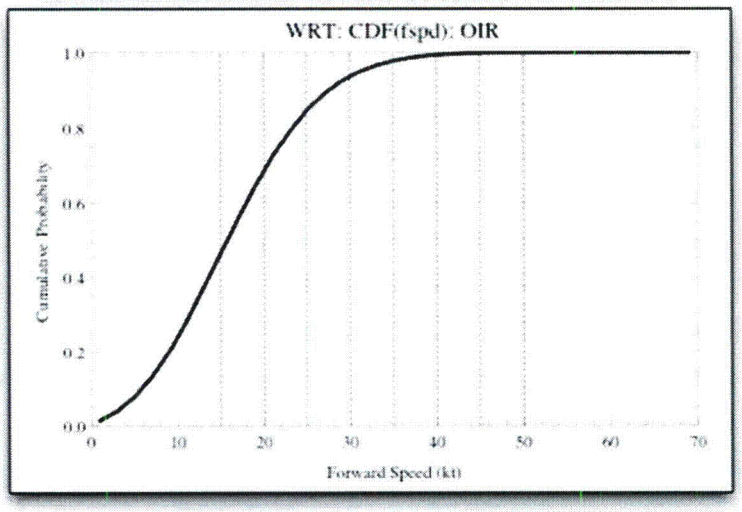

Probability of fspd (per interval of 5 kt)

fspd	15	20	25	30	35	40	45	50
Pr(fspd)	0.2317	0.1951	0.1234	0.0625	0.0261	0.0093	0.0027	0.0006
An. Freq(fspd)	0.0954	0.0803	0.0508	0.0257	0.0107	0.0038	0.0011	0.0003

Figure 2.4-28: The PDF, CDF, tabulated probabilities and annual frequencies for the rmw parameter within the OIR based on the WRT dataset.

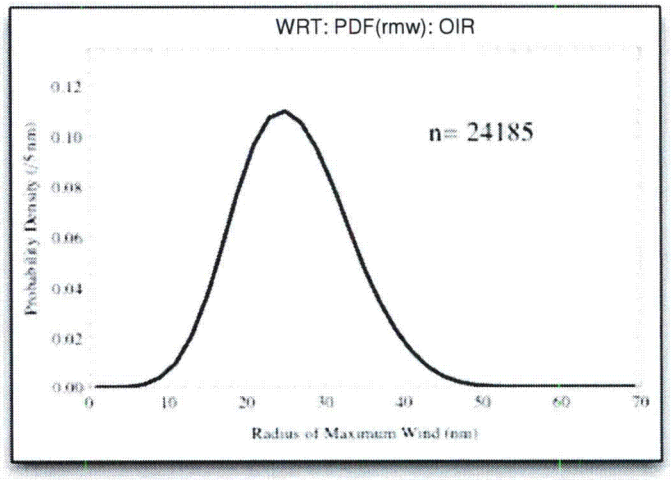

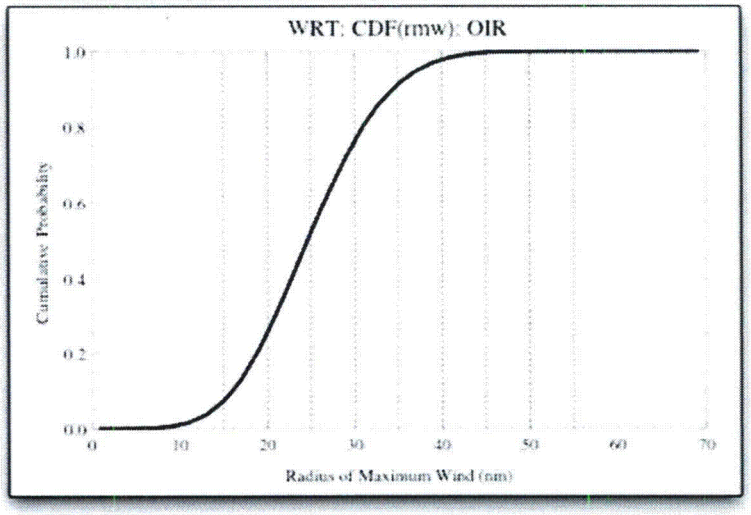

Probability of rmw (per interval of 5 nm)

rmw	15	20	25	30	35	40	45	50	55
Pr(rmw)	0.1173	0.2369	0.267	0.1997	0.1022	0.0368	0.0084	0.0012	0.0002
An_Freq(rmw)	0.0483	0.0976	0.11	0.0822	0.0421	0.0152	0.0035	0.0005	0.0001

Figure 2.4-29: Storm intensity (vm) extracted from the 3M data set as a function of storm bearing based on the calculated PMH intensity data set rank. The regression line represents a second-order polynomial function developed from a least-squares fit to the interval-specific vm values.

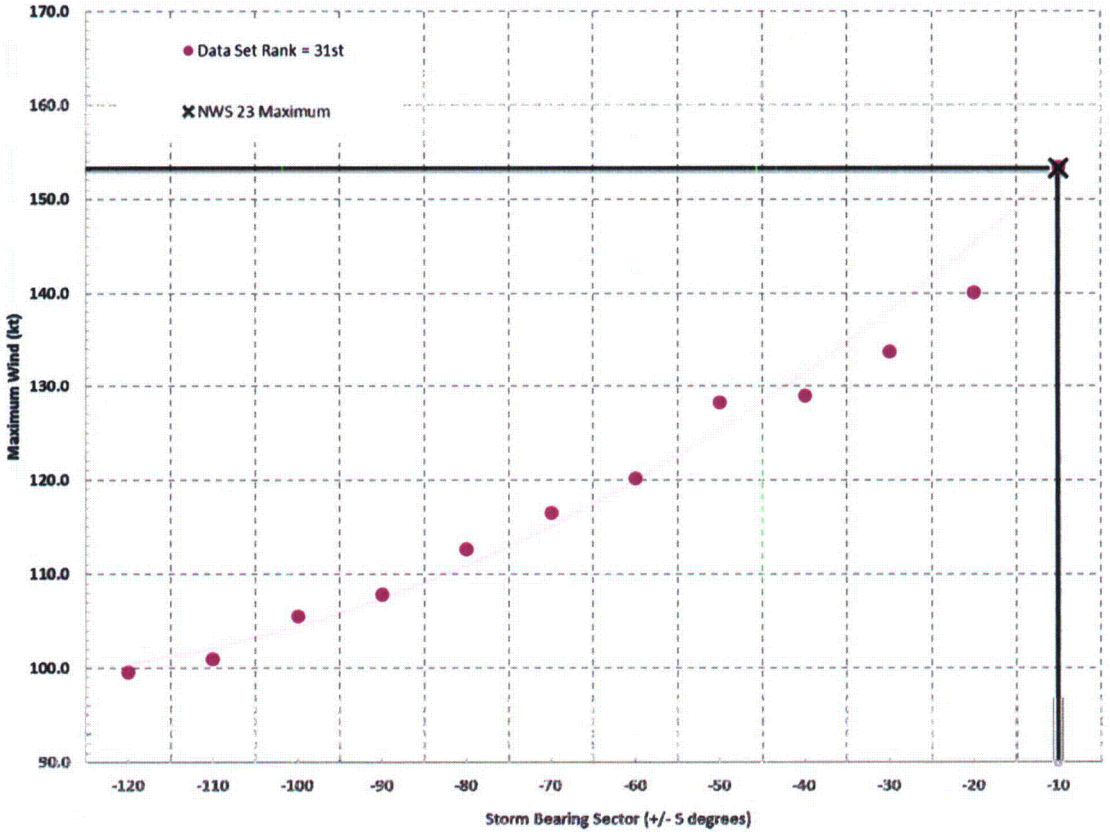

Figure 2.4-30: Scatter plot pairs representing WRT (left panels) and 3M (right panels) data. PMH parameter bounds for storm forward speed (fspand radius of maximum winds (rmw) are depicted in red. The limits depicted in the right panels are identical to the limits depicted in the left panels.

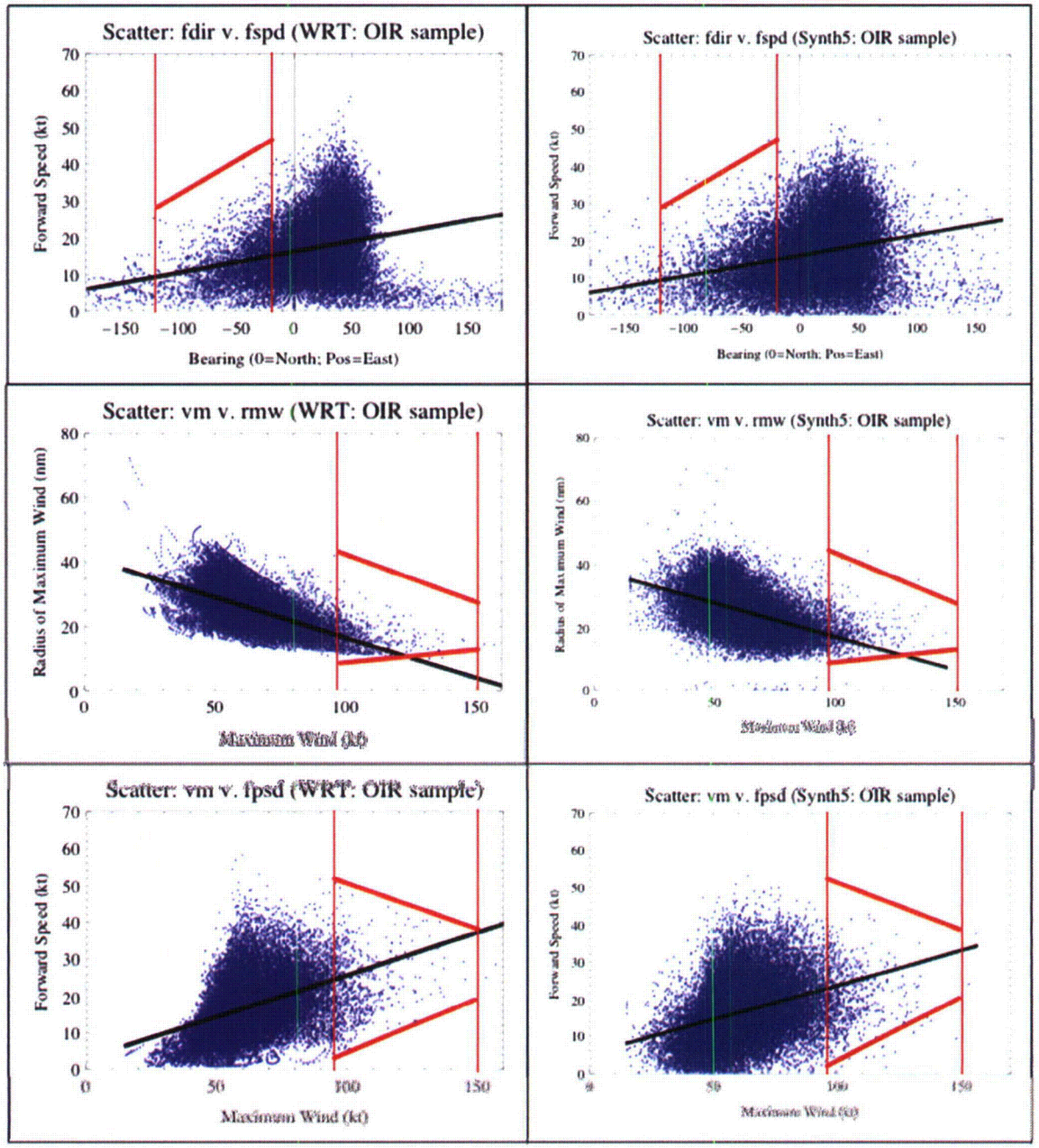

Figure 2.4-31: Simulated storm tracks – bearings ranging from -120° to -20°.

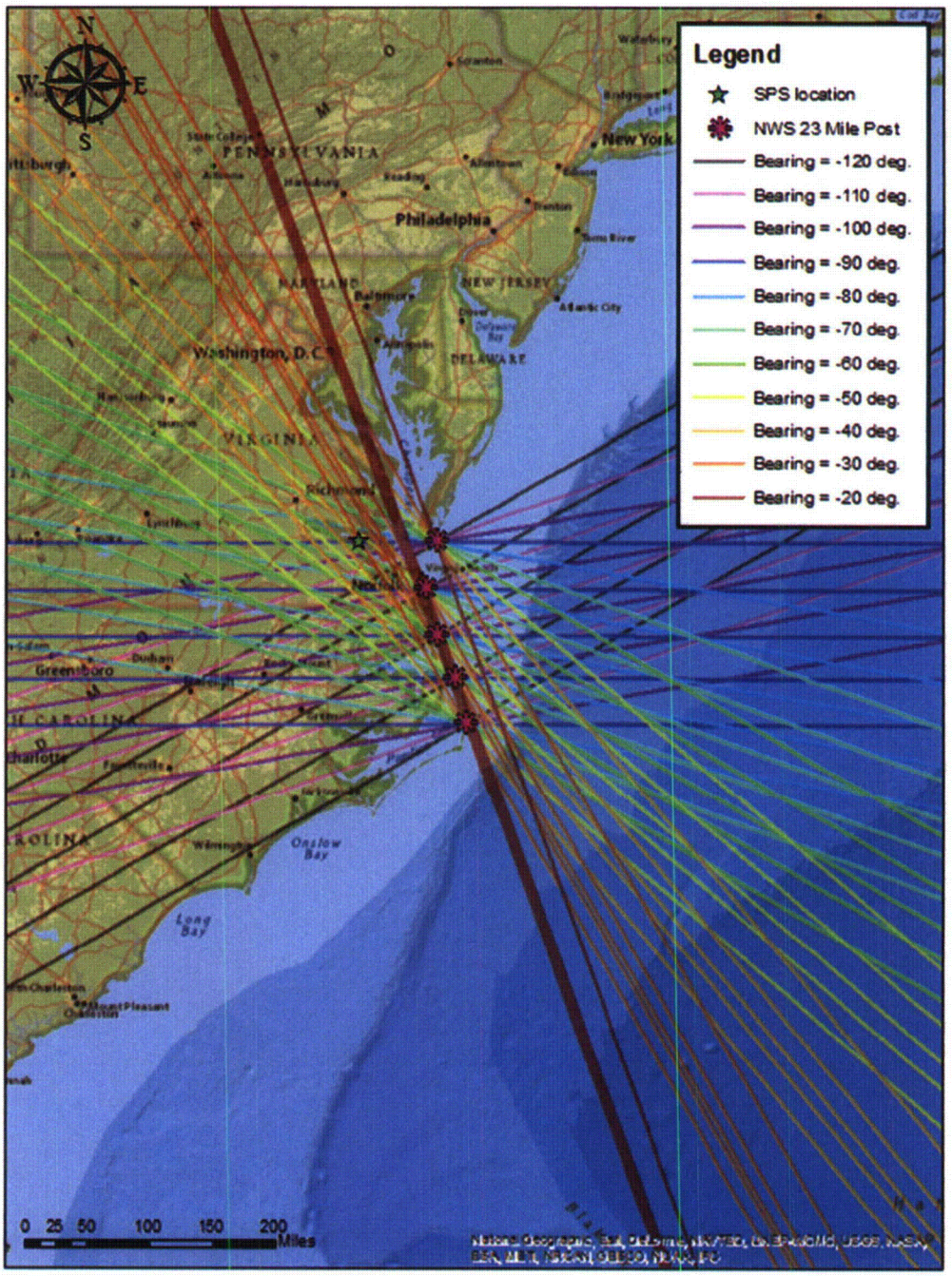

Figure 2.4-32: SLOSH hor3 model basin – SPS vicinity.

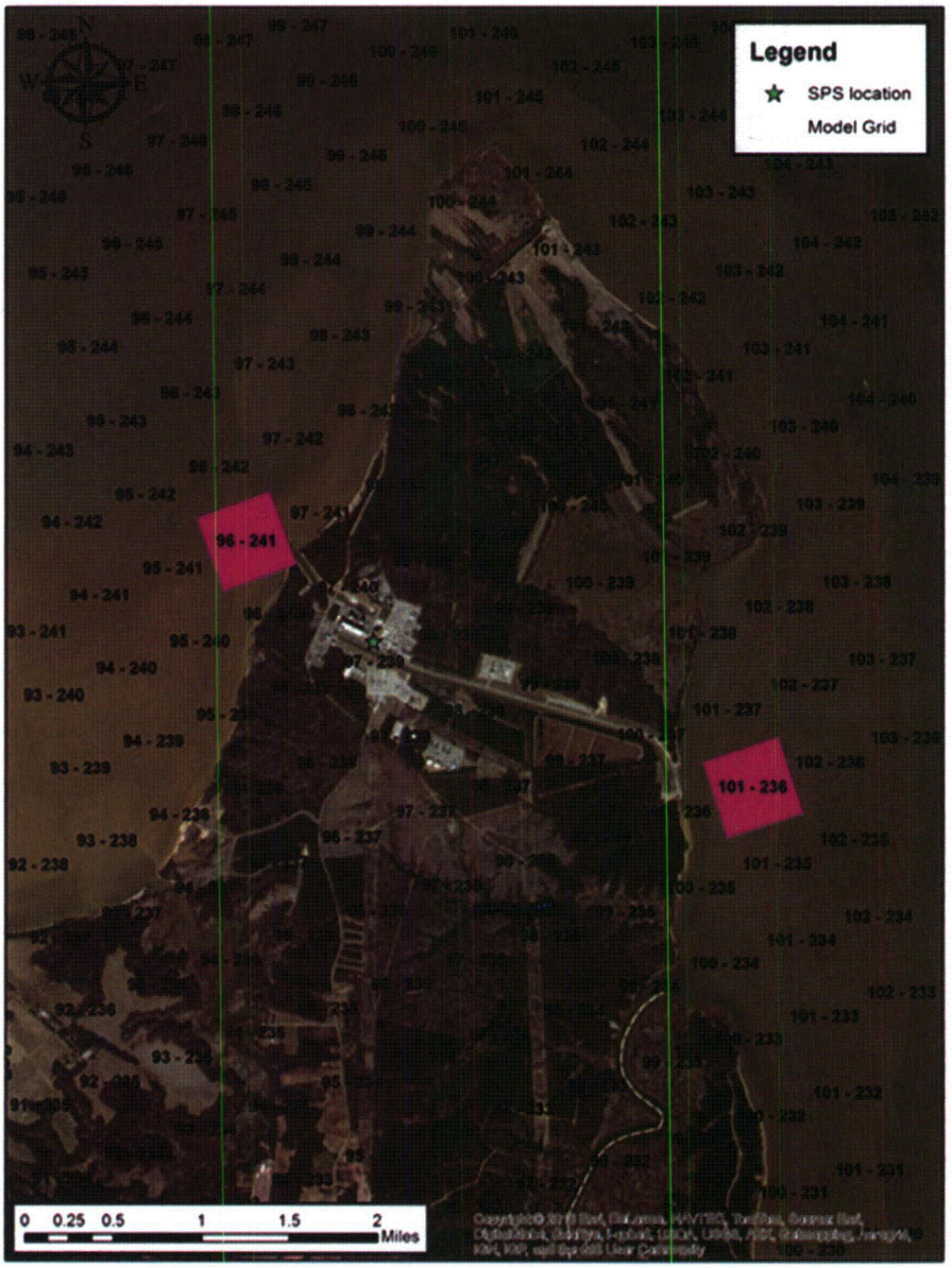

Figure 2.4-33: SLOSH hor3 model basin – SPS region. Cell identifications (i.e., I,J) shown for proximal NOAA tidal gaging and subordinate stations.

Figure 2.4-34: Screening results – SLOSH-simulated stillwater elevation as a function of storm bearing and forward speed.

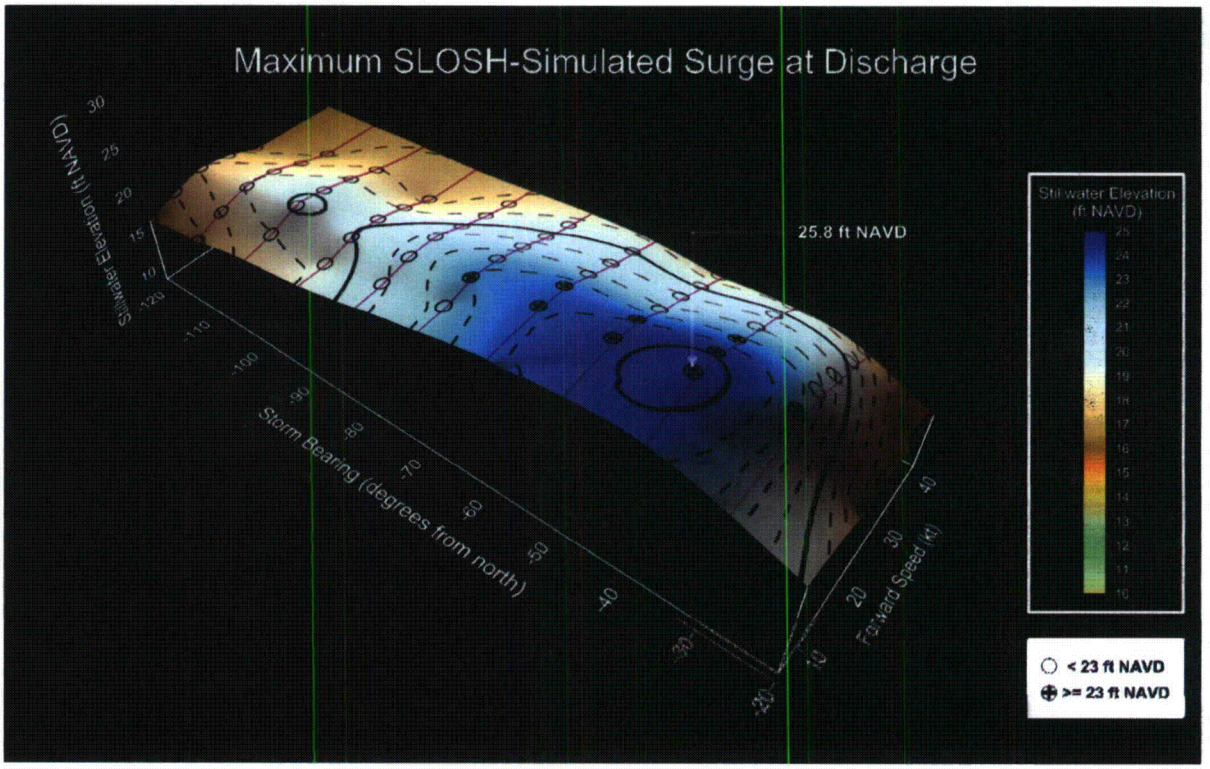

Figure 2.4-35: Screening results – SLOSH-simulated stillwater elevation as a function of storm bearing and radius to maximum winds.

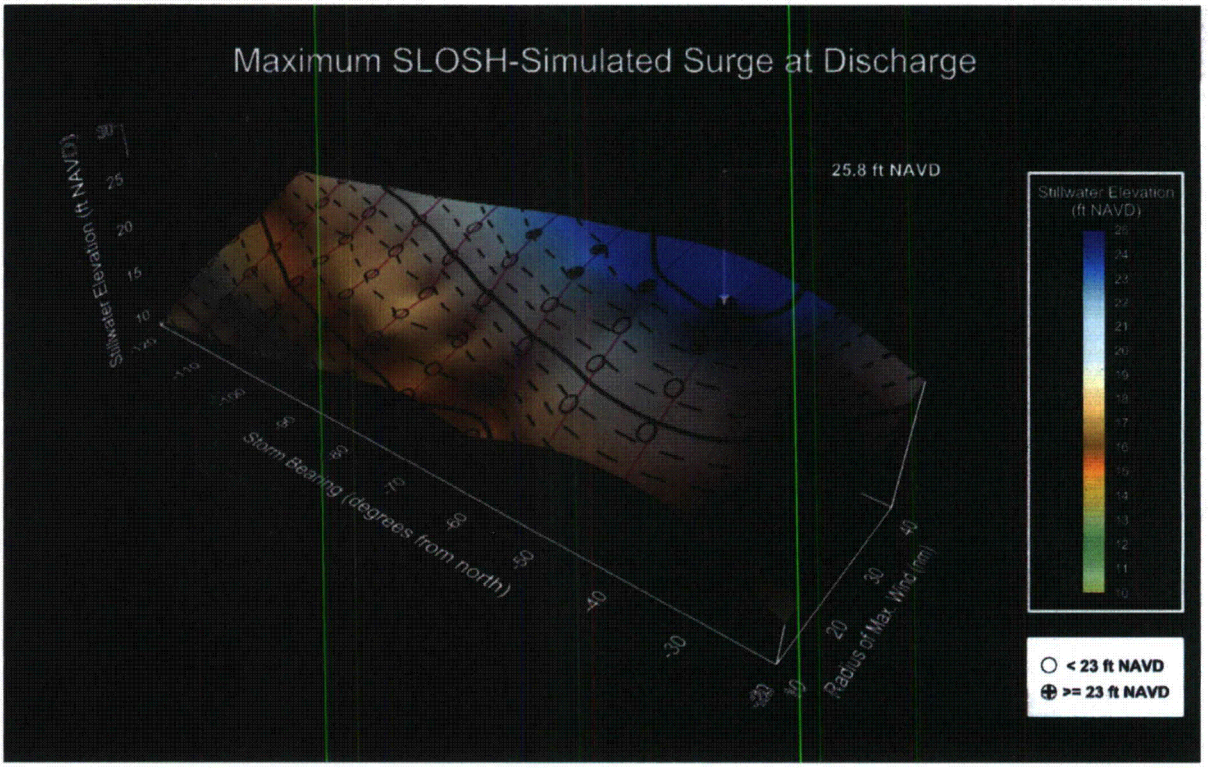

Figure 2.4-36: Simulated storm tracks in the SPS vicinity – bearings ranging from -120° to -20°.

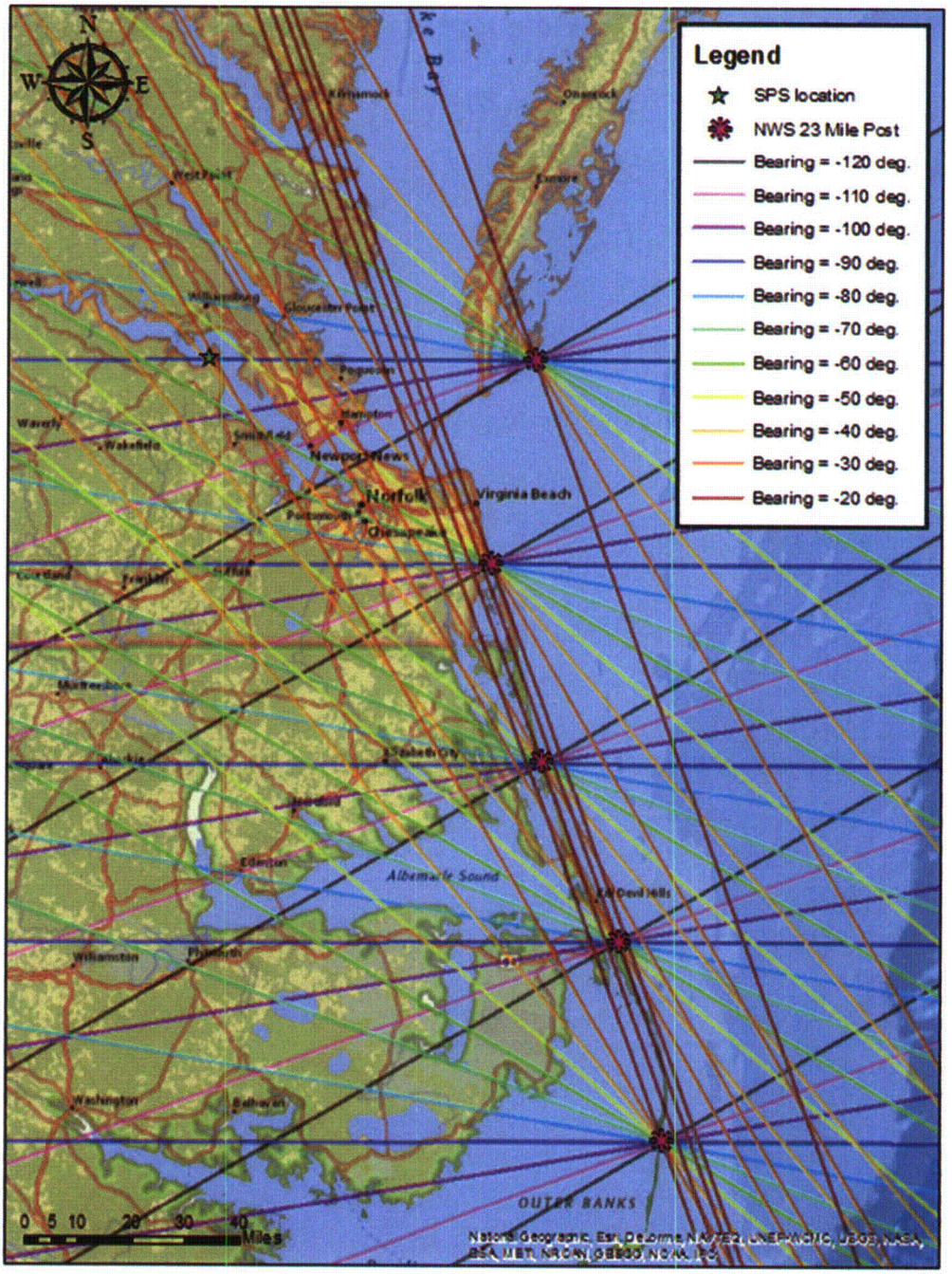

Figure 2.4-37: Comparison of stillwater surge-frequency relationships at SPS developed using the JPM and JPM-OS based on SLOSH results.

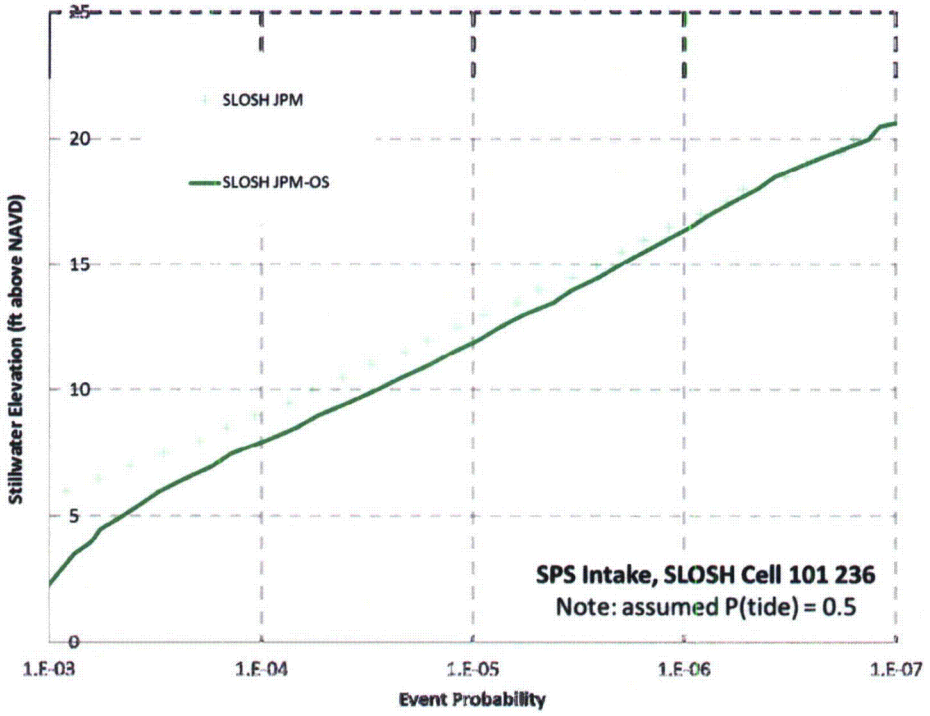

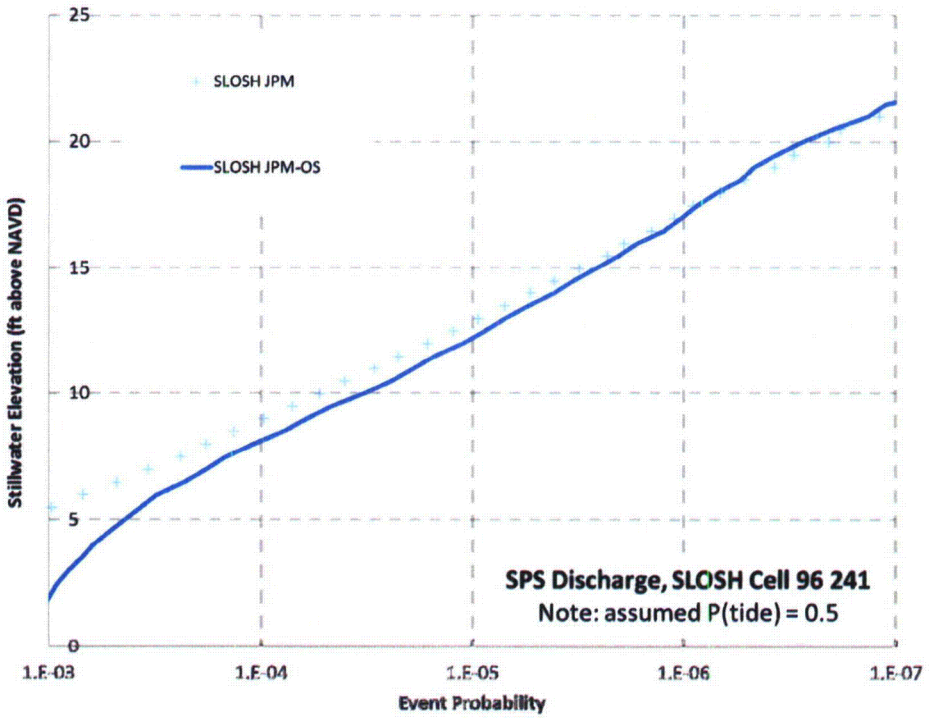

Figure 2.4-38: Refined stillwater surge-frequency relationships at SPS calculated using JPM-OS and ADCIRC including adjustments for uncertainty, error and SLR. The intial JPM / SLOSH and JPM-OS / ADCIRC (no uncertainty or SLR adjustments) relationships are provided for reference.

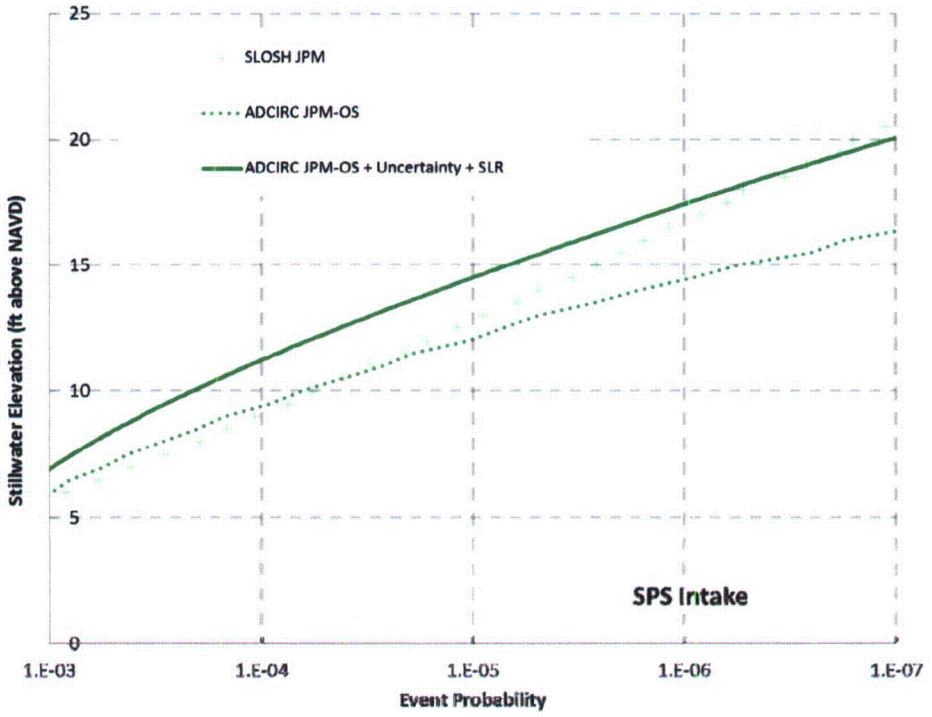

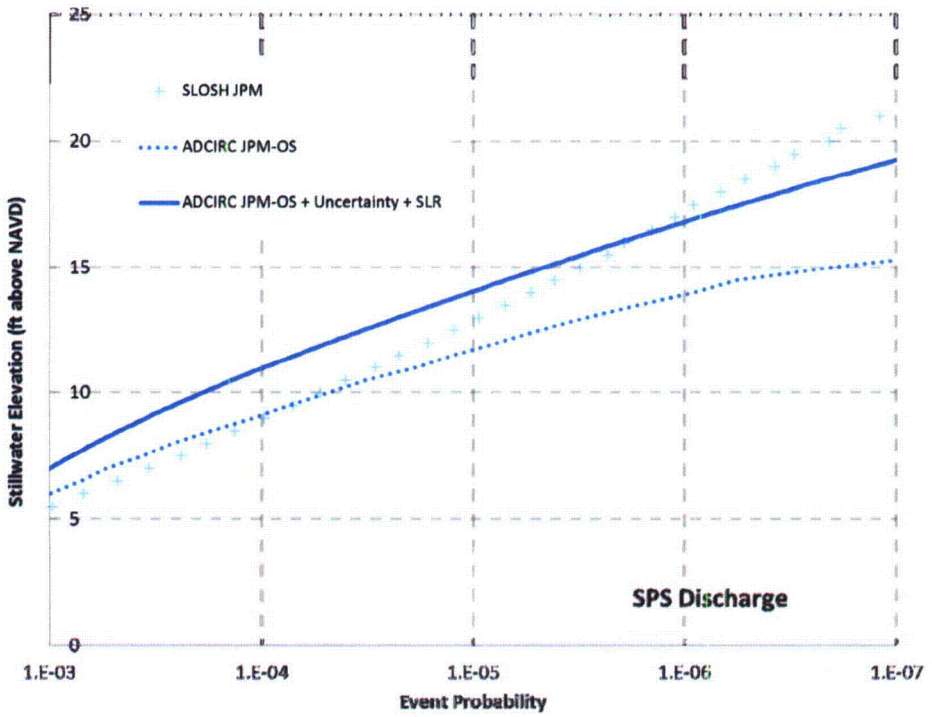

Figure 2.4-39: Refined stillwater surge-frequency relationship (converted to MSL vertical datum) at SPS calculated using JPM-OS and ADCIRC including adjustments for uncertainty, error and SLR.

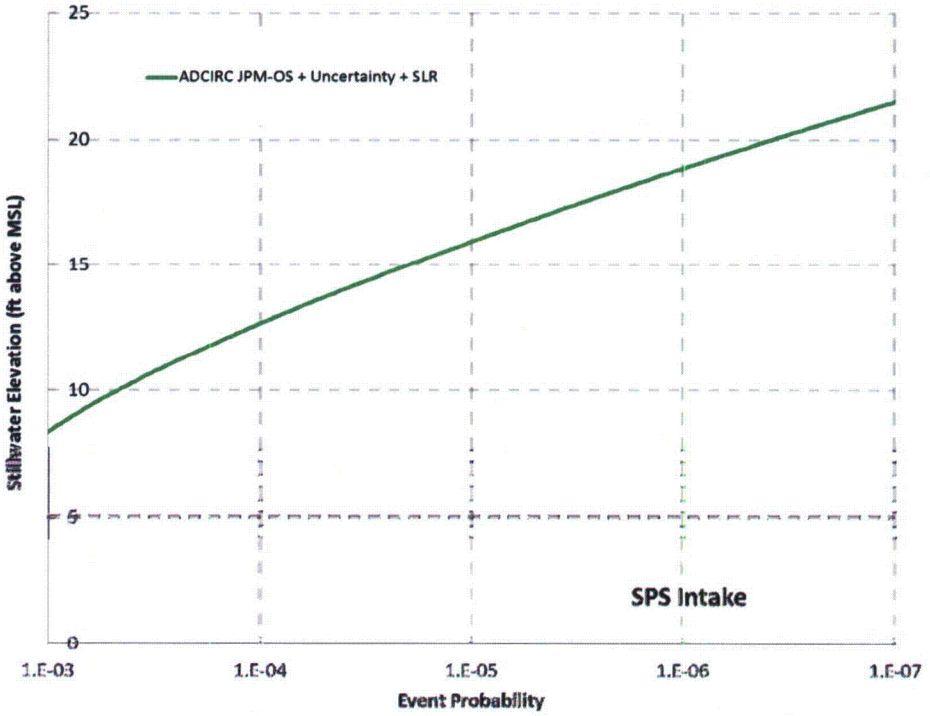

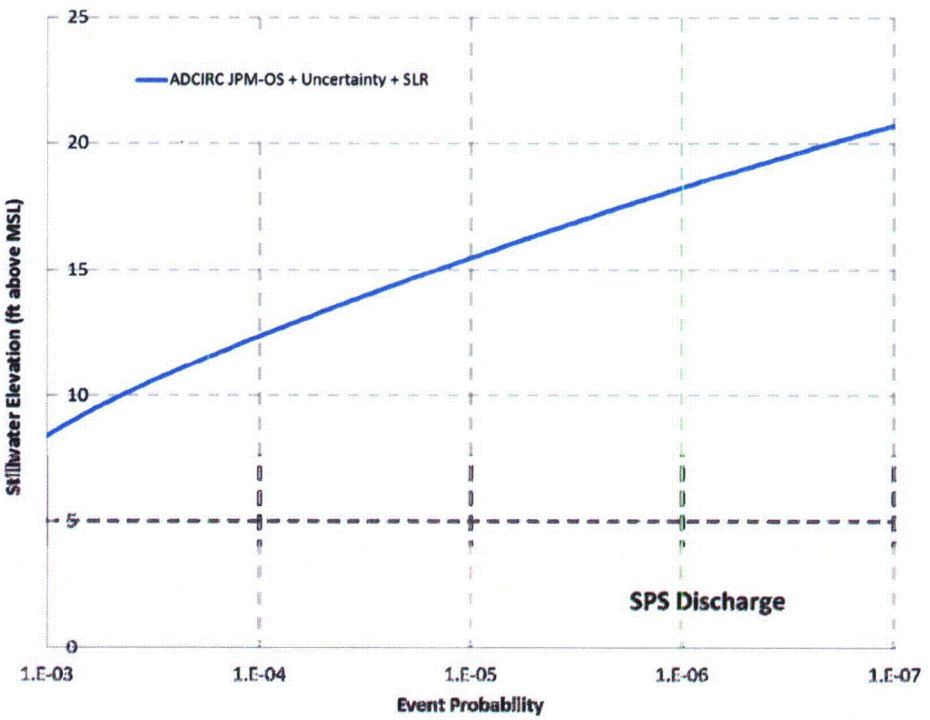

2.5. Seiche

An evaluation of the seiche flood hazard at SPS was performed. Three enclosed or semi-enclosed surface water bodies at SPS have been identified as requiring evaluation. The water bodies include: 1) the James River, a large river estuary surrounding and abutting SPS; 2) the intake canal, an enclosed water body; and 3) the semi-enclosed discharge canal (see Figure 2.5-1).

2.5.1. Method

Seiche at SPS was evaluated with consideration of meteorological, astronomical, wind-generated waves, tsunamis and seismic forcing as the causative mechanism for seiche in the James River, intake canal and discharge canal. The hierarchical-hazard assessment approach (HHA) described in NUREG/CR-7046 (NRC, 2011) was applied at SPS to determine whether a seiche in either James River, intake canal or discharge canal could result in significant flooding. The initial step is the determination of the natural period of oscillation in each water body. The period is estimated analytically and verified by observations where available. Next the period of each external forcing mechanism is examined as a possible driver of the system. Amplification of surface height oscillations can occur when the forcing period is close to the natural period of the basin, a phenomena known as resonance. If resonance is possible, further analysis of observed water level data is used to characterize the response to forcing in the basin.

The natural period of oscillation (primary seiche mode) of each water body was calculated using Merian's Formula (Scheffner, 2008). For semi-enclosed basins, Merian's Formula is based on a one-quarter-wavelength standing wave (see Figure 2.5-2 for definitions). The primary seiche mode for a semi-enclosed basin can be estimated using Merian's Formula as follows (Scheffner, 2008 and Rabinovich, 2009):

$$T = \frac{4l}{(1+2n)\sqrt{gh}} \qquad \text{(Equation 1)}$$

where:

T is the period (seconds)
l is the length of the basin (feet)
g is the acceleration due to gravity (feet per square second)
h is the average depth of the basin (feet)
$\sqrt{gh}$ is the shallow water wave speed
n = the number of nodes along the axis of the basin (0 for the primary mode of a semi-enclosed basin), n=0,1,2...

For an enclosed basin the standing wave is reflected at both ends and thus the system has two anti-nodes. The node in an enclosed system is located at the midpoint of the basin, see Figure 2.5-2. Merian's Formula for an enclosed basin is Equation 2 below (Scheffner, 2008 and Rabinovich, 2009):

$$T = \frac{2l}{n\sqrt{gh}} \quad \text{(Equation 2)}$$

where:

T is the period (seconds)
I is the length of the basin (feet)
g is the acceleration due to gravity (feet per square seconds)
h is the average depth of the basin (feet)
$\sqrt{gh}$ is the shallow water wave speed
n = the number of nodes along the axis of the basin, 1 for the primary mode in an enclosed basin

A spectral analysis was performed to compare the estimated period of the primary seiche mode with the observed periodicity of the James River using six-minute water level data at four NOAA water level stations (see Figure 2.5-3): Sewell's Point (Station 8638610), Kingsmill (Station 8638424), Tettington (Station 8638450), and Hopewell (Station 8638481), (NOAA ,2012b) . The spectral analysis was performed by applying the built in discrete Fast Fourier Transform (FFT) in Matlab R2011b (Matlab, 2012).

The natural period of the surface water bodies were estimated and compared to the periods of potential forcing mechanisms (meteorological, astronomical, wind-generated waves, tsunamis and seismic events). The frequency content and acceleration for the Safe Shutdown Earthquake (SSE) and Operating Basis Earthquake (OBE) were developed in the SPS UFSAR (DOMINION, 2014). Amplification of surface height oscillations can occur when the forcing period is close to the natural period of the basin, a phenomena known as resonance. If resonance is possible, further analysis of observed water level data is used to characterize the response to forcing in the basin. If the observed response is strongly damped then the flooding risk posed by the seiche is mitigated.

2.5.2. Results

2.5.2.1. Determination of the Natural Period of James River

The James River is the southern-most (and closest to the Atlantic Ocean) of several large river estuaries on the western side of the Chesapeake Bay. Near the mouth, the river is wide and ranges from 65 to 100 feet deep. Upstream from the mouth, the river becomes narrower and shallower. About 59 miles upriver from the mouth, the river narrows significantly at Tettington. The river narrows again about 22 miles upstream of Tettington, at Hopewell (see Figure 2.5-3). Both locations are potential reflection points for a seiche in the river. At the mouth of the river, near Sewell's Point, the tidal range is small, about 31.5 inches. The range diminishes up river as far as Hopewell and is amplified again upstream from Hopewell to Richmond where the maximum range is about 39.4 inches.

The James River was evaluated as a semi-enclosed basin. The primary resonance mode, which will result in the largest oscillations at the anti-nodes, was analyzed (Rabinovich, 2009). The James River at Tettington and Hopewell were both considered as potential reflection points because at these locations the river narrows significantly. In both cases, the node is located at the mouth of the river near Sewell's Point. River reach lengths were calculated between

reflection points and the river mouth, and depth data was acquired (NOAA, 2012a). The river measures approximately 310,000 feet from Sewell's Point to Tettington and 425,000 feet from Sewell's Point to Hopewell. Average depths from 26 to 39 feet were calculated. Merian's formula (Scheffner, 2008) provides an estimated period ranging from 10 to 12 hours using Tettington as a reflection point, and 13 to 16 hours using Hopewell as a reflection point. A summary of river geometry and resulting seiche periods is provided in Table 2.5-1.

The natural periods of the river were also evaluated by performing a spectral analysis on three months of measured six-minute water level data from the NOAA four stations (NOAA, 2012b). The analysis was performed by applying a discreet Fast Fourier Transform using frequencies from the minimum frequency of ~0.011 cycle/day to the Nyquist sampling frequency of 120 cycles/day. The results of the spectral analysis are presented in Figures 2.5-4 through 2.5-7.

The spectral analysis of the observed water level shows no direct evidence of a seiche. There is no significant energy at any of the estimated seiche frequencies. All of the spectral peaks in Figures 2.5-4 through 2.5-7 are known tidal constituents observed in most coastal and estuarine environments. The power in the peaks for the principle components show no sign of amplification toward the head of the river. Only the higher frequency over-tides, that are due to non-linear interaction in the shallow river, are amplified at Hopewell. Based on the measured water level data, no seiche dynamics were observed in the James River.

2.5.2.2. Evaluation of External Forcing Mechanisms on James River

The external forcing mechanism which were analyzed are earthquakes, tsunamis, meteorological conditions including gusts and storms and astronomical tides.

Earthquakes: The response spectra for the OBE and SSE (DOMINION, 2014) show only small acceleration at the 7 to 12 second range. These periods are outside the natural periods calculated for the James River.

Tsunamis: The period of tsunami waves range from several minutes up to 1 hour (UCSD, 2013). Ten minutes is the shortest period typical of a tsunami as described by the NOAA Pacific Tsunami Warning Center (NOAA, 2009). Resonance within the James River will not occur due to the difference in the natural period of the river and the typical range of tsunami wave periods.

Meteorological: Meteorological forcing does not have sufficient energy at the James River's frequency to drive a seiche in the James River. Local convection, diurnal heating and cooling, and a high energy band at the synoptic scale (Wells, 1997 and Svensson et al, 2011.) were considered.

Astronomical: The astronomical tides are the primary forcing for flow in the James River estuary. The tides drive a surface height oscillation of about 2.8 feet near SPS (NOAA, 2005e). The period of the semi-diurnal tides falls within the range of seiche periods calculated for the James River. Since a potential source of resonance exists in the James River the characteristics of the resonant frequency was examined.

The semi-diurnal constituents all diminish from Sewell's Point to Kingsmill and Scotland near SPS (NOAA, 2005a, NOAA, 2005b, NOAA, 2005c, NOAA, 2005d). Amplification of these components only occurs far upstream of SPS at Richmond. For the largest tidal constituent, the

M2 amplitude, at Kingsmill is 91-percent of the value at Sewell's Point. At Scotland it is 78-percent and at Richmond it is slightly amplified, at 115-percent of the value at Sewell's Point. The harmonic frequencies or overtides such as M4, M6 and MK3 increase upriver, however these compound tides are the result of non-linear wave dynamics that transfer energy from lower frequencies to higher frequencies as part of the dissipation process (Parker, 1999) and their amplitudes are very small. This transfer of energy is not related to amplification due to forcing at resonance. If a strong resonance existed, large amplitudes would be observed near the head of the river and amplification of tidal constituents on the order of 10 to 20 times the value at the mouth would be observed. There is no evidence to support a strong resonant seiche of this kind in observed water level data of the James River.

The response of the river to a strong forcing event illustrates the lack of resonant response to tidal forcing. Water levels at three stations (Sewell's Point, Tettington, and Richmond) over the course of a large storm surge during November 2009 are shown in Figure 2.5-8, Figure 2.5-9 and Figure 2.5-10. The figures show the predicted astronomical tide for the time period of the storm, the actual observed water levels and the difference between the observed and predicted values. Measuring the difference between the observed and predicted values is an approximate method for filtering out the tidal signal. At Sewell's Point and Tettington, the tidal signal was largely removed. However, at Richmond Locks the tidal prediction overestimates the observed tide and the resulting difference contains tidal like oscillations (see Figure 2.5-9). At all three stations the water levels return to normal in a few days and shows only small oscillations around an elevated mean. The behavior observed in the James River is characteristic of an over-damped oscillator as described in Figure 2.5-11. This time series is characteristic of the James River system response to strong forcing and indicates that there is no resonant seiche mode in part because the system is highly-damped due to frictional dissipation. Analysis shows that the James River is an over-damped system and thus does not support oscillatory behavior.

2.5.2.3. Determination of the Natural Period of Intake and Discharge Channels

The 100-foot wide intake canal runs 9,200 feet from the east side of the peninsula to the plant. is pumped into the intake canal from the James River, but the canal is not connected to the river. The discharge canal varies in width from 100 to 140 feet and runs 3,500 feet from SPS to the west side of the peninsula, where it is open to the river. Channel lengths were calculated in ArcGIS. Depths in the intake canal range from 20 to 25 feet (DOMINION, 2014). The discharge canal was dredged to an elevation of -17.5 feet MSL (DOMINION, 2014), depths in the channel are dependent on tidal elevation. Based on Sewell's Point, the nearest NOAA station NOAA, 2005e) the tidal range of discharge canal depths is 16.1 to 18.9 feet.

The periods of the intake and discharge canals were calculated in both the longitudinal and transverse directions. Based on the channel dimension in the longitudinal direction, the period of the primary mode range from 9 to 10 minutes in the discharge canal and 11 to 12 minutes in the intake canal. In the transverse direction, the periods of the primary modes ranges from 8 to 12 seconds in the discharge canal and 7 to 8 seconds in the intake canal. An overview of the channel dimensions and associated periods are provided in Table 2.5-2 and Table 2.5-3.

2.5.2.4. Evaluation of External Forcing Mechanisms on Intake and Discharge Channels

The external forcing mechanism which were analyzed are earthquakes, tsunamis, meteorological conditions including gusts and storms and astronomical tides.

Earthquakes: The frequency content of earthquakes is typically less than 10 seconds. The response spectra for the OBE and SSE (DOMINION, 2014) show only small acceleration at the 7 to 12 second range, indicating that significant seiches in the transverse direction are not expected to occur within either the intake or discharge canals.

Tsunamis: A tsunami in the James River could have a period roughly equal to the natural period of a longitudinal seiche in the discharge canal. However, the discharge canal is only weakly coupled to the river due to the narrow entrance and tsunamis are not expected to propagate into the discharge canal due to the orientation of the opening.

Meteorological: Meteorological forcing such as wind gusts typically have a period of approximately 1 minute (Wells, 1997). This period is not equivalent to the period of the primary seiche mode in either the transverse (approximately 10 seconds) or longitudinal (approximately 10 minutes) directions. Additionally, gusts are unlikely to create a consistent oscillating source of sufficient strength on either the intake or discharge canals to cause a significant seiche.

Astronomical: The astronomical tides in the James River have periods that are several orders of magnitude larger than the longitudinal period of the discharge canal and thus would not cause resonance. Wind-generated waves could occur with periods in the ranges of the transverse period of the discharge canal. However, the geometry of the discharge canal does not allow a transverse seiche to be caused by forcing from the James River, so wind-generated waves could not cause resonance in the transverse direction. The intake canal is disconnected from the James River therefore, there is no risk of forcing from tides or waves.

2.5.3. Conclusions

Significant seiches on the James River, intake canal and discharge canal at SPS are not expected based on the screening analysis performed using Merian's formula, a statistical analysis of historical water level data and literature review. No further analysis or modeling is necessary.

2.5.4. References

2.5.4-1 Dominion, 2014. Updated Safety Analysis Report, Surry Power Station. Revision 46.02.

2.5.4-2 Matlab, 2012. Matlab R2011b, The Mathworks Inc., Version 7.14, 1 March 2012.

2.5.4-3 NOAA, 2005a. 37 component tidal harmonic constituents at Sewell's Point. Website: http://tidesandcurrents.noaa.gov/data_menu.shtml?Stn=8638610%20Sewell' %20Point,%20VA&type=Harmonic%20Constituents. Accessed: 25 November 2012.

2.5.4-4 NOAA, 2005b. 37 component tidal harmonic constituents at Kingsmill. Website: http://tidesandcurrents.noaa.gov/data_menu.shtml?Stn=8638424% 20Kingsmill%20VA&type=Harmonic%20Constituents. Accessed: 25 November 2012.

2.5.4-5 NOAA, 2005c. 37 component tidal harmonic constituents at Scotland. Website: http://tidesandcurrents.noaa.gov/data_menu.shtml?Stn=8638433 Scotland, VA&type=Harmonic Constituents. Accessed: 25 November 2012.

2.5.4-6 NOAA, 2005d. 37 component tidal harmonic constituents at Richmond. Website http://tidesandcurrents.noaa.gov/data_menu.shtml?Stn=8638495 Richmond River Locks, James River, VA&type=Harmonic Constituents. Accessed: 25 November 2012.

2.5.4-7 NOAA, 2005e. Sewell's Point, VA Datums. Website: http://www.tidesandcurrents.noaa.gov/data_menu.shtml?Unit=0&format=Apply+Change&stn=8638610+Sewell's+Point%2C+VA&type=Datums. Accessed 10 December, 2012.

2.5.4-8 NOAA, 2009. Pacific Tsunami Warning Center, Frequently Asked Questions. Website: http://ptwc.weather.gov/faq.php#4. Accessed 8 May, 2013.

2.5.4-9 NOAA, 2012a. National Geophysical Data Center, NGDC Coastal Relief Model. Website: http://www.ngdc.noaa.gov/mgg/coastal/crm.html. Accessed: 3 December 2012

2.5.4-10 NOAA, 2012b. Historic Water Level Data: Six Minute Water Level. NOAA Website: http://tidesandcurrents.noaa.gov/station_retrieve.shtml?Type=Historic+Tide+Data. Accessed: 28 November 2012.

2.5.4-11 NRC, 2011. Design-Basis Flood Estimation for Site Characterization at Nuclear Power Plants, NUREG/CR-7046, United States Nuclear Regulatory Commission (USNRC), November 2011.

2.5.4-12 Parker, 1999. Coastal and Estuarine Studies: Coastal Ocean Prediction, Chapter 11, Tide Height and Current Prediction. The American Geophysical Union, 1999.

2.5.4-13 Rabinovich A.B., 2009. "Seiches and Harbor Oscillations". In: Kim, Y.C. ed. Handbook of Coastal and Ocean Engineering. World Scientific, Singapore, 2009, 193–236.

2.5.4-14 Scheffner, 2008. "Water Levels and Long Waves." In: Demirbilek, Z., Coastal Engineering Manual, Part II, Coastal Hydrodynamics Chapter 5-6, Engineer Manual 1110-2- 1100, U.S. Army Corps of Engineers, Washington, D.C.

2.5.4-15 Svensson et al, 2011. Evaluation of the Diurnal Cycle in the Atmospheric Boundary Layer Over Land as Represented by a Variety of Single-Column Models: The Second GABLS Experiment. Springer Sciene +Business Media B.V., 2011.

2.5.4-16 UCSD, 2013. Wave Measurement – Tsunami Events, The Coastal Data Information Program (CDIP), University of California, San Diego, October, 2011.

2.5.4-17 Wells, 1997 Wells, N. "The Atmosphere and Ocean, A Physical Introduction." John wiley & sons Ltd, 1997.

Table 2.5-1: Parameters for length, depth and the resulting period of oscillation for the James River

Reflection Point	Length[1] (feet)	Depth[2] (feet)	Period[3] (hours)
Tettington	308,742	26.25	11.8
Tettington	308,742	39.37	9.6
Hopewell	424,890	26.25	16.2
Hopewell	424,890	39.37	13.3

(1) Length measured using ArcMap computer program using shape files and datasets provided by NGDC CRM (NOAA, 2012a).
(2) Depth estimated from NGDC CRM Bathymetry (NOAA, 2012a).
(3) Calculated using Merian's Formula.

Table 2.5-2: Parameters for length, depth and the resulting period of oscillation in the longitudinal direction for the canals at SPS

Canal	Length[1] (feet)	Depth[2] (feet)	Period[3] (minutes)
Intake	9187	20.0	12.1
Intake	9187	24.9	10.8
Discharge	3511	18.9	9.5
Discharge	3511	16.1	10.3

(1) Length measured using ArcMap computer program using shape files and datasets provided by NGDC CRM (NOAA, 2012a).
(2) Intake Canal depths are operational regulated (DOMINION, 2014). The Discharge Canal depths are based on invert elevation - 17.5 ft MSL (DOMINION, 2014) plus/minus 1.4 ft MHHW/MLLW (NOAA, 2005e).
(3) Calculated using Merian's Formula.

Table 2.5-3: Parameters for length, depth and the resulting period of oscillation in the transverse direction for the cooling water canals at SPS

Transverse	Width[1] (feet)	Depth[2] (feet)	Period[3] (seconds)
Intake	98.43	20.0	7.8
Intake	98.43	24.9	6.9
Discharge	98.43	16.1	8.7
Discharge	98.43	18.9	8.0
Discharge	137.8	16.1	12.1
Discharge	137.8	18.9	11.2

(1) Length measured using ArcMap computer program (Reference 8.2) utilizing shape files and datasets provided by NGDC CRM (NOAA, 2012a).
(2) Intake Canal depths are operational regulated (DOMINION, 2014). The Discharge Canal depths are based on invert elevation - 17.5 ft MSL (DOMINION, 2014) plus/minus 1.4 ft MHHW/MLLW (NOAA, 2005e).
(3) Calculated using Merian's Formula.

Figure 2.5-1: Schematic diagram of the SPS site including major structures and water bodies. The James River is shown to the East and West of the site. The intake and discharge canals are also specified.

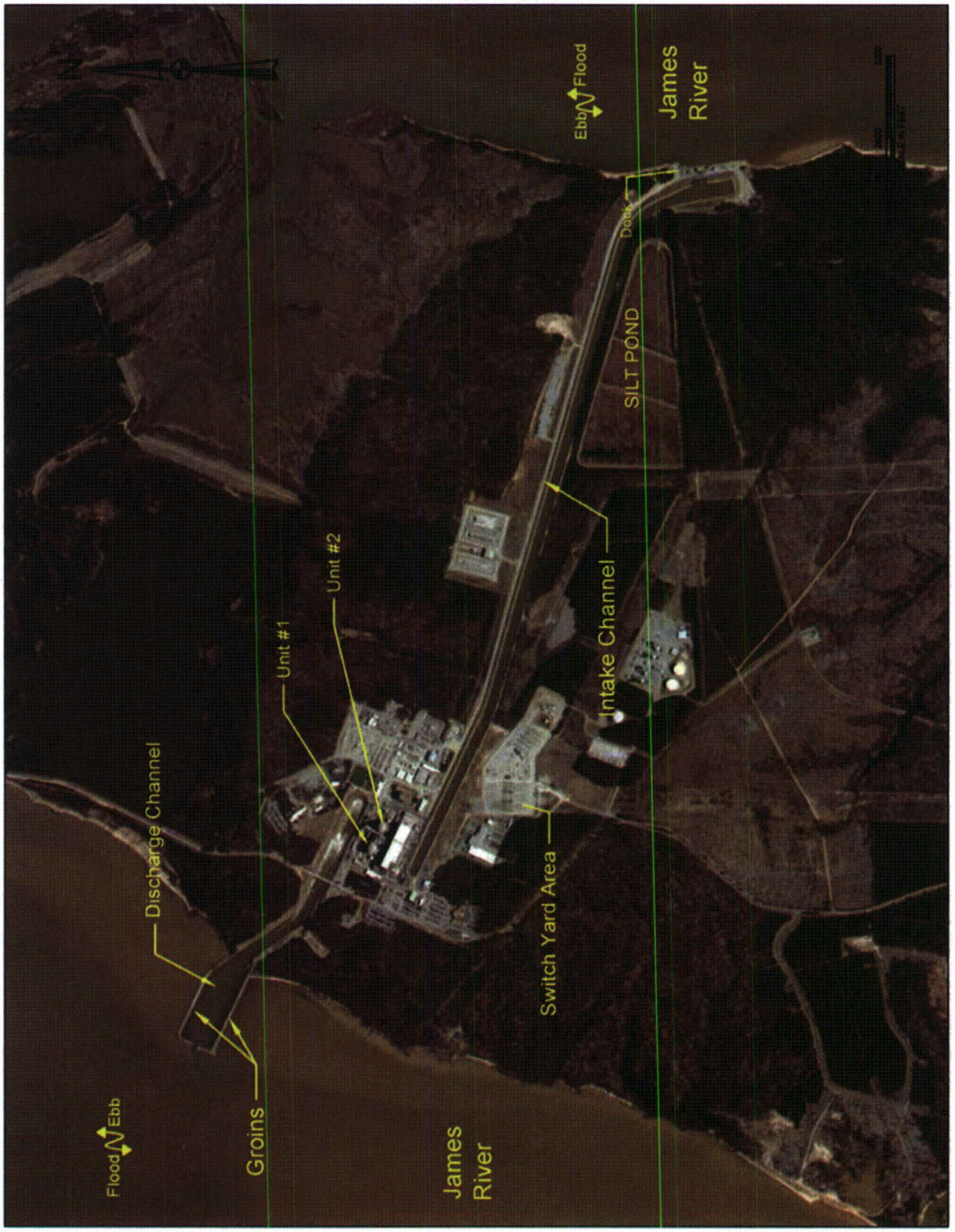

Figure 2.5-2: Diagram of the first three resonant modes of an enclosed (left) and semi-enclosed (right) basin (Scheffner, 2008).

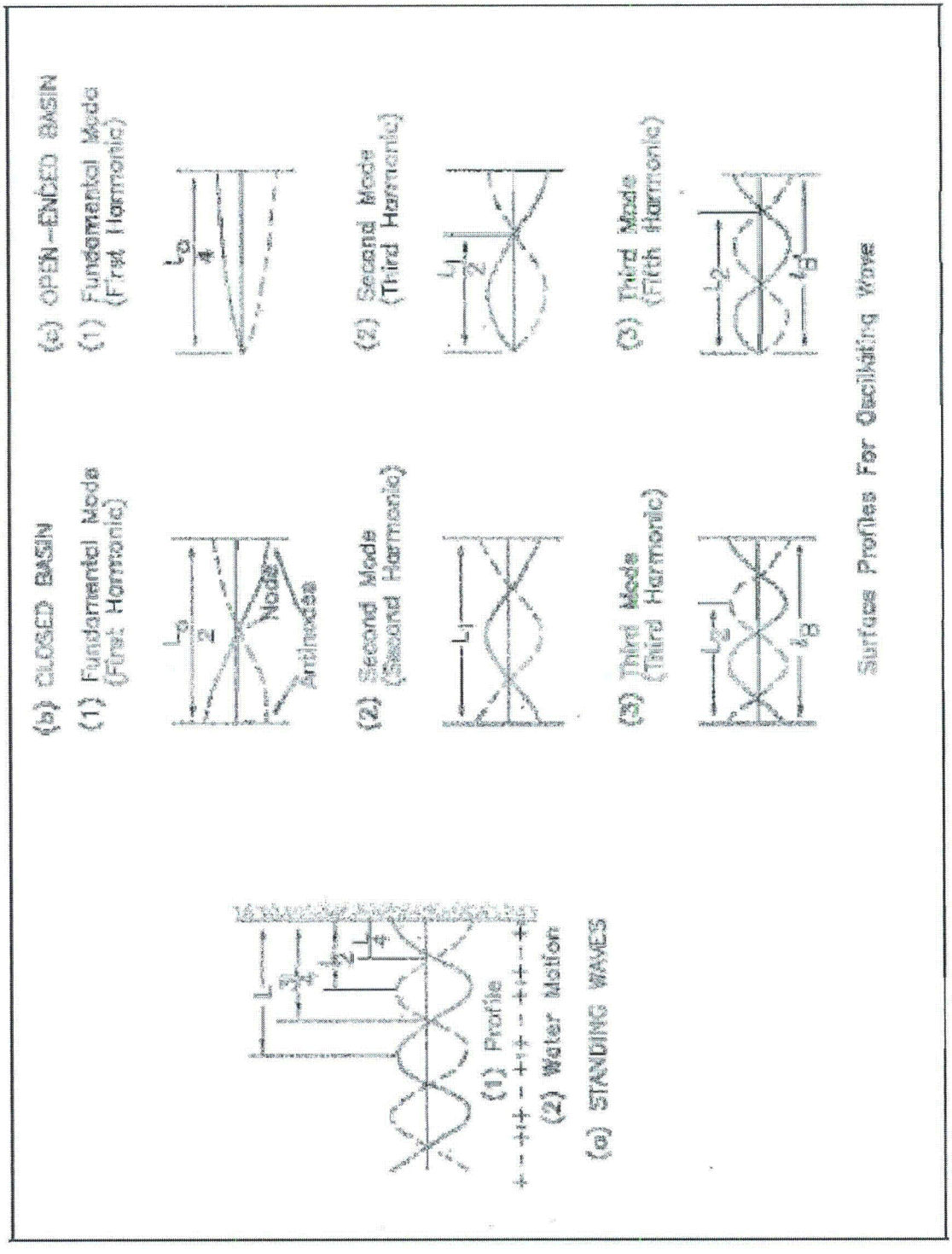

Figure 2.5-3: Map of the James River including the location of SPS and several NOAA Water Level Stations on the River.

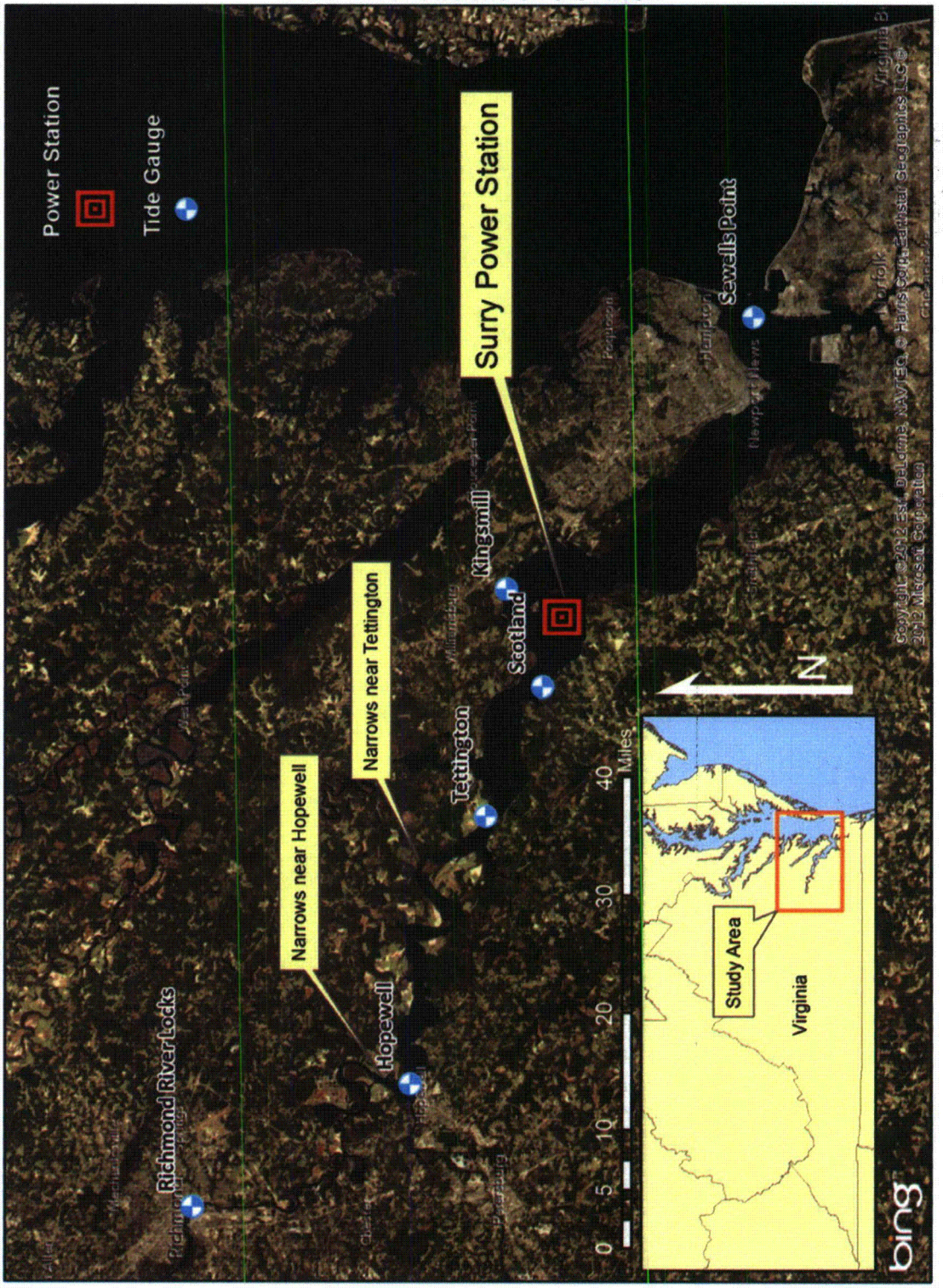

Figure 2.5-4: Spectral analysis of surface height time series at Hopewell on the James River. The y-axis has units of spectral power in this case proportional to meters squared. The x-axis has units of frequency in days or cycles per day.

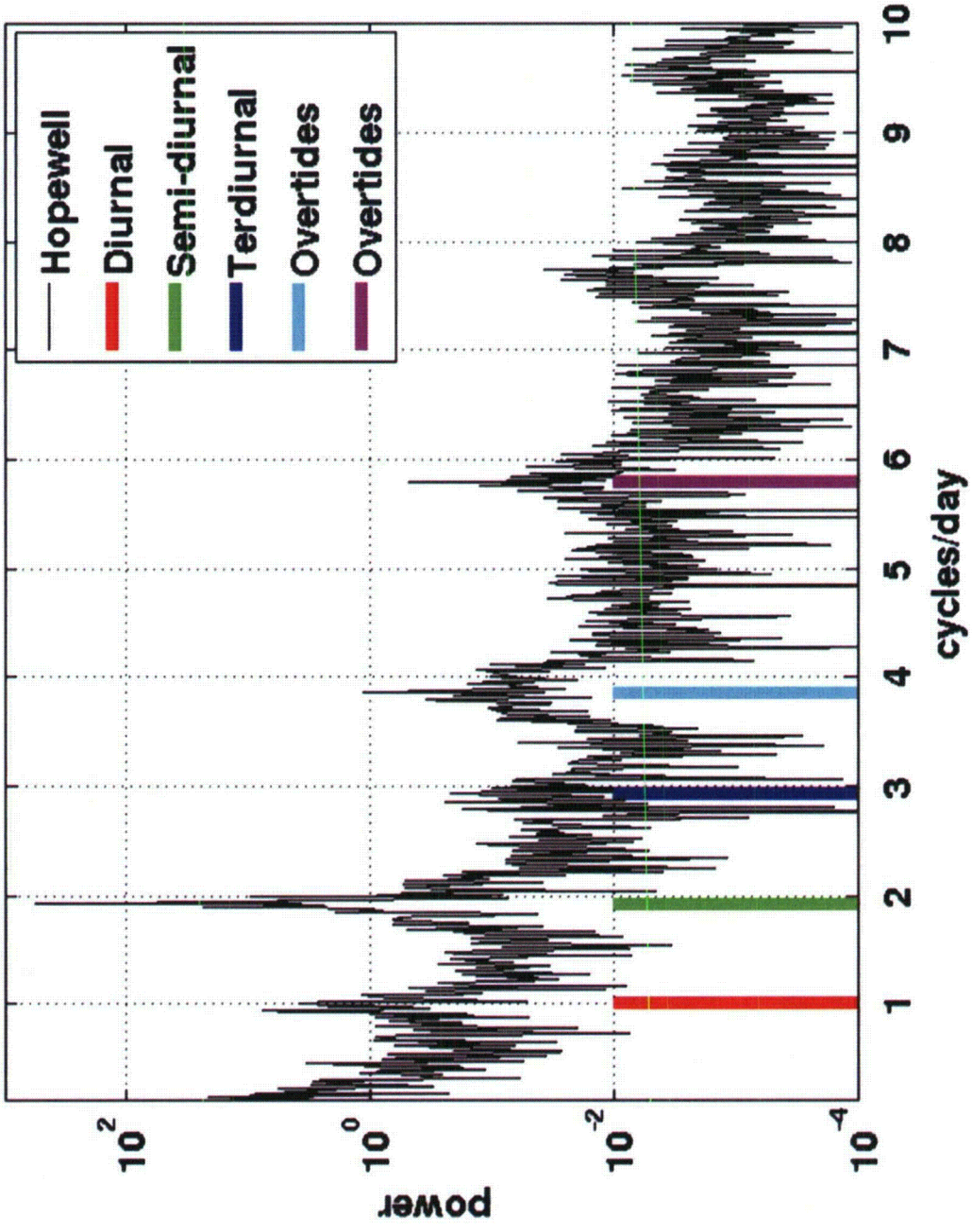

Figure 2.5-5: Spectral analysis of surface height time series at Kingsmill on the James River. The y-axis has units of spectral power in this case proportional to meters squared. The x-axis has units of frequency in days or cycles per day.

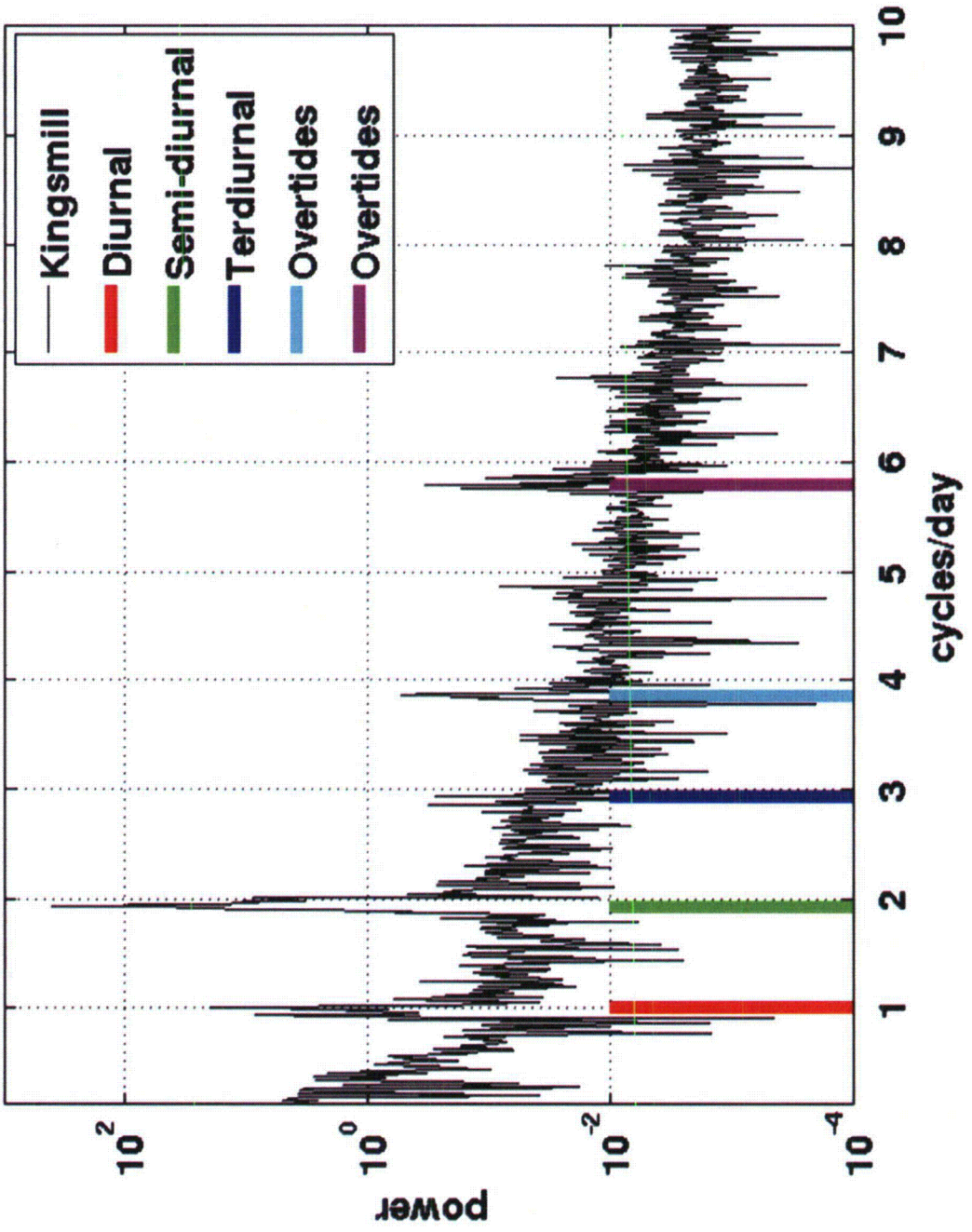

Figure 2.5-6: Spectral analysis of surface height time series at Sewell on the James River. The y-axis has units of spectral power in this case proportional to meters squared. The x-axis has units of frequency in days or cycles per day.

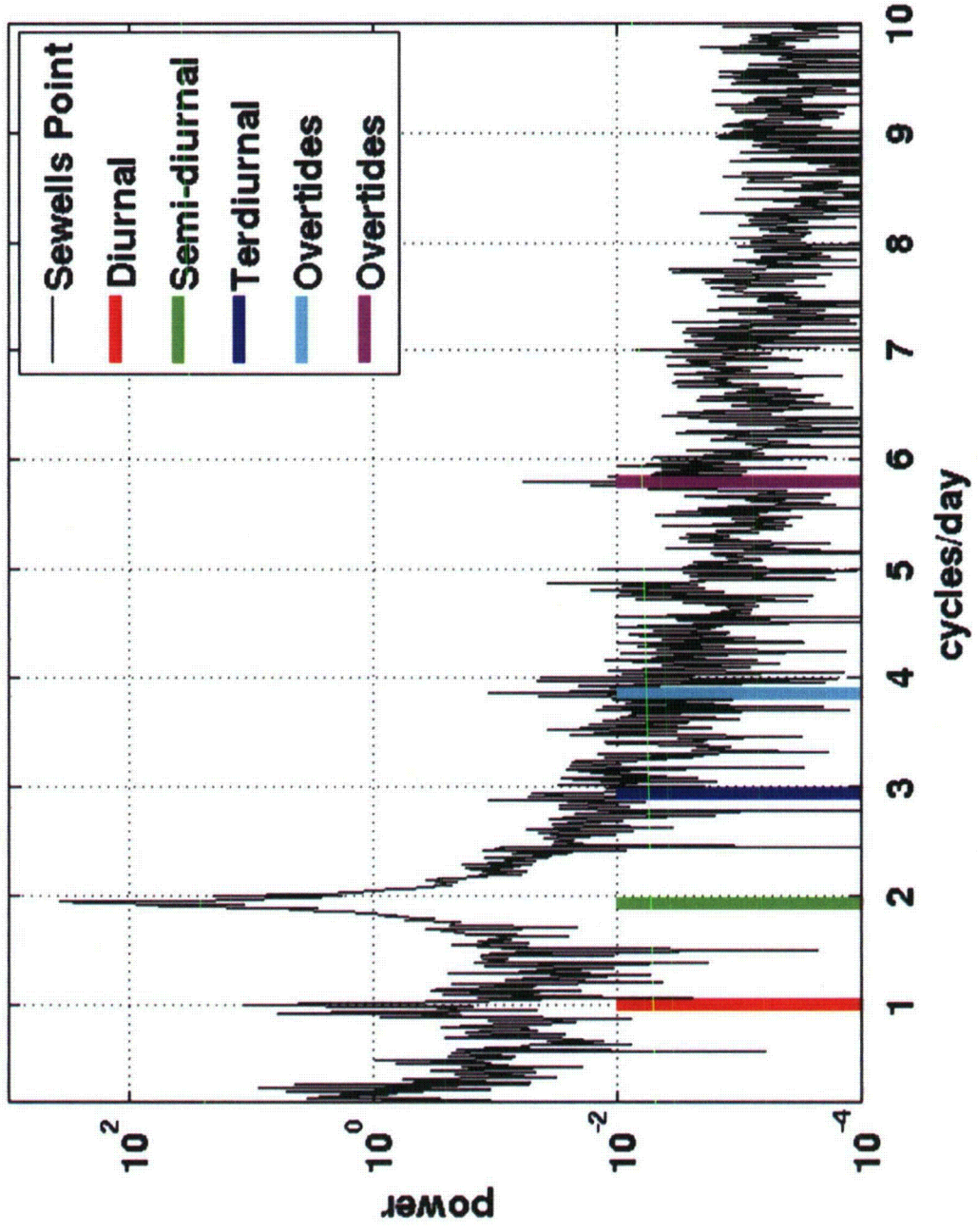

Figure 2.5-7: Spectral analysis of surface height time series at Tettington on the James River. The y-axis has units of spectral power in this case proportional to meters squared. The x-axis has units of frequency in days or cycles per day.

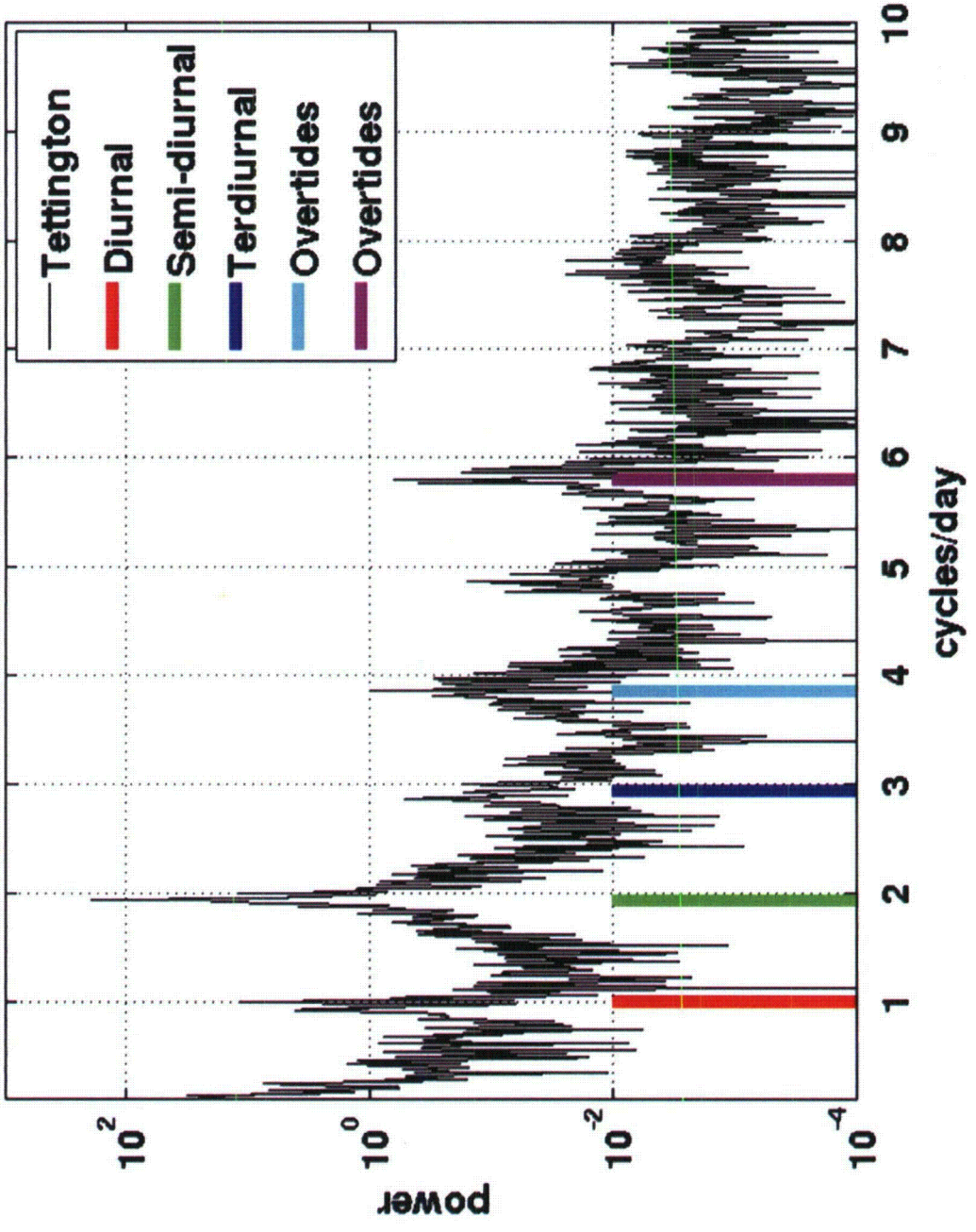

Figure 2.5-8: Observed responses to a storm surge event on November 12, 2009 in the James River at the NOAA Sewell's Point water level station.

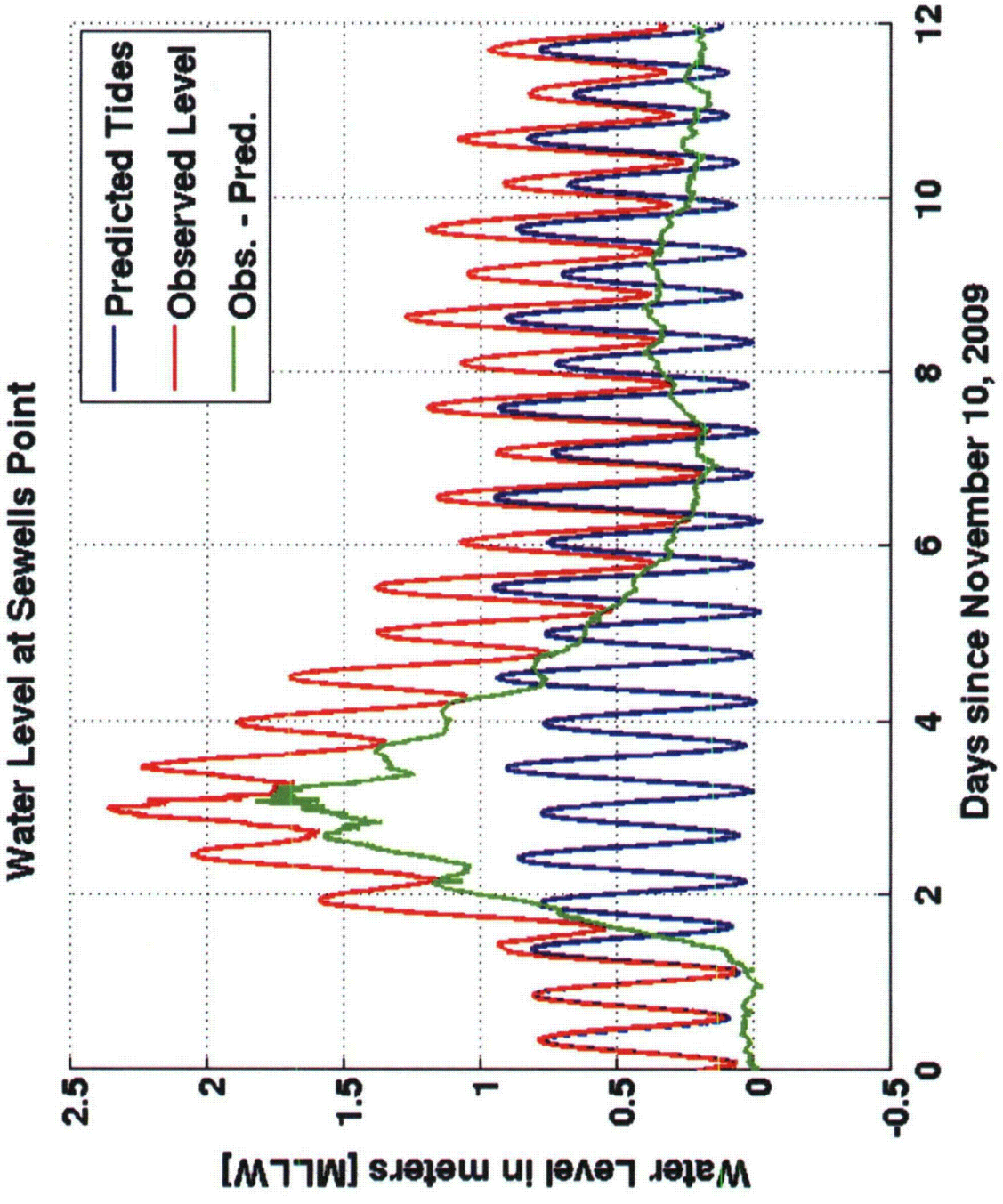

Figure 2.5-9: Observed responses to a storm surge event on November 12, 2009 in the James River at the NOAA Tettington water level station.

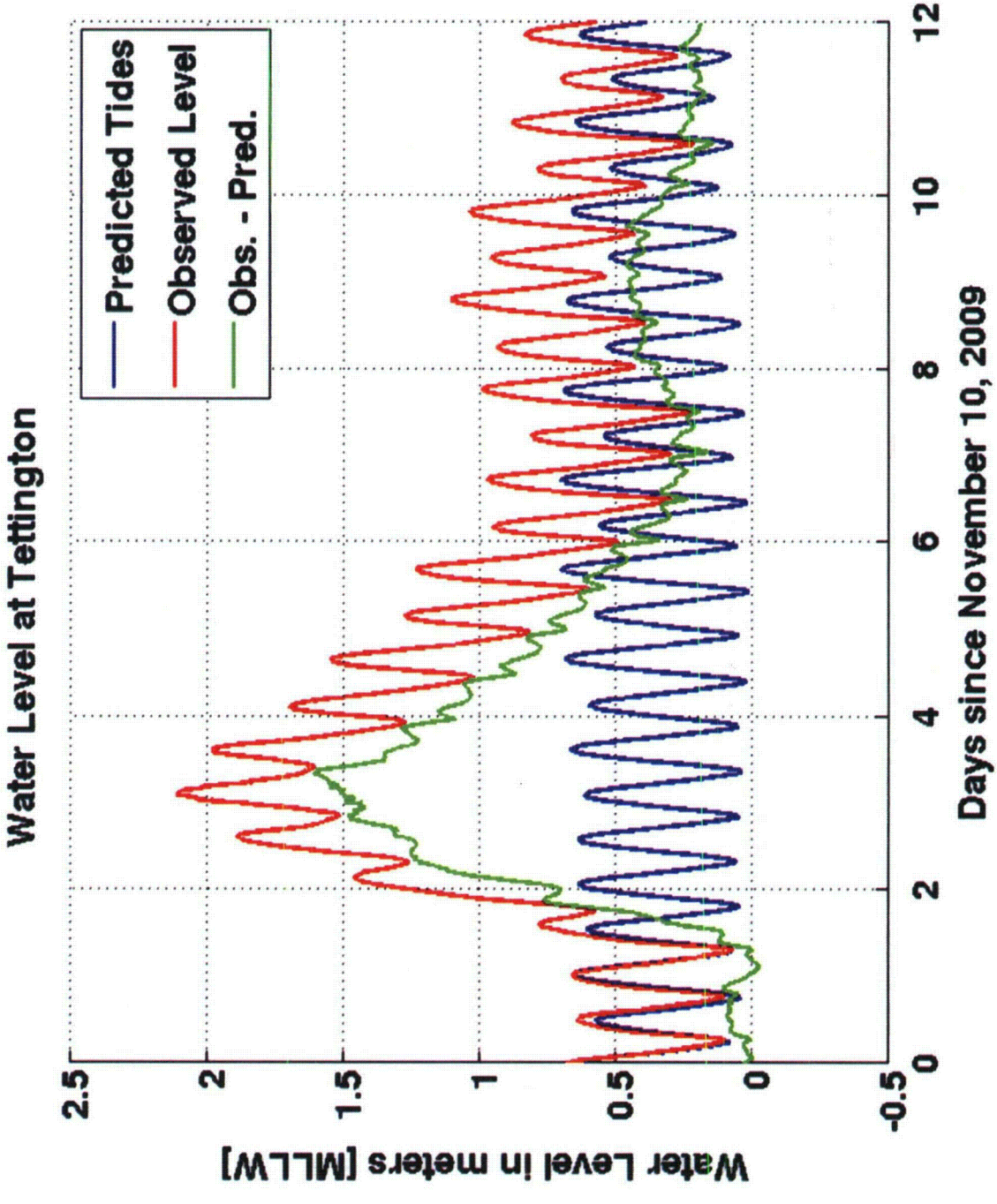

Figure 2.5-10: Observed responses to a storm surge event on November 12, 2009 in the James River at the NOAA Richmond Locks water level station.

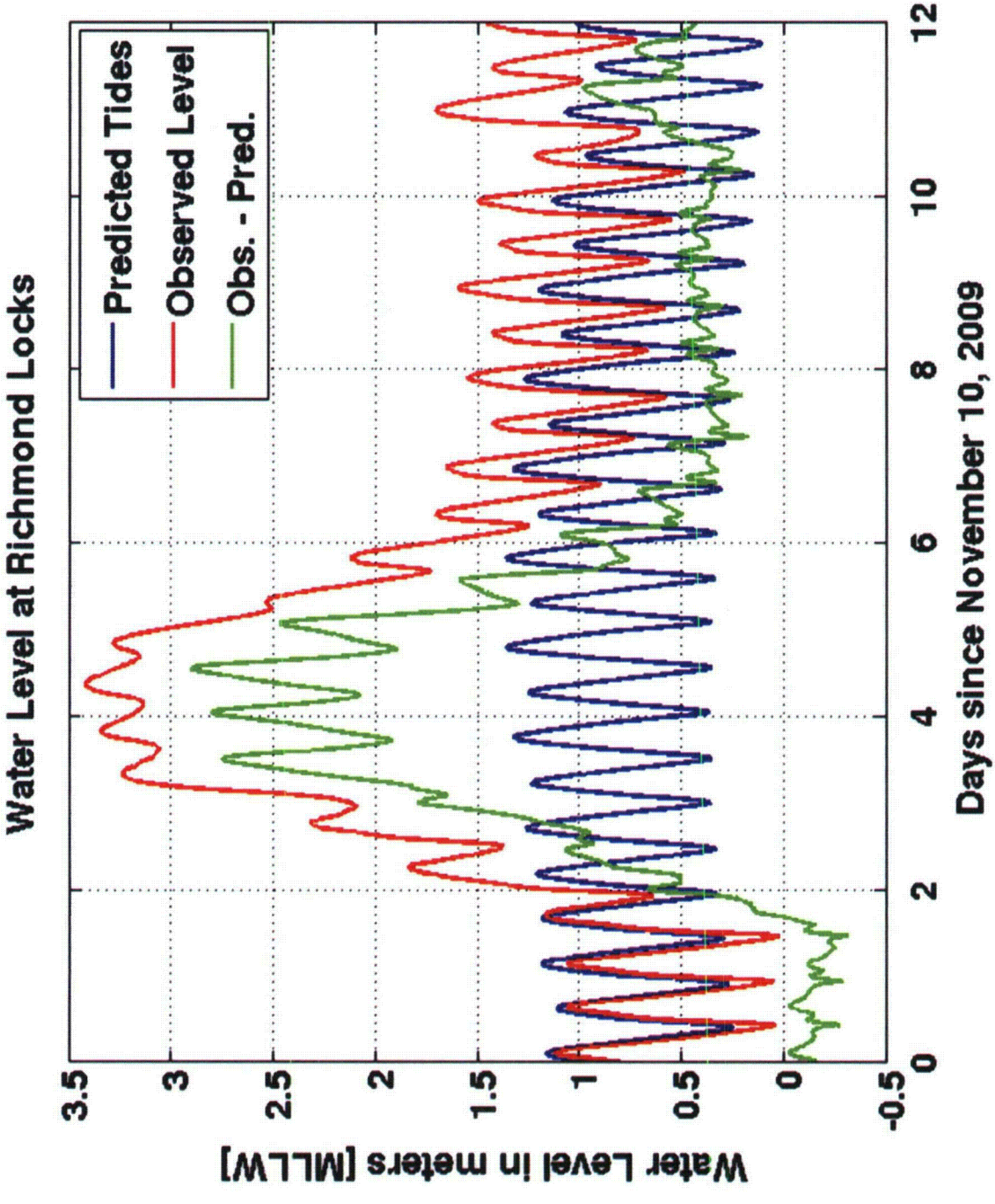

Figure 2.5-11: Idealized diagram of damped oscillations showing characteristic critically damped, under-damped and over damped examples.

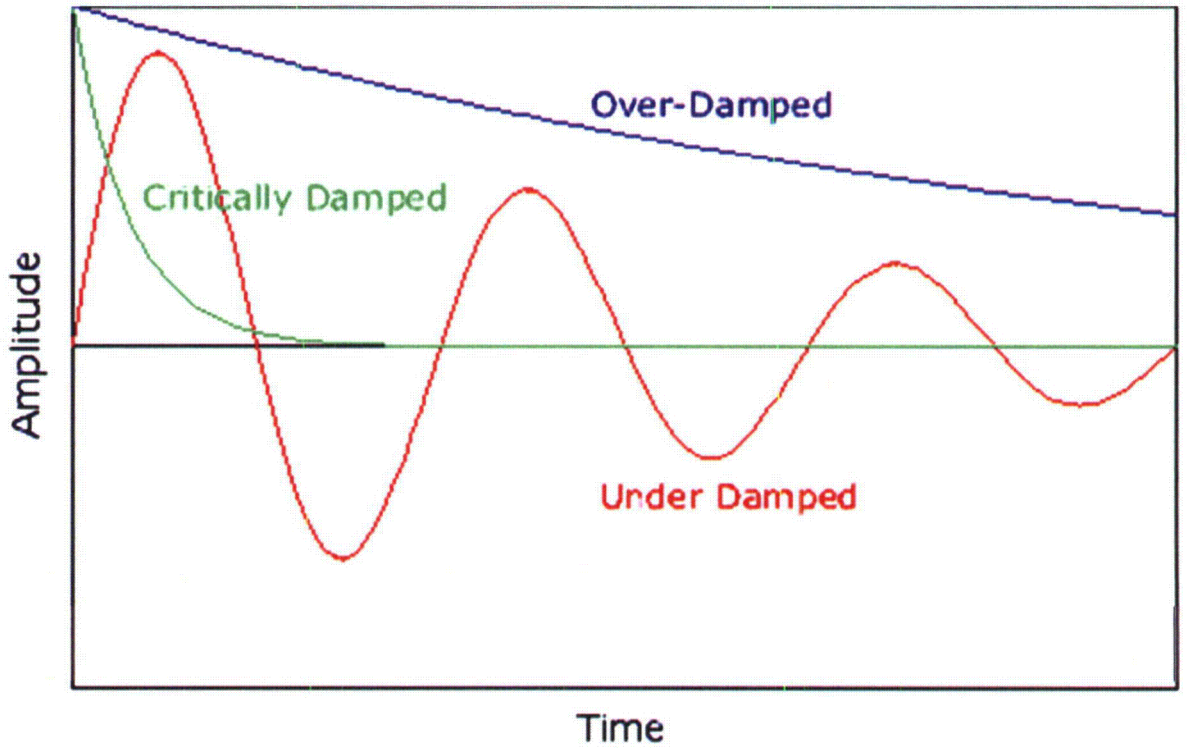

Note: 1. Over-damped: The system returns (exponentially decays) to equilibrium without oscillating.

2. Critically damped: The system returns to equilibrium as quickly as possible without oscillating.

3. Under-damped: The system oscillates (at reduced frequency compared to the undamped case) with the amplitude gradually decreasing to zero

2.6. Tsunami

This section evaluates the Probable Maximum Tsunami (PMT) at SPS. Due to its location (about 50 miles from the coast), direct inundation of SPS from coastal tsunami runup will not occur. However, given its location on a tidal river which is connected to the ocean, SPS could potentially experience bores induced by a coastal tsunami propagating up the James River; therefore, evaluation of both the coastal tsunami hazard and impact to SPS (located up river) are performed.

2.6.1. Method

In accordance with the guidelines presented in NUREG/CR-6966 (NRC, 2009), a hierarchical assessment approach is used to evaluate the tsunami hazard. Relative to tsunami hazards, the hierarchical hazard assessment approach (HHA) consists of the following steps:

1. A Regional Screening Test involving an evaluation of the regional hazard based on a review of the historical record and the best available scientific data (NGDC, 2012). Review of published first-order modeling performed for the National Oceanic and Atmospheric Administration (NOAA), as part of the National Tsunami Hazard Mitigation Program (NTHMP; http://nthmp.tsunami.gov/index.html), and others, for the United States (U.S.) East Coast.

2. A Site Screening Test to compare the location and elevation of the plant site with the areas affected by tsunamis in the region. This screening test considers the local site characteristics of ground elevation (the plant grade relative to the water surface elevation) and the distance of the plant from the shoreline.

3. A Detailed Tsunami Hazard Assessment is performed if the screening tests do not conservatively establish the safety of the plant. A detailed, site-specific tsunami hazard assessment typically involves identification and modeling of applicable (near-field and far-field) tsunamigenic sources, numerical modeling of wave propagation from the tsunamigenic source to the near shore and numerical inundation modeling of the plant site and vicinity.

The completion of a site screening test, required as a next step by the hierarchal hazard assessment (HHA) approach presented in NUREG/CR-6966 (NRC, 2009), was precluded by the complex geography of the region, particularly the site location on the James River and the possible dynamic effects of tidal currents in enhancing tsunami flooding at the site. Therefore, a modeling approach that incorporates the complex geographic features of the region as well as the dynamic tide effects was used. The methodology includes the following steps:

1. Definition of the antecedent water levels in the vicinity of SPS—the 10-percent exceedance high tide (e.g., high tide level that is equaled or exceeded by 10 percent of the maximum monthly tides over a continuous period).

2. Parameterization of the 3 far-field and 1 near-field tsunami sources.

3. Simulation of tsunami generation and propagation through relatively coarse computational nested grids ranging from 1 arc-minute spherical grid (in deep water) to 20 arc-second resolution (about 600 meter). Simulations of the tsunamigenic sources

were performed using a combination of the Fully Nonlinear Boussinesq Wave Model with TVD Solver (FUNWAVE-TVD) and the Non-Hydrostatic Wave Model (NHWAVE) computer models.

4. Simulation and calibration of the regional tidal forcing on the 154 meter resolution Cartesian grid. This simulation is forced by time series of the tide elevation and current obtained from a separate regional tidal database, OSU Regional Tidal Solution for the East Coast of America (Egbert et al., 1994 and Egbert et al., 2002).

5. Combined tsunami and tide simulations in a series of nested grids ranging from 154 meter to 10 meter resolution for the immediate vicinity of SPS. Simulations were conducted for different phases of the tide to identify the worst case flooding scenario at SPS.

6. Generation of maps and time-series graphs describing tsunami impacts at SPS.

7. Estimation of drawdown due to each tsunamigenic source.

Computational modeling of tsunamis was performed by subject matter expert, Dr. Stéphan Grilli, PhD, P.E. of the University of Rhode Island.

2.6.2. Results

2.6.2.1. Screening

The results of the SPS regional tsunami screening test indicate a region of potential tsunami hazard near SPS. The screening test identifies four sources with the potential to cause significant tsunamis in the region, which include:

1. An extreme co-seismic tsunami (M9.0) generated in the Caribbean Subduction Zone (Puerto Rican Trench).
2. An extreme co-seismic tsunami (M9.0) generated within the Azores-Gibraltar Convergence Zone similar to the 1755 Lisbon earthquake.
3. A subaerial landslide representing an extreme flank failure (450 km^3) at the Cumbre Vieja Volcano in the Canary Islands.
4. A near-field extreme submarine mass failure similar to the Currituck historical case, which is used as a proxy for the largest possible submarine mass failure (SMF) in the area. The Currituck event was a translational landslide that occurred along the continental margin off the coast of Virginia and North Carolina between 22,500 and 43,300 years ago (Grilli et al., 2011). It is considered to be one of the largest submarine landslides to have occurred off the U.S. East coast.

For the re-evaluation, parameters for these four sources have been updated based on the most recent tsunami inundation modeling along the U.S. East Coast done for the National Tsunami Hazard Mitigation Program (NTHMP), which is summarized as follows:

1. Puerto Rican Trench (PRT) M9 co-seismic source: As part of recent NTHMP work, several PRT parameters were revised slightly, including the number and locations of sub-sources and the earthquake magnitude (from M8.9 to M9) (Grilli et al, 2013a).

2. Lisbon M9 co-seismic source: The Lisbon source was reanalyzed in recent NTHMP analysis (Grilli et al, 2013b). Because there is considerable uncertainty in the parameters of this historical source (particularly the strike angle), the NTHMP analysis modeled a number of possible sources to determine worst case impacts along the upper U.S. East Coast. In total, 16 different scenarios at different strike angles all with a M9 magnitude were simulated. The scenario with the worst case impact for the upper U.S. East Coast was identified in the NTHMP and used as the "worst case" scenario herein.

3. Cumbre Vieja Volcano (CVV) 450 km^3 subaerial landslide source: For this analysis the results of the detailed three-dimensional (3D) modeling work (Abadie et al., 2012) are used to specify the tsunami source. As part of recent NTHMP analysis, detailed inundation modeling from this source was performed for selected areas of the U.S. East Coast (Grilli et al., 2013c). The closest reference station to SPS is located offshore of Delaware. This station experiences the highest tsunami surface elevation of all locations, the same source propagation methodology is used herein.

4. Currituck SMF proxy: A detailed analysis of the historical Currituck submarine landslide, in combination with recent geotechnical and geological analyses (some performed as a collaboration between the University of Rhode Island (URI) and the United States Geological Survey [USGS]) has been used to parameterize and model the event. The analysis includes a reconstruction of the geometry and kinematics of the slide and simulation of the resulting tsunami generation (Grilli et al., 2013d).

2.6.2.2. Antecedent Water Level

In accordance with ANSI/ANS-2.8-1992 (ANSI, 1992), this tide can be determined from recorded tide data or from predicted astronomical tide tables. The full period of record (1927-2014) of verified monthly water levels (in feet NAVD88) was obtained from the from NOAA Station 8639610 at Sewells Point, VA (NOAA, 2014a). The monthly high tide data was sorted and ranked, and the Weibull plotting position was used to calculate the exceedance probability for each high tide value in the table. The Weibull plotting position equation was applied as follows:

$$Pe = 100\left(\frac{m}{(n+1)}\right)$$

where:

Pe = the probability of exceedance

m = rank

n = total number of monthly high tide values

The 10 percent exceedance high tide was calculated to be 3.1 feet NAVD88. The updated mean sea level trend at the Chesapeake Bay Bridge Tunnel, Virginia is 5.96 millimeters per

year (NOAA, 2014b). This gives an expected 50-year sea level rise rate of 0.98 feet. The resultant 10% exceedance high tide was determined to be elevation 4.1 feet NAVD88.

2.6.2.3. Determination of Tidal Forcing

The James River has significant tidal forcing, use of maximum static water elevations for tsunami simulations is not sufficient to properly characterize the PMT at the site. Simulations have shown potential amplification of the tsunami waves directly after the high tide and indicated that the tsunami waves propagated further on a rising tide in the lower portion of the river and at the maximum high tide further upstream (Tolkova, 2012).

The dominant tidal constituent at Sewells Point, VA (NOAA Station 8638610) is the M2 (semi-diurnal) tide, which is nearly five times greater than the next two constituents (N2 and S2). Therefore, the M2 tide was considered representative of the general tidal conditions in the region. The OSU Regional Tidal Solution for the East Coast of America (Egbert et al., 1994 and Egbert et al., 2002) was used to obtain the M2 constituent for all boundary points within the 154 meter resolution computer model grid.

2.6.2.4. Tsunami Source Parameters

Far-Field Co-Seismic Tsunami - Puerto Rican Trench M9

The Caribbean subduction zone is a source of large earthquakes that could potentially cause an extreme tsunami impacting the U.S. East Coast and thus the SPS site. As analyzed by ten Brink et al. (ten Brink et al., 2008), the largest hazard from the area would be an earthquake that ruptures the entire subduction zone north of Puerto Rico (i.e., the PRT) resulting in the maximum slip possible, approximately 10 meters for a M9 magnitude event.

NOAA has catalogued and parameterized M7.5 subfaults for all major subduction zones in the Short-term Inundation Forecast for Tsunamis (SIFT) database (Gica et al., 2008). For this study, an extreme M9 co-seismic source from the PRT is defined using a combination of 12 NOAA SIFT M7.5 unit sources. To account for the greater magnitude (M9), assuming a moderately shallow rupture and a shear modulus equal to 45 GPa (for subducting material), a slip of 14.8 meters is defined for each of the sub-faults. This approach to parameterizing the PRT source is similar to recent modeling carried out as a part of the NTHMP (Grilli et al., 2013a).

The Okada method is an analytical solution for a semi-infinite homogeneous medium (the seafloor) with a dislocation specified along an oblique plane. The maximum seafloor deformation predicted by this solution was specified as a hot start on the free surface (due to the near incompressibility of water and small rise time). The initial water velocity was set to zero for initializing the simulation of this source. The resulting initial sea surface amplitude used for modeling ranges from about -20 feet to +26 feet. This source was re-interpolated in the 1 arc-minute grid and used to perform basin scale propagation simulations with FUNWAVE-TVD as described in Section 2.6.2.5.

Far-Field Co-Seismic Tsunami – Lisbon M9

The Azores-Gibraltar plate boundary (a.k.a., Azores convergence zone) is another possible source of earthquakes that could cause an extreme tsunami impacting the U.S. East Coast.

There are numerous potentially active faults within the convergence zone, including the Gorringe Bank Fault, the Marque de Pombal Fault, the St. Vincente Fault, and the Horseshoe fault. It is not clear which faults are presently active in the region; however, these faults, collectively, are considered to be the source of some of the largest historical earthquakes and tsunamis in the Atlantic Ocean, including the M8.5-8.9 1755 Great Lisbon Earthquake and tsunami (Grilli et al., 2011).

The Lisbon Earthquake was reanalyzed in the recent NTHMP work (Grilli et al., 2013b) because of uncertainty in the source parameters, particularly the strike angle. To determine the worst case impact for the upper U.S. East Coast, 16 scenarios were simulated at different strike angles, each having a M9 magnitude. The scenario with the maximum impacts for the upper U.S. East Coast was selected as the source for this evaluation and is known as "Source Area 1, Case 5" in the NTHMP work. Source Area 1 is located in the region west of the Madeira Tore Rise (Figure 2.6-1). It has a 15 degree strike angle and a 20 meter slip, with a depth of 5 kilometers, length of 317 kilometers, width of 126 kilometers, dip of 40 degrees, and a rake of 90 degrees (Grilli et al., 2013b).

The initial sea surface elevation ranges from -7 feet (-2 meters) to +33 feet (+10 meter) using Okada's method. This source was re-interpolated in the 1 arc-minute grid and used to perform basin-scale propagation simulations with FUNWAVE-TVD as described in Section 2.6.2.5.

Far-Field Subaerial Landslide - Cumbre Vieja Volcano

A complete flank collapse of the Cumbre Vieja Volcano (CVV) on La Palma, in the Canary Islands (Figure 2.6-2), is another potential source of an extreme tsunami that could impact the U.S. East Coast. The tsunami source corresponding to the extreme flank collapse of the CVV considered by Abadie et al. 2012 as their worst case (a 450 km^3 volume) was used to initialize FUNWAVE-TVD. The initial surface elevation and current velocities for this source were computed by Abadie et al. 2012. After filtering and depth integration, these results were specified in FUNWAVE-TVD to simulate propagation across the Atlantic Ocean.

Propagation was performed initially in the region around La Palma using a 500 meter Cartesian grid (Grilli et al., 2013c). At about 20 minutes after initiation, waves are directed toward the west-northwest (i.e. towards the upper U.S. East Coast) and have amplitudes ranging from -50 meters to +50 meters (-164 feet to +164 feet). This source was re-interpolated in the 1 arc-minute grid and used to perform basin scale propagation simulations with FUNWAVE-TVD as described in Section 2.6.2.5.

Near-Field Submarine Mass Failure

When large SMFs occur on or near the continental shelf break, they have the potential to generate significant near-field tsunamis. Although only a few historical landslide tsunamis have been clearly identified in the region, simulations performed for the NTHMP indicate that SMFs may govern the tsunami hazard along much of the U.S. East Coast (Grilli et al., 2013d).

The most notable submarine landslide complex along the continental margin adjacent to the U.S. East Coast is known as the Currituck landslide. It is considered the largest SMF known to have occurred along the U.S. East Coast. These large tsunami waves correspond to an area directly west of the Currituck failure (Figure 2.6-3). The landslide occurred about 100 km off of the coast of Virginia and North Carolina between 22,500 and 43,300 years ago (Grilli et al.,

2011 and Locat et al., 2009). It was likely a single event caused by an earthquake, although two separate large failures that likely failed in sequence were identified. The SMF down-slope length was about 30 kilometers, the width about 20 kilometers, and the maximum thickness varied between 250-750 meters (ten Brink et al., 2008). The NTHMP work parameterized a SMF Currituck proxy (Grilli et al., 2013d). The parameters used are summarized in Table 2.6-1. The SMF is assumed to have a Gaussian shape and a total volume of about 135 cubic kilometers.

2.6.2.5. Model Inputs

FUNWAVE-TVD is a fully nonlinear and dispersive Boussinesq long wave model used to propagate tsunami waves and quantify inundation and drawdown. The governing equations in FUNWAVE-TVD are discretized on a regular grid, either spherical or Cartesian. A nested gridding scheme is implemented to allow for higher spatial resolution of the model near the tsunami sources and the coastline(s) being studied. The gridding scheme is based on a one-way coupling method, which works by computing time series of free surface elevation and currents in the coarser grid, for a large number of numerical gauges (stations) defined along the boundary of the finer grid. Computations in the finer nested grid are then performed using these time series as boundary conditions. Two formulations of equations in different coordinate systems are used in FUNWAVE-TVD – one in spherical coordinates, which includes Coriolis effects, but is only weakly nonlinear in its current implementation (Kirby et al., 2013); the other in Cartesian coordinates, which is fully nonlinear, but is only valid for smaller, local or regional grids due to the earth curvature (Shi et al., 2012). The first coordinate system is used for early stages of long-distance propagation of a potential tsunami over oceanic scales, and the latter is used for calculating regional propagation and coastal impact.

Each source, with the exception of the SMF, was initialized on a 1 arc-minute spherical grid. Given the close proximity of the source event to SPS, the SMF source was initialized on a higher resolution 20 arc-second grid (approximately 600 meters). A series of increasingly higher-resolution grids are nested within FUNWAVE-TVD to transition from the full model extent to areas of very fine resolution (approximately 10 meter by 10 meter grid) near SPS. The gridding approach used by FUNWAVE-TVD generally increases resolution from one grid to the next by a factor of 3 to 4; this is as a typical range that has been found in earlier work to ensure good accuracy and convergence of the nested simulations (Grilli et al., 2013a; Grilli et al., 2013b; Grilli et al., 2013c and Grilli et al., 2013d).

NHWAVE is a three-dimensional non-hydrostatic wave model and is used to compute tsunami generation from the near-field (SMF) source. The geometry and kinematics of the SMF are modeled and specified as bottom boundary conditions in the model. NHWAVE solves Euler equations in a "sigma-layer" 3D discretization. Results are reported at 12 NOAA water level stations in the region of the SPS (Table 2.6-2; also see Figure 2.6-4).

The far-field sources were modeled with FUNWAVE-TVD using coarse resolution 1 arc-minute and 20 arc-second spherical nested grids. Computations were then performed in a series of nested Cartesian grids (154 meter, 39 meter and 10 meter), in combination with tidal forcing, as the tsunami approached the area of interest and the SPS site.

The near-field (SMF) source was modeled with NHWAVE, the simulations were carried out in a Cartesian grid with 500 meter horizontal resolution. For consistency with the far-field source simulations, the resulting surface elevation and water velocity fields were then interpolated onto

the 20 arc-second resolution FUNWAVE-TVD grids. Computations were performed in three levels of nested Cartesian grids (154 meter, 39 meter and 10 meter), in combination with tidal forcing. Tables 2.6-3, 2.6-4 and 2.6-5 describe the grid dimensions and stations used as boundary conditions for each of the model grids.

Bathymetry and topography were interpolated in each model grid from a variety of sources, including:

1. NOAA's 1 arc-minute resolution ETOPO1 database (obtained from gravitational anomaly and reconciled with coastal relief models in shallower water) (Amante and Eakins, 2009).

2. The 3 arc-second (approximately 90 meter) resolution NGDC Coastal Relief Model (CRM), which extends in the northeast from the coastal zone to the continental shelf (NOAA, 2013).

3. The 1/3 arc-second (approximately 10 meter) resolution NTHMP Virginia Beach DEM (Taylor et al., 2008) combined with 1/3 arc-second (approximately 10 meter) resolution FEMA Region III Coastal Storm Surge DEM (Forte et al., 2011).

The fine-grid simulations were performed using both tidal and tsunami forcing, linearly superimposed along the boundary of the 154 meter grid. These simulations account for both the change in water level cause by the tide and the nonlinear dynamic effects of tidal currents in potentially enhancing tsunami flooding at the site. Prior to performing the combined tide-tsunami simulations, computations were performed using only tidal forcing on the 154 meter resolution grid (see Table 2.6-4). The purpose of these computations was to: 1) verify that FUNWAVE-TVD was accurately simulating the dominant tidal component (M2) in the Chesapeake Bay and the James River; and 2) calibrate the M2 tidal forcing to reproduce the antecedent water level at NOAA Sewells Point station.

This calibrated tidal forcing was combined with the incident tsunami time-series for each of the four sources using linear superposition of both surface elevation and current along the boundary of the 154 meter grid. Combined tide/tsunami simulations were then performed on the three fine scale grids (154 meter, 39 meter, and 10 meter). For these combined simulations, the phase of the tide was varied to maximize flooding at the SPS site.

Bottom friction and breaking dissipation in incident wave trains are also important in the higher resolution (near shore) grids. In all model grids a bottom friction coefficient for coarse sand of 0.0025, was used; this is conservative since friction is typically larger near shore and onshore. Wave breaking is modeled in FUNWAVE-TVD by using a breaking criterion (set to surface elevation equal to 0.8 times the local depth in this case) to detect areas of breaking events and then disabling dispersive terms in these areas (Shi et al., 2012). The threshold for wetting/drying of model grid cells was set to 1 centimeter.

To identify phases of the tide that could cause worst case inundation at SPS, the following scenarios were considered:

1. Synchronizing the maximum tidal elevation with arrival of maximum tsunami waves at the SPS site, thus causing maximum elevation by way of superposition (referred to as Case TT1). The maximum leading elevation of the tsunami wave was synchronized with the maximum tide at the southeast corner of the 154 meter grid.

2. Synchronizing large ebb currents in the James River near the SPS site (with arrival of the maximum tsunami waves, thus creating the potential for shoaling of the incoming tsunami wave (referred to as Case TT2). The incoming tsunamis was synchronized with the peak ebb currents at mid-tide along the boundary of the 154 meter grid.

2.6.2.6. Model Simulations for Tide Plus Tsunami

Results of the detailed tsunami modeling calculation at SPS are summarized below. Results for Case TT1 are presented for each of the four sources. Results for Case TT2 are presented for the two tsunami sources that produce the worst case inundation at the SPS site under Case TT1 conditions (CVV and the Currituck SMF) to examine whether this process might result in greater inundation at the SPS site. For each tsunami source, the initial propagation of the wave and the overall features of the generated tsunami at or near the shelf break are discussed in terms of surface amplitudes and wavelength of the leading wave. Detailed modeling results, such as runup and inundation at SPS, are presented for the finest (10 meter resolution) grid. In some cases, predictions of inundation from coarser grids are presented to confirm the relevance and accuracy of simulations. Inundation levels in the figures are presented in meters above elevation 0.586 meters NAVD88 (the MHW at Sewells Point and the SLR component of the high antecedent water level). The results are also translated into NAVD88 and the plant datum of MSL.

For each source event, maps of the maximum inundation (runup) levels resulting from FUNWAVE-TVD simulations were calculated. In addition, time series of water surface elevations were output from each model run at various stations in the vicinity of SPS (Figure 2.6-4 and Table 2.6-2).

Far-field subaerial landslide (Cumbre Vieja Volcano 450 km^3) plus Tide (Case TT1):

Figure 2.6-5 shows the tide plus tsunami elevation computed at Station 3 (NOAA Station 8638421, Burwell Bay, VA) and Station 4 (NOAA Station 8638424, Kingsmill, VA) and the "SPS River Station" located just east of the site in the middle of the James River, in the 10 meter grid. The leading tsunami and tide elevations are almost synchronized. However, higher surface elevations are obtained for later times, likely due to an enhancement of smaller incident tsunami waves by ebbing tidal currents.

The maximum surface elevation is approximately 7 to 7.2 feet MSL (5.54 to 5.71 feet NAVD88), near the SPS Protected Area and SPS Low Level Intake are also shown in Figure 2.6-6 and Figure 2.6-7. The tsunami resulting from an extreme flank failure of the CVV requires approximately 8 hours to travel across the Atlantic Ocean to the continental shelf break and approximately 6.5 additional hours to travel from the shelf break to SPS site.

Far-field co-Seismic Tsunami - Puerto Rican Trench plus Tide (Case TT1):

Figure 2.6-8 shows a comparison of surface elevations computed at Station 3 (NOAA Station 8638421, Burwell Bay, VA) and Station 4 (NOAA Station 8638424, Kingsmill, VA) and the "SPS River Station" located just east of the site in the middle of the James River. At the "SPS river station" location, the water surface elevation reaches 1.39 meters (4.56 feet) NAVD88.

The maximum surface elevations in the vicinity of the SPS Protected Area and SPS Low Level Intake are also shown in Figure 2.6-6 and Figure 2.6-7and range from elevations 6.0 to 6.1 feet MSL (4.53 to 4.7 feet NAVD88). The travel time to the site is 7.3 hours

Far-field co-Seismic Tsunami-Lisbon plus tide (Case TT1):

Figure 2.6-9 shows a comparison of surface elevations computed at Station 3 (NOAA Station 8638421, Burwell Bay, VA), Station 4 (NOAA Station 8638424, Kingsmill, VA) and the "SPS river station", located just east of the site. At the "SPS river station" location, the elevation reaches approximately elevation 5.8 feet MSL (1.34 meters (4.40 feet) NAVD88).

The maximum surface elevations in the vicinity of the SPS Protected Area and SPS Low Level Intake are also shown in Figure 2.6-10 and Figure 2.6-11. The elevation reaches approximately elevation 5.9 to 6.1 feet MSL (4.5 to 4.7 feet NAVD88) near the SPS site. The travel time to the site is 11.5 hours.

Near-Field Submarine Mass Failure plus tide (Case TT1):

Figure 2.6-12 shows a comparison of surface elevations computed at Station 3 (NOAA Station 8638421, Burwell Bay, VA) and Station 4 (NOAA Station 8638424, Kingsmill, VA) and at the "SPS river station", located just east of the site.

The maximum water surface elevation reaches 6.4 to 6.5 feet MSL (4.99 to 5.02 feet NAVD88) in the vicinity of the SPS Protected Area and SPS Low Level Intake. The maximum surface elevations in the vicinity of the plant are shown in Figure 2.6-13 and Figure 2.6-14. The tsunami inundation resulting from this SMF will take 4.5 hours to reach SPS

Far-field subaerial landslide (CVV) plus tide (Case TT2):

Figure 2.6-15 shows a comparison of surface elevations computed at Station 3 (NOAA Station 8638421, Burwell Bay, VA) and Station 4 (NOAA Station 8638424, Kingsmill, VA) and the "SPS river station", located just east of the site.

The maximum water surface elevation reaches 5.8 to 6.2 feet MSL (4.37 to 4.76 feet NAVD88) in the vicinity of the SPS Protected Area and SPS Low Level Intake. The maximum surface elevations in the vicinity of the plant are shown Figure 2.6-16 and Figure 2.6-17.

Near-Field Submarine Mass Failure plus tide (CaseTT2):

Figure 2.6-18 shows a comparison of surface elevations computed at Station 3 (NOAA Station 8638421, Burwell Bay, VA) and Station 4 (NOAA Station 8638424, Kingsmill, VA) and the "SPS river station", located just east of the site.

The maximum water surface elevation reaches 5.8 to 6.2 feet MSL (4.37 to 4.76 feet NAVD88) in the vicinity of the SPS Protected Area and SPS Low Level Intake. The maximum surface elevations in the vicinity of the plant are also shown in Figure 2.6-19 and Figure 2.6-20.

2.6.2.7. Low Water Drawdown Due to Tsunami

Estimates for drawdown during the four tsunami simulations at high tide were developed using the near-field time series results at output station 2, shown in Figure 2.6-4. Drawdown at Station 2 provides conservative estimates of drawdown at both the site and low level intake structure.

Drawdown from the four tsunamigenic sources coincident with the 90 percent low tide were estimated by subtracting the largest tsunami trough of each tsunamigenic source (negative amplitude from each high tide simulation at Sewells Point), from the 90 percent low tide. This method provides a conservative estimate for drawdown at SPS locations.

The 90 percent low tide is defined as the low tide level that is equal to or less than 90 percent of the minimum monthly tides over a continuous period (e.g., 10 percent of low tides are below this value). The 90 percent low tide is calculated by:

1. Statistical analysis of recorded tide data from the NOAA Sewells Point, VA (Station 8639610) using the Weibull plotting position equation.

The 90 percent low tide at Sewell's Point is -3.7 feet NAVD88. The maximum drawdown at low tide is a result of the SMF co-seismic source, resulting in a maximum drawdown of -0.4 meters (-1.3 feet) (see Figure 2.6-21) below the 90 percent low tide antecedent water level of -1.1 meters [-3.7 feet] NAVD88 at Sewells Point, which is equivalent to Elevation -3.6 feet MSL at SPS. Using the negative amplitude at Sewells Point is a conservative approach as the amplitude of the tsunami wave will be damped as it propagates up the James River towards SPS.

2.6.2.8. Tsunami-induced Seiche Potential

In a river basin such as the James River the periods are approximately 10 hours to 16 hours (see Section 2.5), which are beyond the typical tsunami periods calculated herein. The largest tsunami periods observed were approximately 1.4 hours (see Figures 2.6-5, 2.6-9, and 2.6-15).

Computer simulations for all tsunamigenic sources were performed for adequate durations (i.e. two tidal cycles) to capture (if any) tsunami induced seiche motion. The M2 tidal constituent is the principal lunar semidiurnal constituent, which consists of two high waters and two low waters a day (NOAA, 2000). Therefore, two tidal cycles indicates 48 hours of simulation time, which is an adequate duration to capture seiche motion. In a time domain simulation (FUNWAVE), if resonant conditions are present then the possible amplification of incident tsunami wave height that would occur would be evident in the time-series plots (Figures 2.6-5, 2.6-6, 2.6-8, 2.6-12, 2.6-15, and 2.6-18). The results for all tsunamigenic sources indicate that a seiche will not occur due to the PMT.

2.6.3. Conclusions

A detailed tsunami hazard assessment was conducted to identify applicable near-field and far-field tsunami sources and model wave propagation to the near shore and inundation at SPS. Four potential tsunamigenic sources were identified: (a) a M9 earthquake that ruptures the PRT, (b) a M9 earthquake occurring at the Azores-Gibraltar convergence zone, (c) an extreme flank collapse of the CVV, and (d) a SMF on the continental slope directly south of the site. A

summary of the results is presented in Table 2.6-6. Maximum water surface elevations near SPS are approximately 7.2 feet MSL.

2.6.4. References

2.6.4-1 Abadie et al, 2012. Abadie, S., J. C. Harris, S. T. Grilli, and R. Fabre. (2012). Numerical modeling of tsunami waves generated by the flank collapse of the Cumbre Vieja Volcano (La Palma, Canary Islands): tsunami source and near field effects. J. Geophys. Res., 117, C05030, doi:10.1029/2011JC007646.

2.6.4-2 Amante and Eakins, 2009. Amante, C. & Eakins, B.W. (2009). ETOPO1 1 arc-minute global relief model: Procedures, data sources, and analysis (19 p.). NOAA Technical Memorandum NESDIS NGDC-24.

2.6.4-3 ANSI, 1992. American National Standards Institute/American Nuclear Society. (1992). ANSI/ANS-2.8-1992: Determining Design Basis Flooding at Power Reactor Sites.

2.6.4-4 Forte et al., 2011. Forte, M., J. Hanson, L. Stillwell, M. Blanchard-Montgomery, B. Blanton, R. Luettich, H. Roberts, J. Atkinson, and J. Miller (2011). Coastal Storm Surge Analysis System Digital Elevation Model – Report 1: Intermediate Submission No. 1.1, ERDC/CHL TR-11-1, US Army Corps of Engineers Work Unit J64C87.

2.6.4-5 Egbert et al., 1994. Egbert, G. D., A. F. Bennett, and M. G. G. Foreman (1994), TOPEX/POSEIDON tides estimated using a global inverse model, J. Geophys. Res., 99(C12), 24821–24852

2.6.4-6 Egbert et al., 2002. Egbert, Gary D., Svetlana Y. Erofeeva, 2002: Efficient Inverse Modeling of Barotropic Ocean Tides. J. Atmos. Oceanic Technol., 19, 183–204.

2.6.4-7 Gica et al., 2008. Gica, E., Spillane, M. C., Titov, V. V., Chamberlin, C. D., and Newman, J. C. (2008). Development of the Forecast Propagation Database for NOAA's Short-Term Inundation Forecast for Tsunamis (SIFT), NOAA Technical Memorandum OAR PMEL-139.

2.6.4-8 Grilli et al., 2011. Grilli, S. T., Harris, J. C., & Tajalli Bakhsh, T. (2011). Literature review of tsunami sources affecting tsunami hazard along the U. S. East Coast. Center for Applied Coastal Research, University of Delaware.

2.6.4-9 Grilli et al., 2013a. Grilli A.R. and S.T. Grilli. (2013a). Modeling of tsunami generation, propagation and regional impact along the upper U.S east coast from the Puerto Rico Trench. Research Report no. CACR-13-02. NTHMP Award, #NA10NWS4670010, National Weather Service Program Office, 18 pps.

2.6.4-10 Grilli et al., 2013b. Grilli A.R. and S.T. Grilli (2013b). Modeling of tsunami generation, propagation and regional impact along the U.S. East Coast from the Azores Convergence Zone. Research Report no. CACR-13-04. NTHMP Award, #NA10NWS4670010, National Weather Service Program Office, 20 pps.

2.6.4-11 Grilli et al., 2013c. Grilli A.R. and S.T. Grilli. (2013c). Far-Field tsunami impact on the U.S. East Coast from an extreme flank collapse of the Cumbre Vieja Volcano (Canary Island). Research Report no. CACR-13-03. NTHMP Award, #NA10NWS4670010, National Weather Service Program Office, 13 pps.

2.6.4-12 Grilli et al., 2013d. Grilli, S.T., C. O'Reilly and T. Tajalli-Bakhsh. (2013). Modeling of SMF tsunami generation and regional impact along the upper U.S. East Coast. Research Report no. CACR-13-05. NTHMP Award, #NA10NWS4670010, National Weather Service Program Office, 46 pps.

2.6.4-13 Kirby et al., 2013. Kirby, J.T., Shi, F., Tehranirad, B., Harris, J.C. and Grilli, S.T. (2013). Dispersive tsunami waves in the ocean: Model equations and sensitivity to dispersion and Coriolis effects. Ocean Modeling, 62, 39-55, doi:10.1016/j.ocemod.2012.11.009.

2.6.4-14 Locat et al., 2009. Locat J., H. Lee, U. ten Brink, D. Twichell, E. Geist, and M. Sansoucy. (2009). Geomorphology, stability, and mobility of the Currituck slide. Marine Geology, 264, 28-40.

2.6.4-15 NGDC, 2012. NOAA National Geophysical Data Center. (n.d.). NOAA/WDC Tsunami Runup. Retrieved November 8, 2012, from NOAA National Geophysical Data Center (NGDC): http://www.ngdc.noaa.gov/nndc/struts/form?t=101650&s=167&d=166

2.6.4-16 NOAA, 2000. "Tide and Current Glossary", NOAA National Ocean Service, Silver Spring, MD, January 2000.

2.6.4-17 NOAA, 2013. NOAA National Geophysical Data Center, U.S. Coastal Relief Model, Retrieved September 2013, http://www.ngdc.noaa.gov/mgg/coastal/crm.html

2.6.4-18 NOAA, 2014a. Station 8638610, Sewells Point, VA. Retrieved March 1, 2014, from http://tidesandcurrents.noaa.gov/stationhome.html?id=8638610

2.6.4-19 NOAA, 2014b. Updated Mean Sea Level Trends 8638863 Chesapeake Bay Bridge Tunnel, Virginia, Retrieved March 1, 2014. http://tidesandcurrents.noaa.gov/sltrends/sltrends_update.shtml?stnid=8638863

2.6.4-20 NRC, 2009. U.S. Nuclear Regulatory Commission, NUREG/CR-6966: Tsunami Hazard Assessment at Nuclear Power Plant Sites in the United States of America. Richland, WA: Pacific Northwest National Laboratory, 2009.

2.6.4-21 Shi et al., 2012. Shi, F., J.T. Kirby, J.C. Harris, J.D. Geiman and S.T. Grilli. (2012). A High-Order Adaptive Time-Stepping TVD Solver for Boussinesq Modeling of Breaking Waves and Coastal Inundation. Ocean Modeling, 43-44, 36-5.

2.6.4-22 Taylor et al., 2008. Taylor, L.A., B.W. Eakins, K.S. Carignan, R.R. Warnken, T. Sazonova, D.C. Schoolcraft, and G.F. Sharman, 2008. Digital Elevation Model of Virginia Beach, Virginia: Procedures, Data Sources and Analysis, NOAA Technical Memorandum NESDIS NGDC-7, National Geophysical Data Center, Boulder, CO, 34 pp.

2.6.4-23 ten Brink et al., 2008. ten Brink, U. S., Twitchell, D., Geist, E., Chaytor, J., Locat, J., Lee, H., Buczkowski, B., Barkan, R., Solow, A., Andrews, B., Parsons, T., Lynett, P., Lin, J., and Sansoucy, M. (2008). Evaluation of tsunami sources with the potential to impact the U.S. Atlantic and Gulf Coasts. Report to the Nuclear Regulatory Commission. USGS. 322 pp.

2.6.4-24 Tolkova, E. 2012. Tide-tsunami interaction on Columbia River, as implied by historical data and numerical simulations. Pure Applied Geophysics, 170(6-8), 115-1126.

Table 2.6-1: Parameters of Currituck SMF proxy used in NHWAVE simulations

SMF Parameter	Parameter Value	Description
SMF T (m)	750	Maximum thickness
SMF b (km)	30	Maximum down-slope length
SMF w (km)	20	Maximum width
SMF slope (deg.)	4	Local mean slope (deg.)
SMF Location	36.39N, 74.61W	Coordinates of initial location
θ (deg. N)	90	Dir. of SMF motion
s_f (km)	15.8	Length of runout
t_f (seconds)	710	Time of motion

Reference: (Grilli et al., 2013d)

Table 2.6-2: Reference NOAA Water Level Stations, with associated data, in Chesapeake Bay and the James River

Station #	NOAA Station Name	NOAA Station ID	Latitude	Longitude	Mean Range (m) (ft)	Diurnal Range (m) (ft)	M2 Amplitude (m) (ft)	M2 Phase (deg. GMT)
1	Chesapeake Bay Bridge Tunnel, VA	8638863	36° 58'	76° 6.8'	0.78 (2.55)	0.88 (2.89)	0.38 (1.246)	220.6
2	Sewells Point, VA	8638610	36° 56.8'	76° 19.8'	0.74 (2.43)	0.84 (2.76)	0.366 (1.202)	261.7
3	Burwell Bay, James River, VA	8638421	37° 3.4'	76° 40.1'	-	-	0.355 (1.165)	299.3
4	Kingsmill, VA	8638424	37° 13.2'	76° 39.8'	0.69 (2.26)	0.80 (2.63)	0.332 (1.088)	318.0
5	Scotland, VA	8638433	37° 11.1'	76° 47'	0.60 (1.96)	0.71 (2.32)	0.286 (0.94)	339.2
6	Tettington, James River, VA	8638450	37° 14.4'	76° 56.6'	0.57 (1.87)	0.67 (2.20)	0.26 (0.853)	10.6
7	Kiptopeke, VA	8632200	37° 9.9'	75° 59.3'	0.79 (2.60)	0.90 (2.94)	0.388 (1.273)	247.5
8	New Point, Comfort Shoal, VA	8637590	37° 15.4'	76° 13.3'	-	-	0.31 (1.016)	256.0
9	Gloucester Point, VA	8637624	37° 14.8'	76° 30'	0.73 (2.38)	0.82 (2.69)	0.361 (1.184)	268.6
10	New Point, VA	8637289	37° 20.8'	76° 16.4'	-	-	0.244 (0.801)	262.7
11	Cape Charles Hbr , VA	8632366	37° 15.8'	76° 1.2'	-	-	0.342 (1.121)	259.4
12	Rappahannock Light, VA	8632837	37° 32.3'	76° 0.9'	0.48 (1.57)	0.57 (1.87)	0.239 (0.785)	301.9

Table 2.6-3: Parameters of Atlantic Ocean basin model grids used for the far-field source definition (Cumbre Vieja 450 km^3, Lisbon M9 and PRT M9) and initial propagation modeling with FUNWAVE-TVD

Source	Min. Lon. E. (Deg.)	Max. Lon. E. (Deg.)	Min. Lat. N. (Deg.)	Max. Lat. N.(Deg.)	Resolution	Spherical /Cartesian
CVV 450 km^3	-82.0000	-5.0000	10.0000	45.0000	1 arc-minute	Spherical
LSB M9	-82.0000	-5.0000	10.0000	45.0000	1 arc-minute	Spherical
PRT M9	-82.0000	-50.0000	10.0000	45.0000	1 arc-minute	Spherical

Table 2.6-4: Parameters of the regional and local model grids used in modeling all tsunami sources with FUNWAVE-TVD

Regional/Local Grids	Min. Lon. E. (Deg.)	Max. Lon. E. (Deg.)	Min. Lat. N. (Deg.)	Max. Lat. N.(Deg.)	Spherical /Cartesian
20 arc-sec (606 meters)	-77.0000	-69.9833	34.8000	39.0167	Spherical
154 meters	-77.0000	-75.2016	36.5000	37.7478	Cartesian
39 meters	-76.9000	-76.2014	36.8500	37.2495	Cartesian
10 meters	-76.7700	-76.6205	37.0338	37.2255	Cartesian

Table 2.6-5: Grid dimensions and boundary conditions stations for local model grids used for the far-field and near-field source modeling with FUNWAVE-TVD

Regional/Local Grids	Number of Stations used as Boundary Conditions					Scale Factor	Grid size Nx *Ny
	Total	**East**	**West**	**South**	**North**		
20 arc-sec (606 meter)	1098	254	0	422	422	3	1264 * 760
154 meter	744	228	0	258	258	4	1029 * 909
39 meter	693	290	0	0	403	4	1608*1157
10 meter	1210	605	605	0	0	4	1381*2208

Table 2.6-6: Summary Table of Tsunamigenic Events

Tsunamigenic Source	Tidal Phase	Water Surface Elevation at the SPS Protected Area (feet MSL)	Water Surface Elevation at the Intake Structure (feet MSL)	Maximum Water Surface Elevation (feet MSL)	Time from Tsunamigenic Source Event to Tsunami Reaching SPS (hours)
CVV	TT1	7.0	7.0	7.0	14.5
PRT	TT1	6.1	6.0	6.1	7.3
Lisbon	TT1	6.1	5.9	6.1	11.5
SMF	TT1	6.5	6.4	6.5	4.5
CVV	TT2	6.2	5.8	6.2	11.8
SMF	TT2	6.2	5.8	6.2	4.7

Figure 2.6-1: Location (bathymetry (< 0) and topography (> 0) as color scale in meters) for an extreme Lisbon M9 co-seismic source.

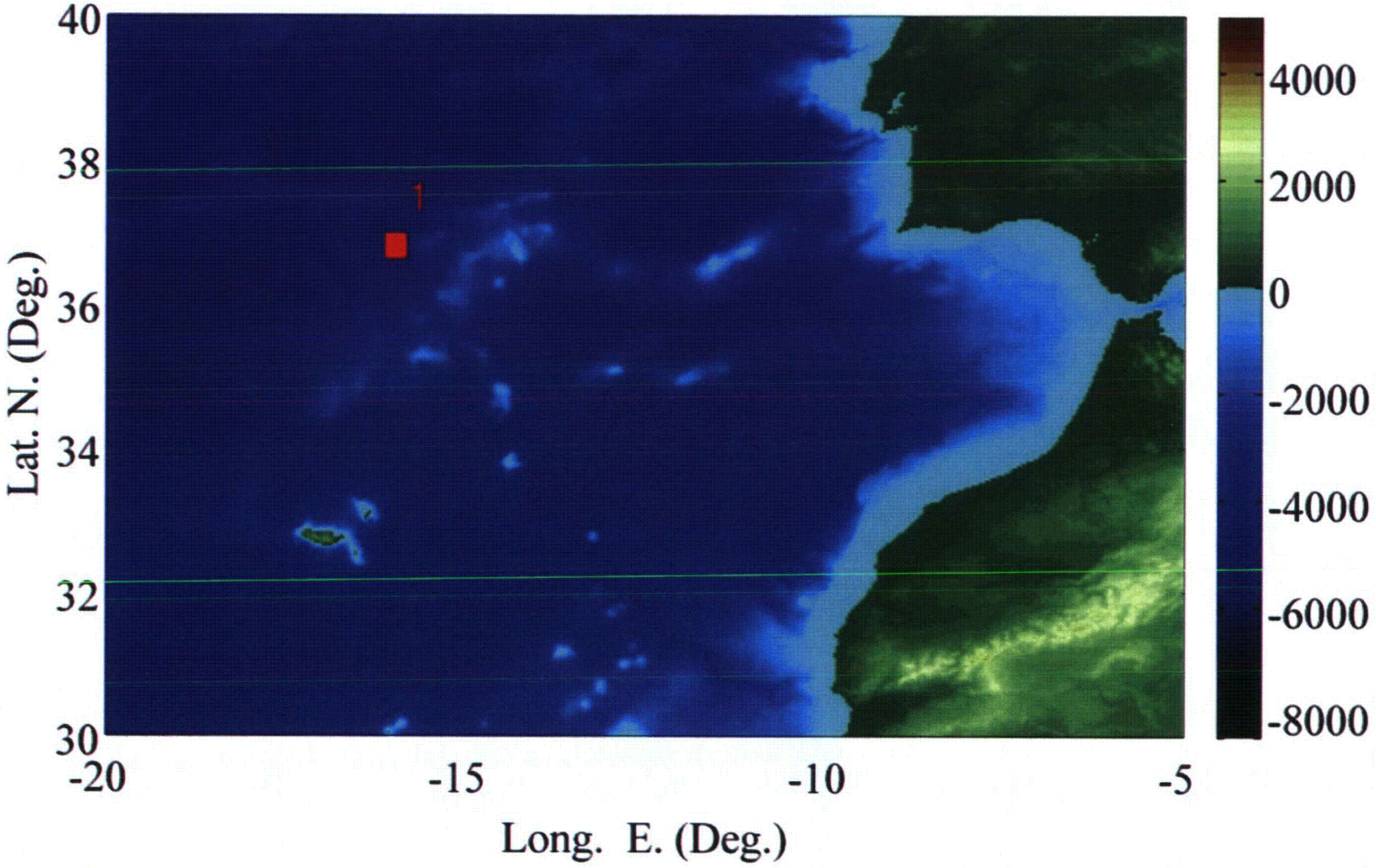

Figure 2.6-2: Far-field Atlantic Ocean basin grid used in simulations of the CVV 450 km^3 subaerial landslide, Lisbon M9 co-seismic, and the PRT M9 co-seismic (sources labeled on figure). The red rectangle in the figure indicates the footprint of the finer regional grid at 20 arc-second (or 606 meter) resolution. Color scale indicates depth (< 0) and topography (> 0) in meters, from the ETOPO-1 database (Amante and Eakins, 2009).

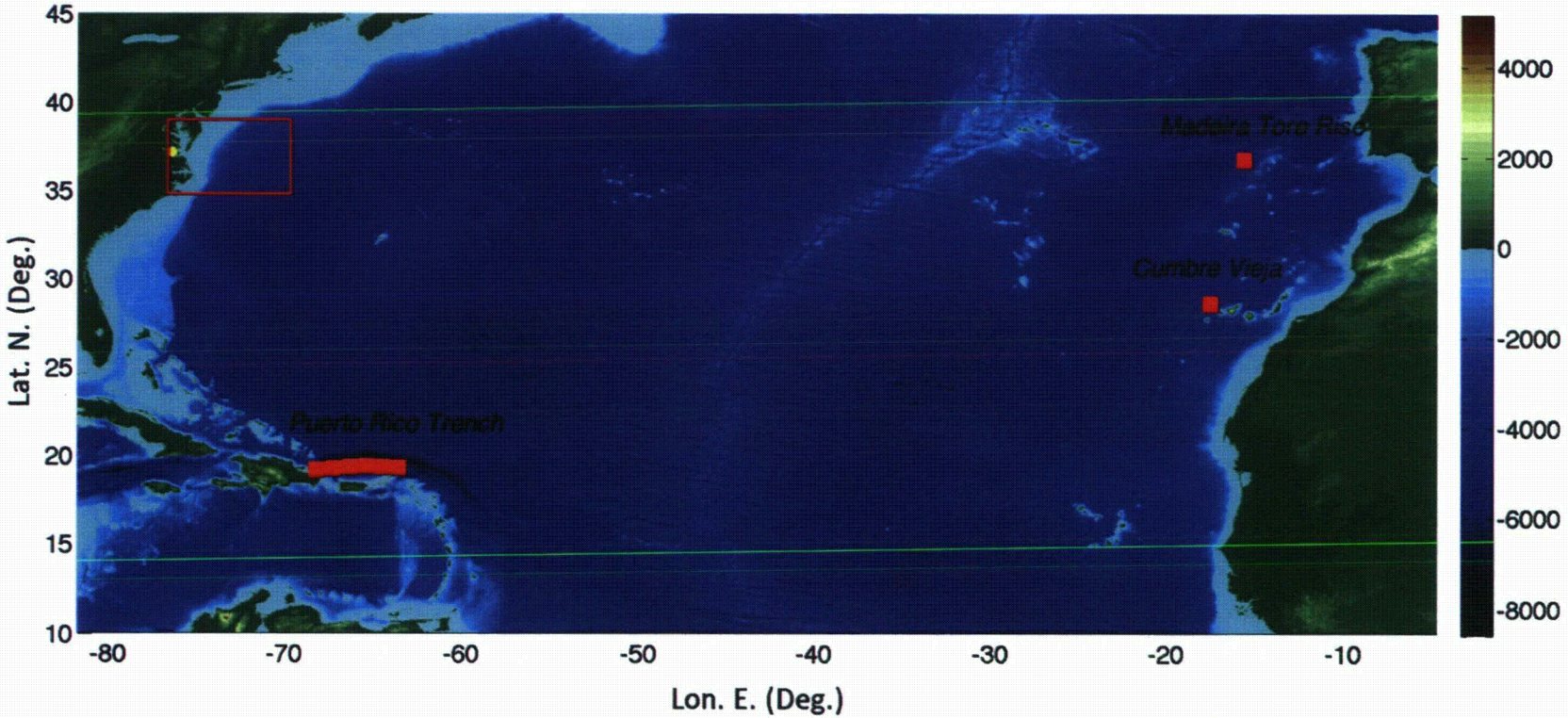

Figure 2.6-3: Location of the historical Currituck SMF. The center of the SMF is at 74.61W and 36.39N. The green ellipse is the footprint of the initial failure. The solid black box marks the boundary of the 500 m resolution grid used in NHWAVE simulations to compute the SMF tsunami source until 13.3 mintues after the event. Color scale indicates depth (< 0) in meters with bathymetric contours marked (from ETOPO-1 and CRM data; Amante and Eakins, 2009 and NOAA, 2013).

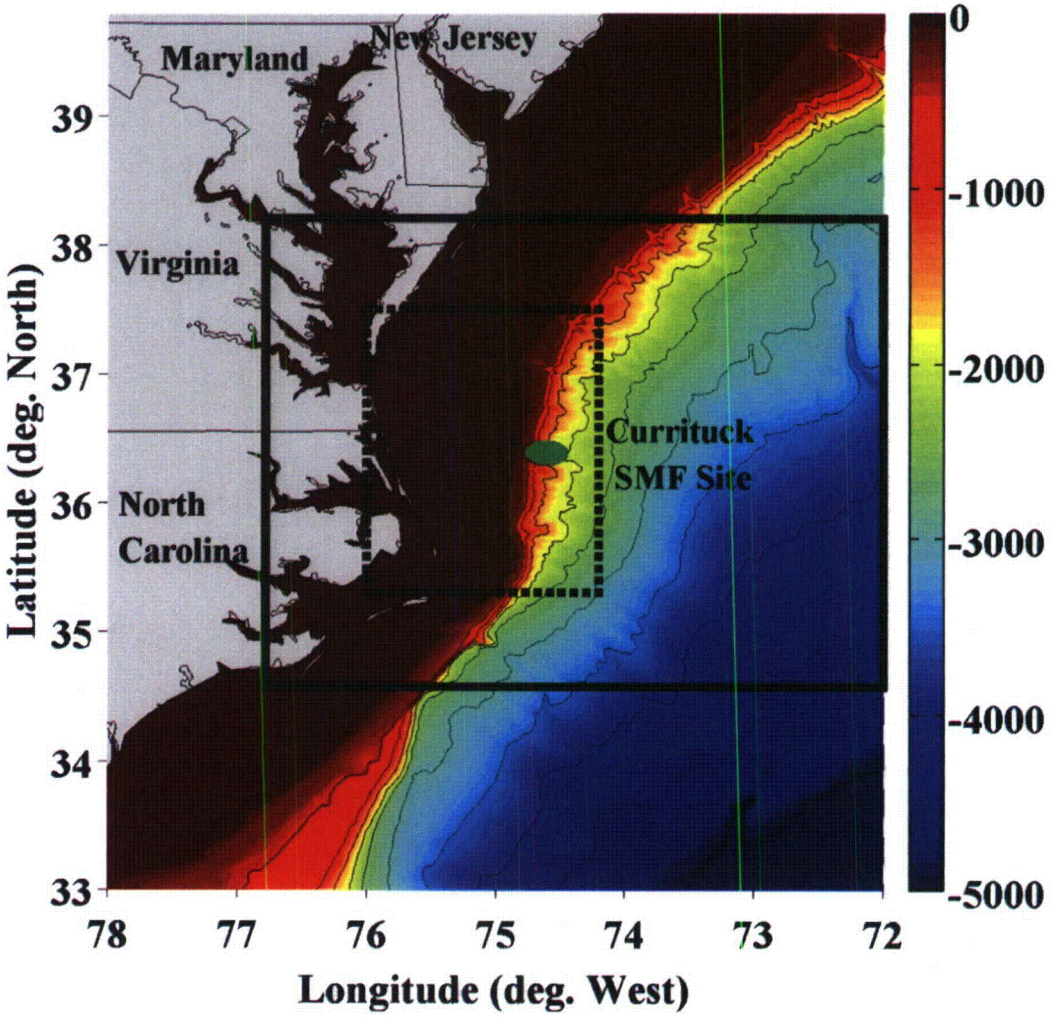

Figure 2.6-4: Location of 12 near shore NOAA stations, as well as the "SPS River Station", used to extract tsunami time-series output. The reference station at Sewells Point, VA is station #2.

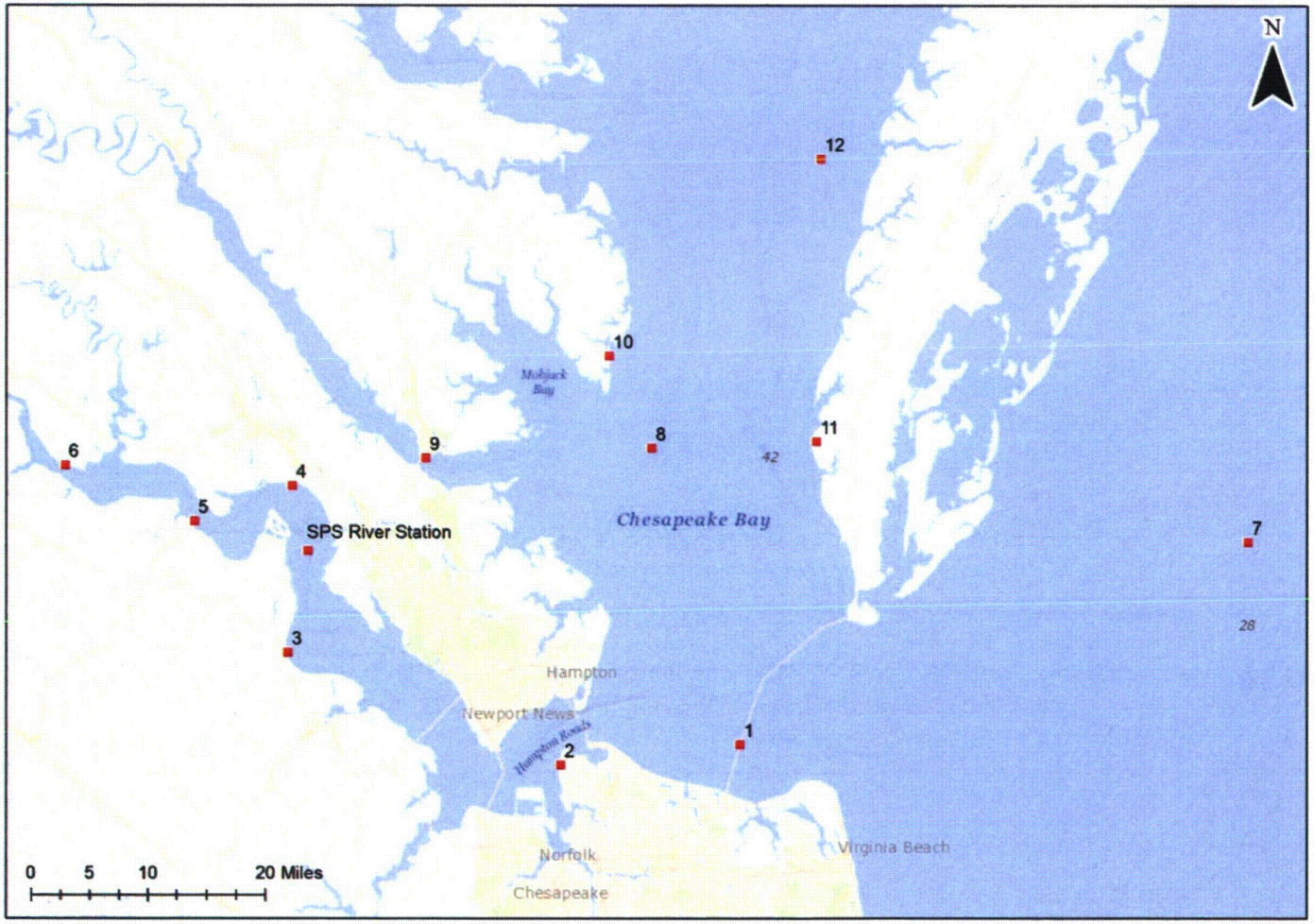

Figure 2.6-5: Time series of surface elevations for the scaled M2 tide plus CVV tsunami (Case TT1), using "MHW+SLR"[1] as a reference level at Station 3 (thick dashed), Station 4 (thick chained) and the SPS river station (thick solid) in the 10 m grid.
Thin red lines show the tide only results at Stations 3 and 4. Time axis indicates time since the start of the CVV event.

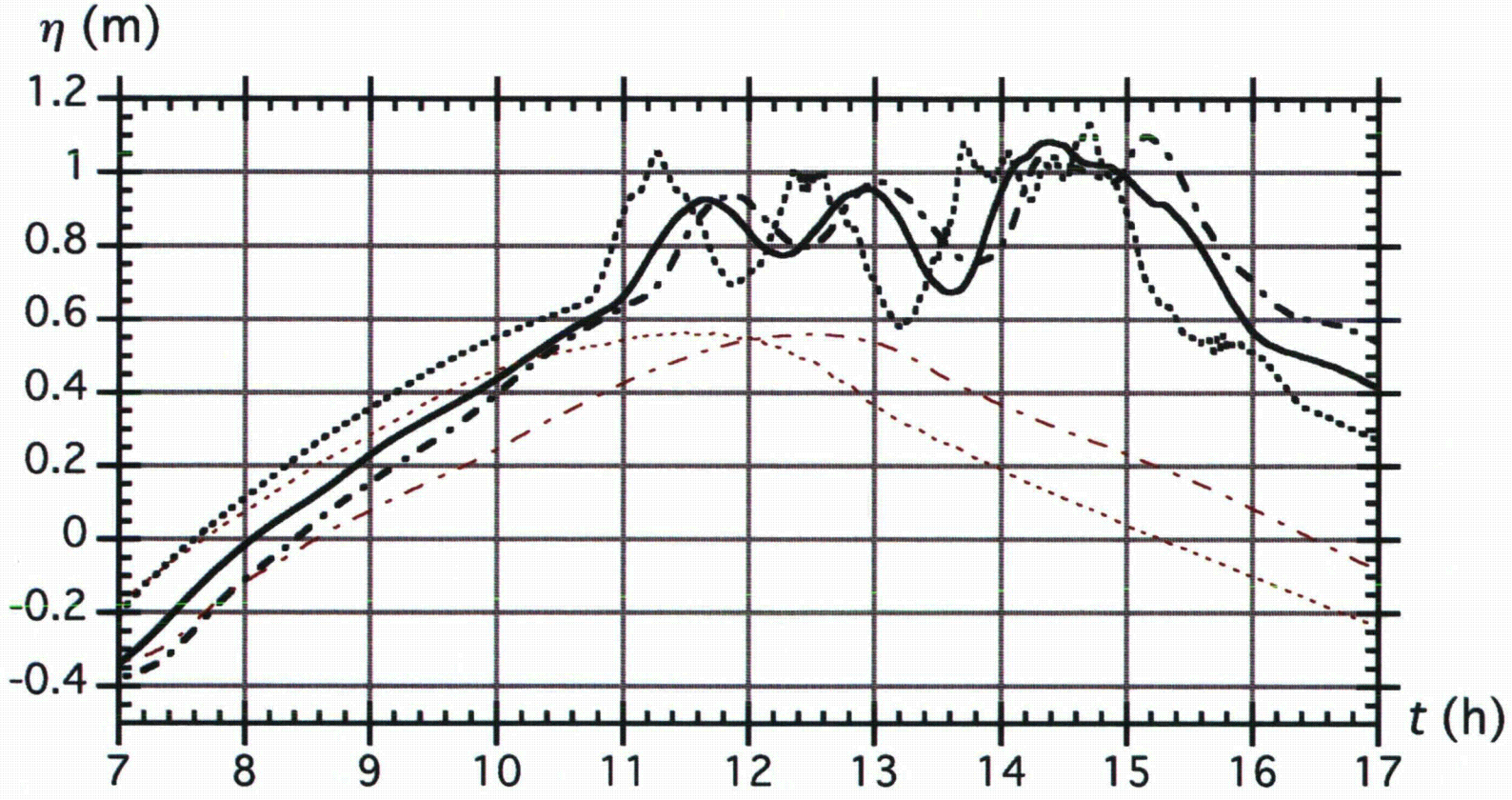

[1] Reference water level "0" is equal to the mean high water (MHW) at Sewells Point plus the SLR component of the AWL (0.287 meters + 0.299 meters = 0.586 meters NAVD88)

Figure 2.6-6: Maximum surface elevation (color scale in meters) for the scaled M2 tide plus PRT tsunami (Case TT1) in the 10 m grid. Reference water level "0" is equal to the mean high water (MHW) at Sewells Point plus the SLR component of the AWL (0.586 meters NAVD88). The black triangle marks the SPS site and the red squares mark the locations of Station 3, Station 4 and the SPS river station.

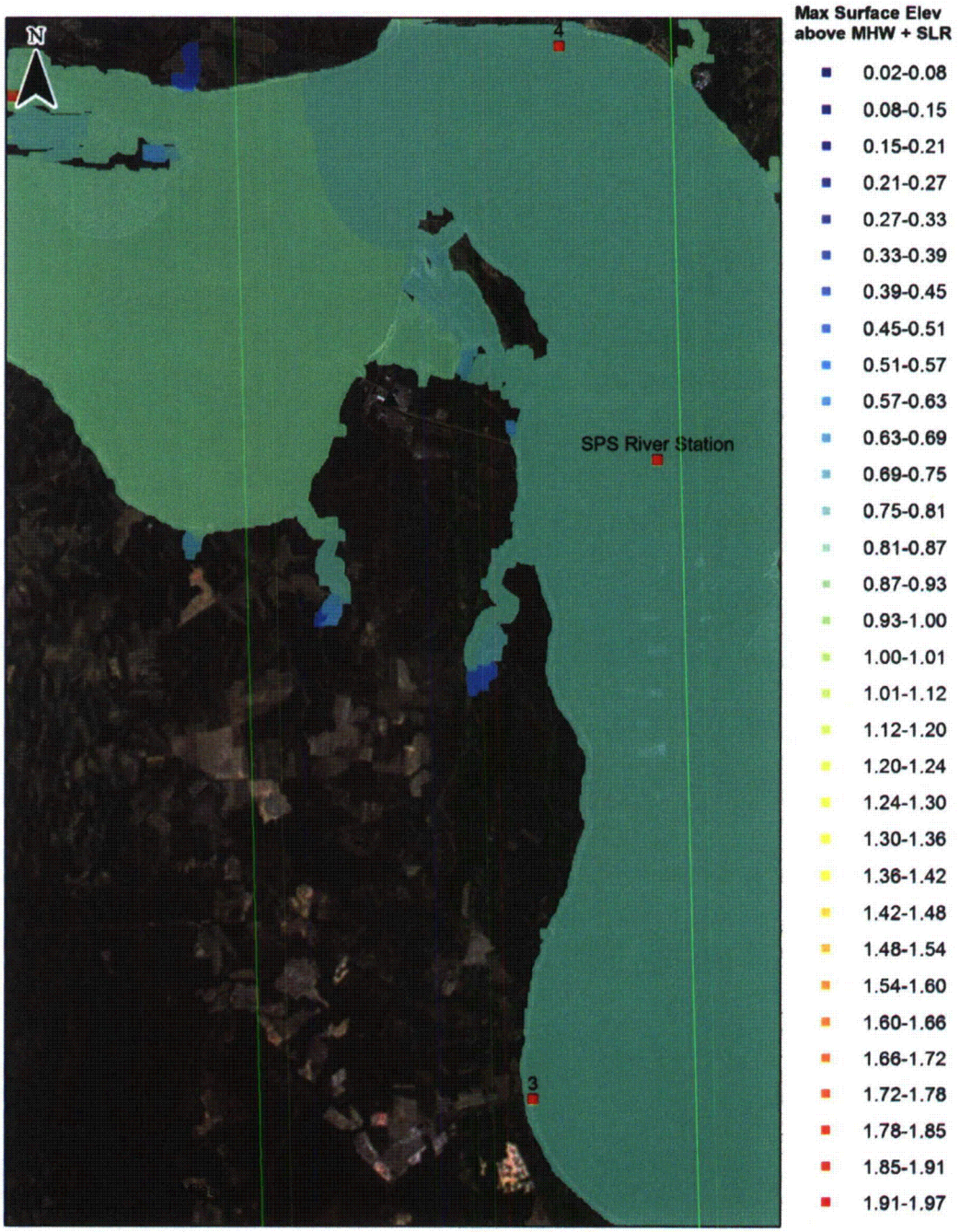

Figure 2.6-7: Maximum surface elevation (color scale in meters) for the scaled M2 tide plus PRT tsunami (Case TT1) in the 10 m grid in the immediate vicinity of the plant.
Reference water level "0" is equal to the mean high water (MHW) at Sewells Point plus the SLR component of the AWL (0.586 meters NAVD88).

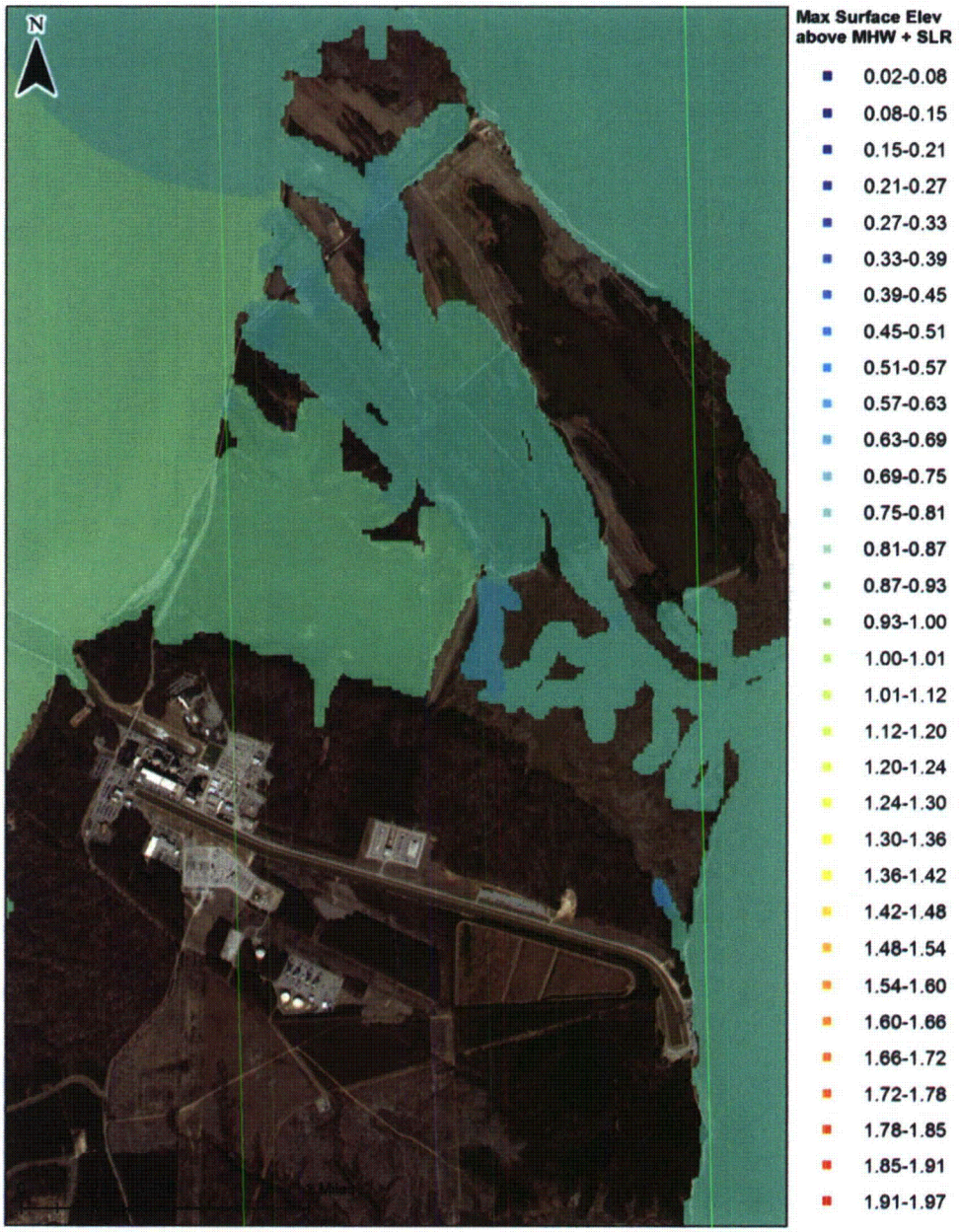

Figure 2.6-8: Time series of surface elevations for the scaled M2 tide plus PRT tsunami (Case TT1) at Station 3 (thick dashed), Station 4 (thick chained), and the SPS river station (thick solid) in the 10 m grid. Reference water level "0" is equal to the mean high water (MHW) at Sewells Point plus the SLR component of the AWL (0.586 meters NAVD88). Thin red lines show the tide only results at Stations 3 and 4. Time axis indicates time since the start of the PRT event.

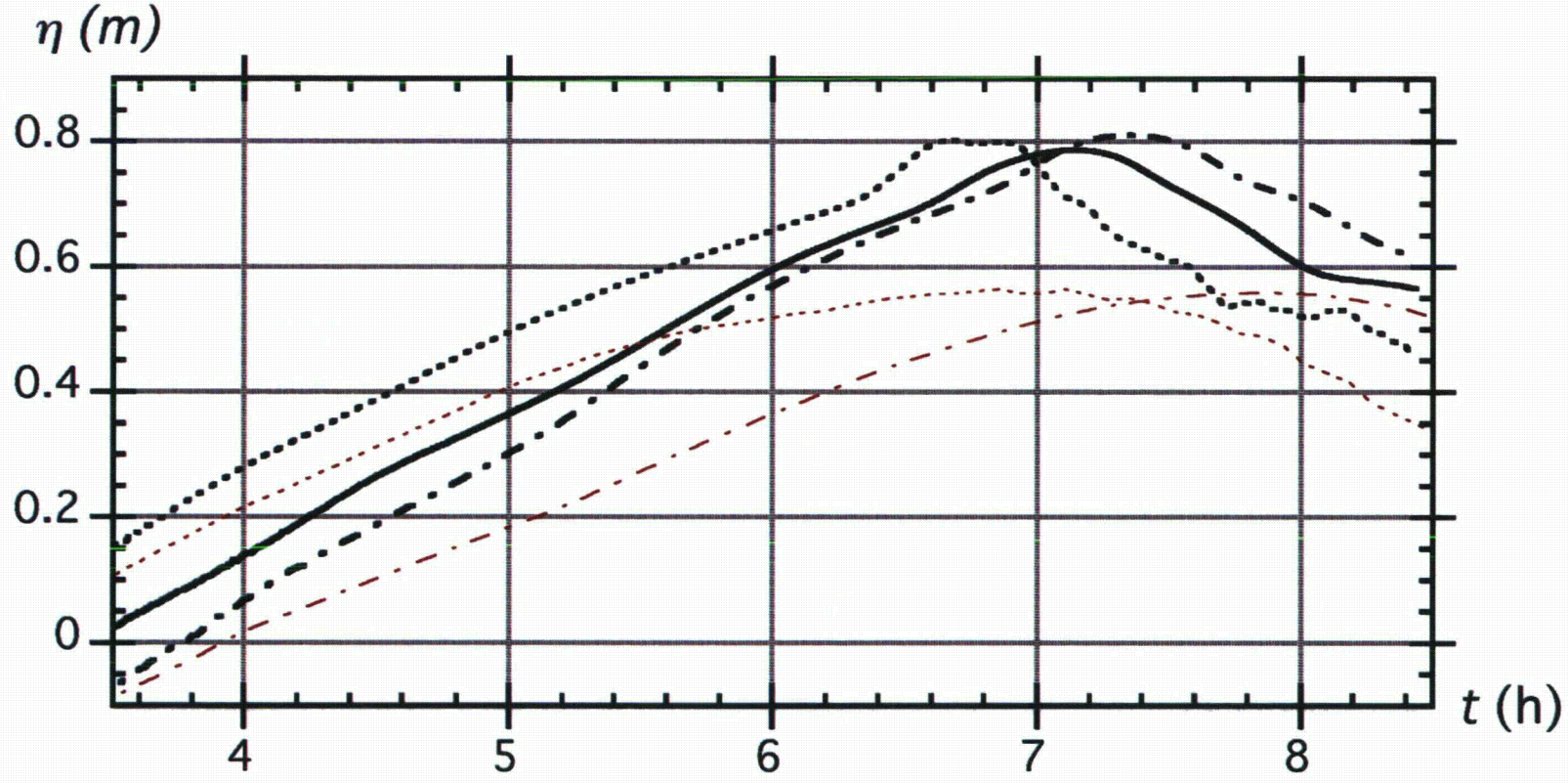

Figure 2.6-9: Time series of surface elevations for the scaled M2 tide plus Lisbon M9 tsunami (Case TT1) at Station 2, (Sewells Point, VA), in the 154 m grid (solid) and in the 39 m grid (dashed). Reference water level "0" is equal to the mean high water (MHW) at Sewells Point plus the SLR component of the AWL (0.586 meters NAVD88). Time axis indicates time since the start of the Lisbon M9 event.

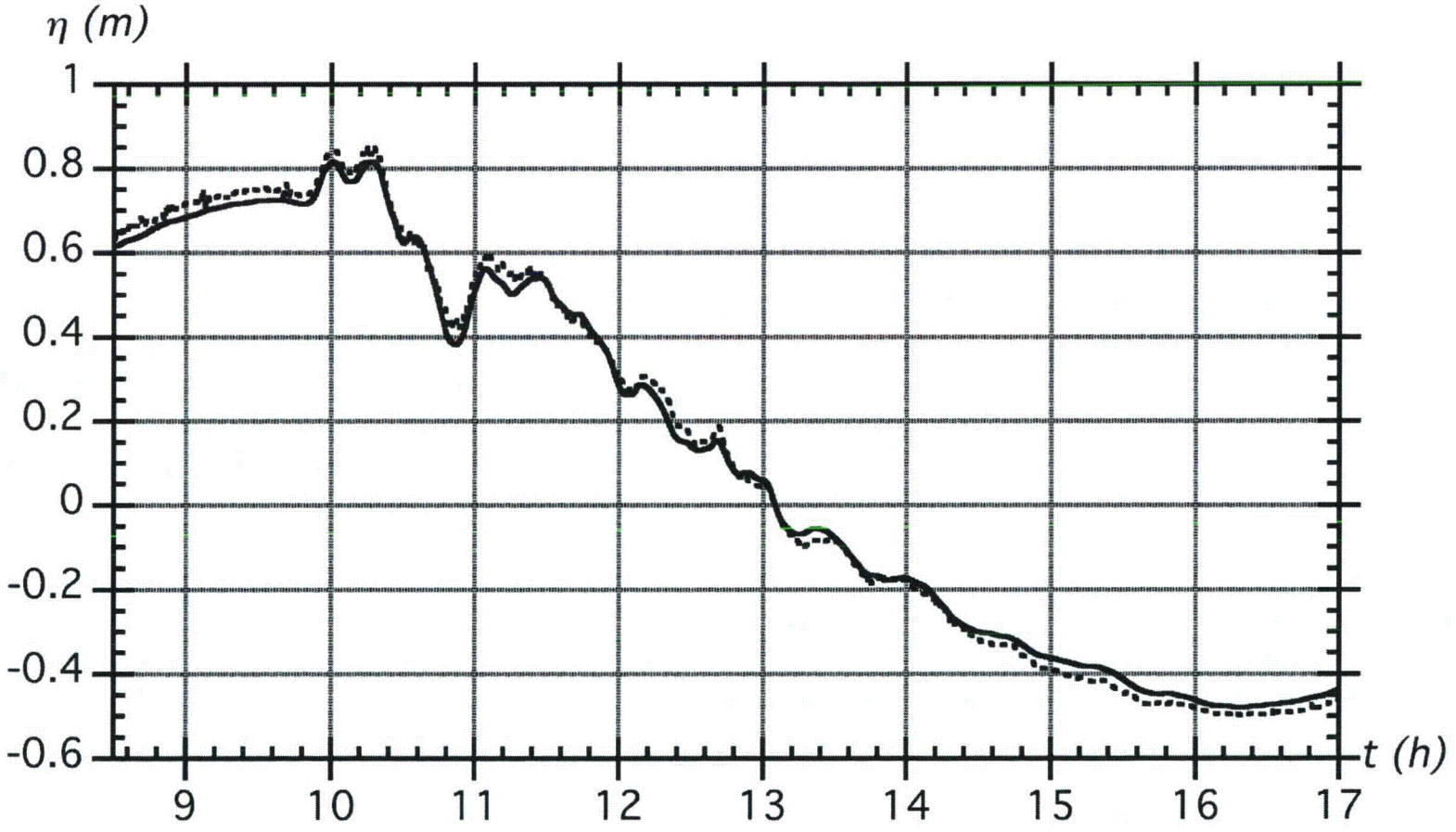

Figure 2.6-10: Maximum surface elevation (color scale in meters) for the scaled M2 tide plus Lisbon M9 tsunami (Case TT1) in the 10 m grid. Reference water level "0" is equal to the mean high water (MHW) at Sewells Point plus the SLR component of the AWL (0.586 meters NAVD88). The black triangle marks the SPS site and the red squares mark the locations of Station 3, Station 4 and the SPS river station.

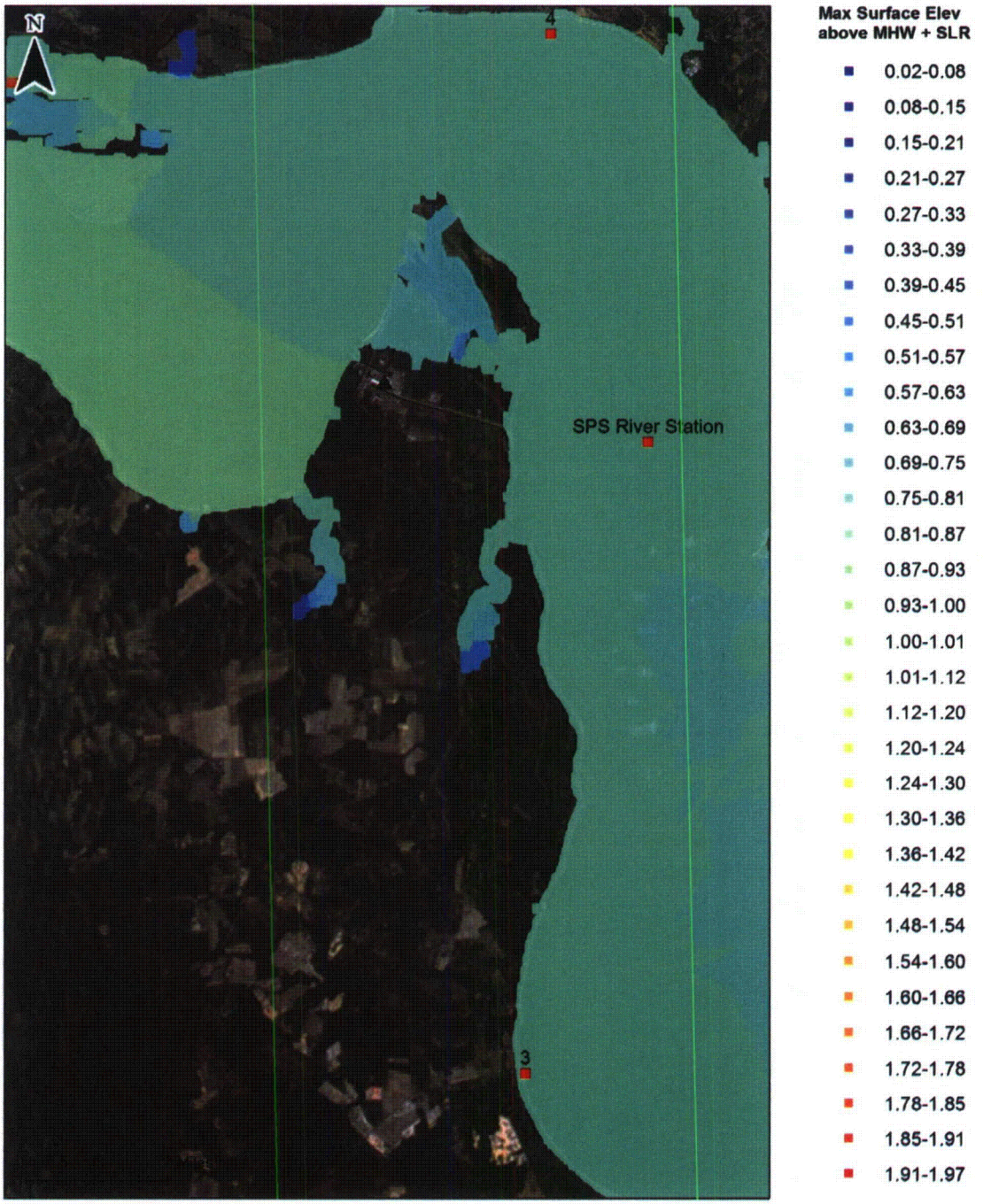

Figure 2.6-11: Maximum surface elevation (color scale in meters) for the scaled M2 tide plus Lisbon M9 tsunami (Case TT1) in the 10 m grid in the immediate vicinity of the plant. Reference water level "0" is equal to the mean high water (MHW) at Sewells Point plus the SLR component of the AWL (0.586 meters NAVD88).

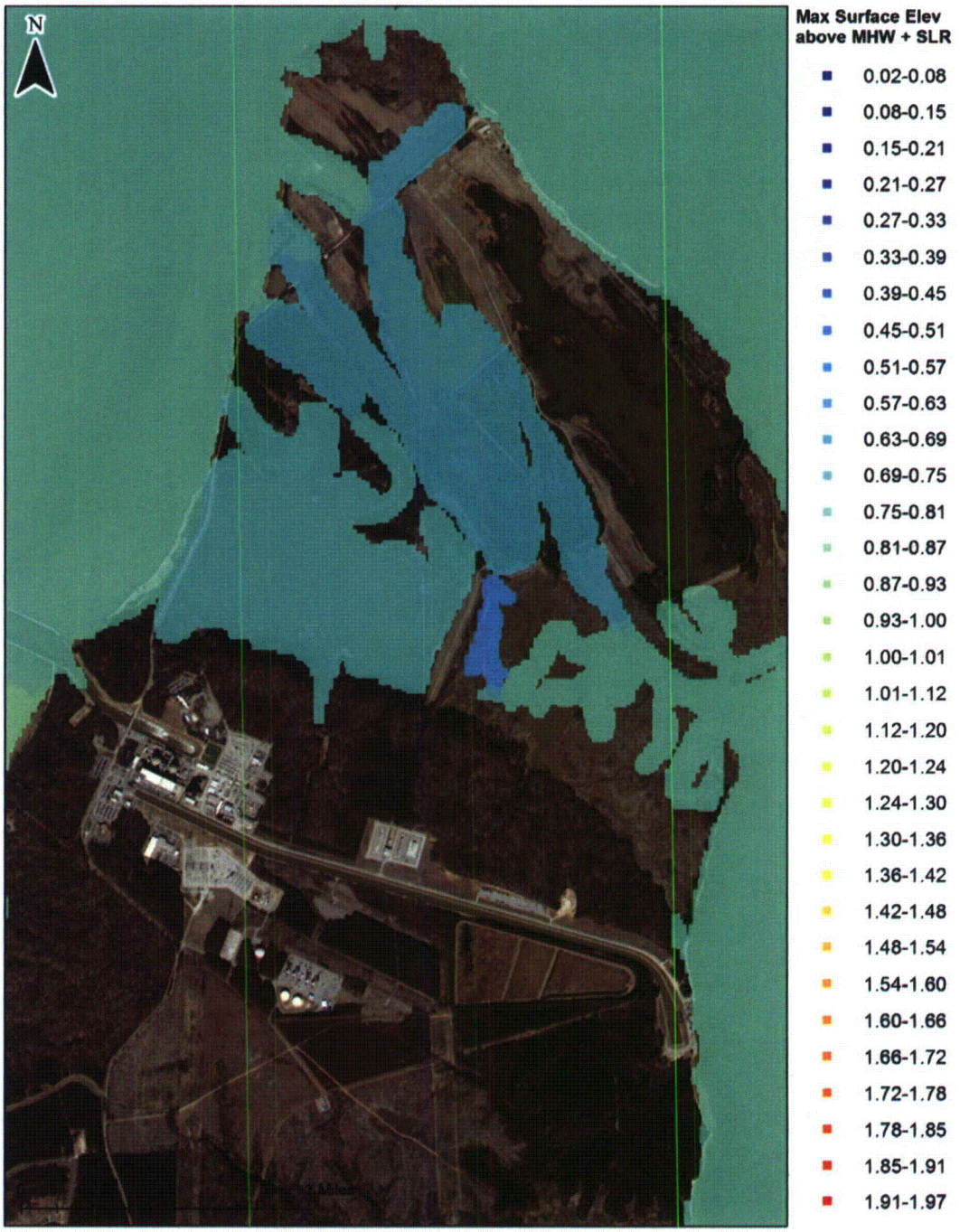

Figure 2.6-12: Time series of surface elevation for the scaled M2 tide plus SMF Currituck proxy tsunami (Case TT1) at (a) Station 2, (Sewells Point, VA), in the 154 m grid (solid) and in the 39 m grid (dashed) and (b) Station 3 (thick dashed), Station 4 (thick chained), and the SPS river station (thick solid) in the 10 m grid. Reference water level "0" is equal to the mean high water (MHW) at Sewells Point plus the SLR component of the AWL (0.586 meters NAVD88). Time axis indicates time since the start of the SMF event.

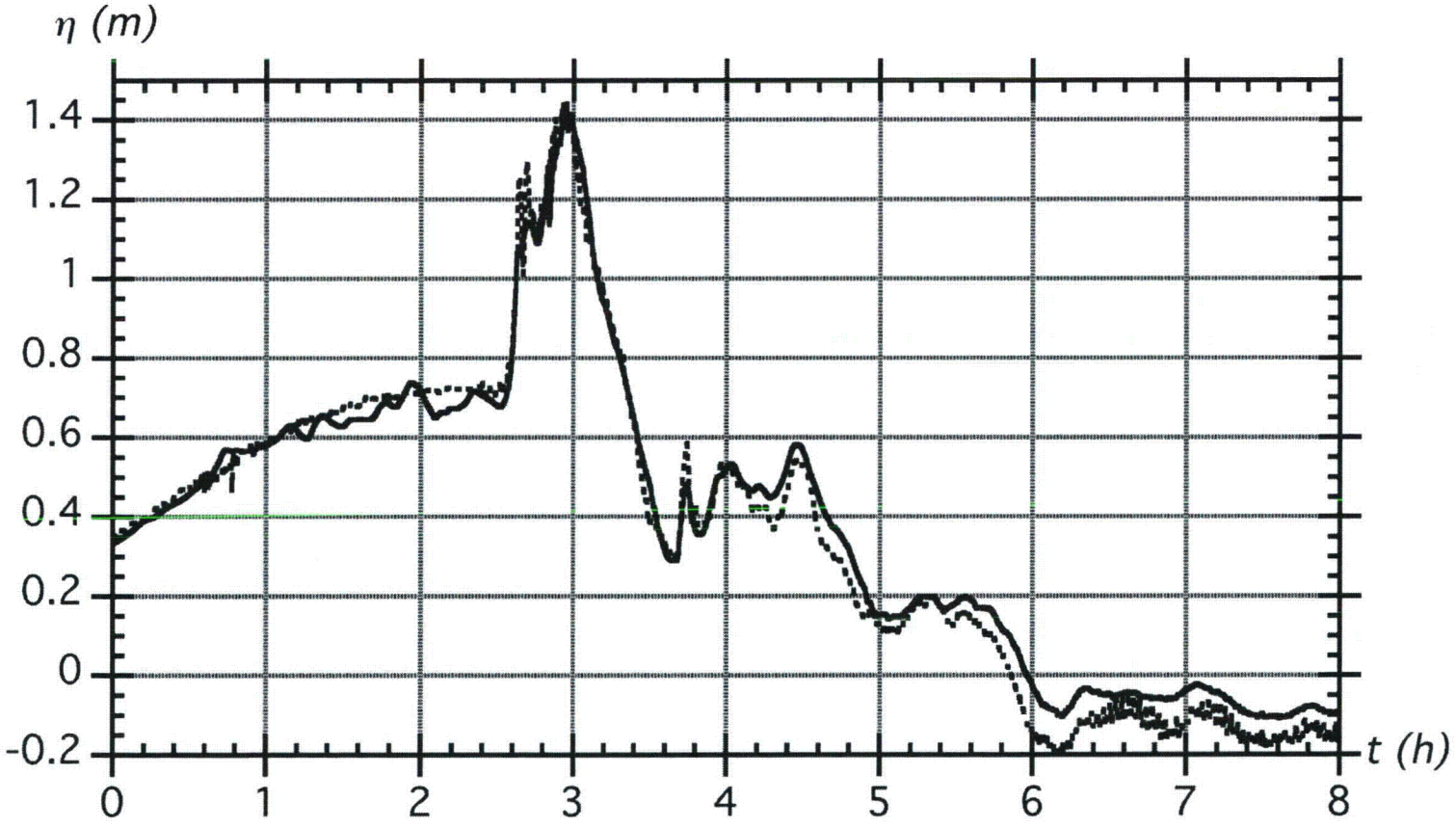

Figure 2.6-13: Maximum surface elevation (color scale in meters) for the scaled M2 tide plus SMF Currituck proxy tsunami (Case TT1) in the 10 m grid. Reference water level "0" is equal to the mean high water (MHW) at Sewells Point plus the SLR component of the AWL (0.586 meters NAVD88). The black triangle marks the SPS site and the red squares mark the locations of Station 3, Station 4 and the SPS river station.

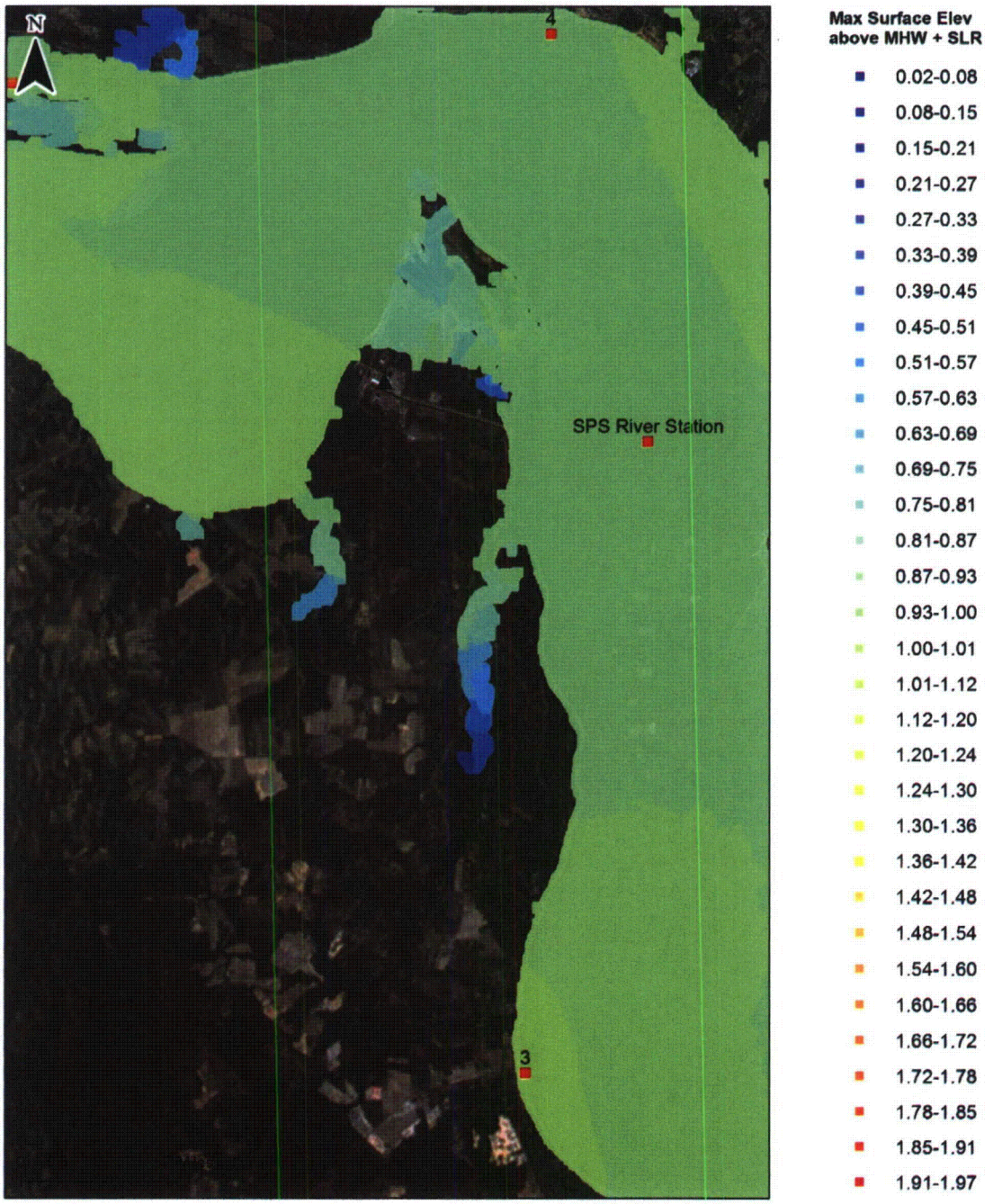

Figure 2.6-14: Maximum surface elevation (color scale in meters) for the scaled M2 tide plus SMF Currituck proxy tsunami (Case TT1) in the 10 m grid in the immediate vicinity of the plant. Reference water level "0" is equal to the mean high water (MHW) at Sewells Point plus the SLR component of the AWL (0.586 meters NAVD88).

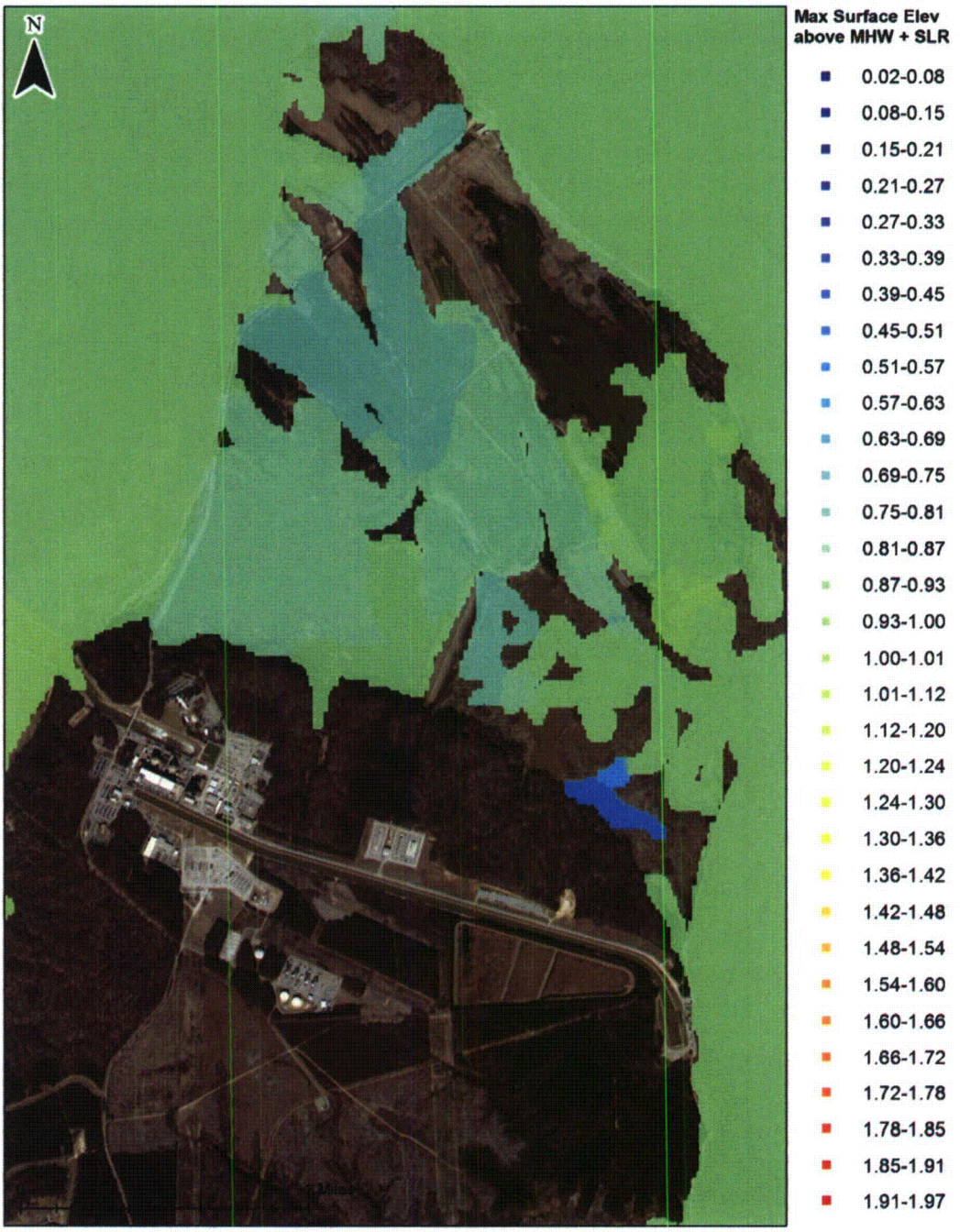

Figure 2.6-15: Time series of surface elevations for the scaled M2 tide plus CVV tsunami (Case TT2) at Station 3 (thick dashed), Station 4 (thick chained), and the SPS river station (thick solid) in the 10 m grid. Reference water level "0" is equal to the mean high water (MHW) at Sewells Point plus the SLR component of the AWL (0.586 meters NAVD88). Thin red lines in show the tide only results at Stations 3 and 4. Time axis indicates time since the start of the CVV event.

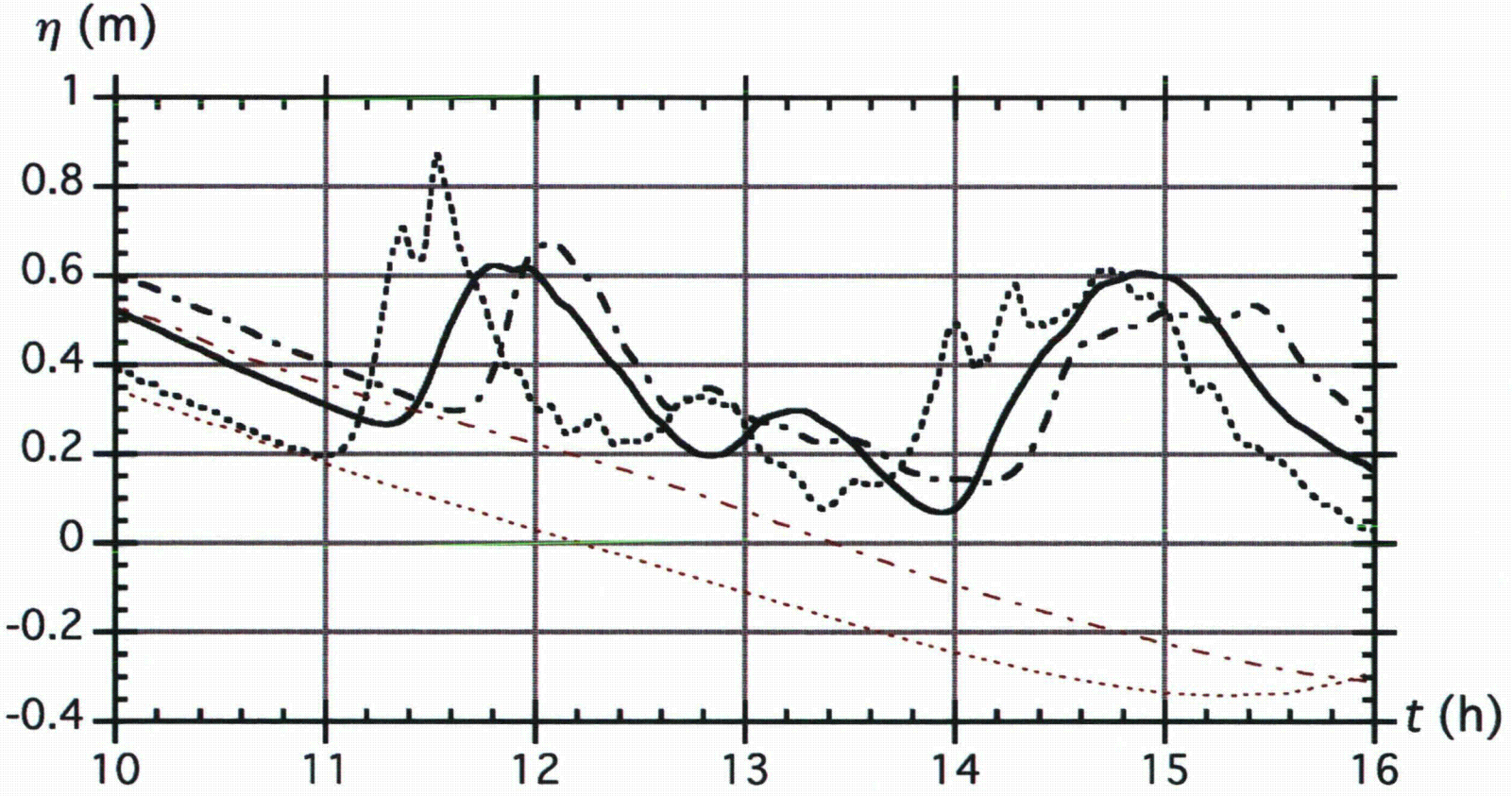

Figure 2.6-16: Maximum surface elevation (color scale in meters) for the scaled M2 tide plus CVV tsunami (Case TT2) in the 10 m grid. Reference water level "0" is equal to the mean high water (MHW) at Sewells Point plus the SLR component of the AWL (0.586 meters NAVD88). The black triangle marks the SPS site and the red squares mark the locations of Station 3, Station 4 and the SPS river station.

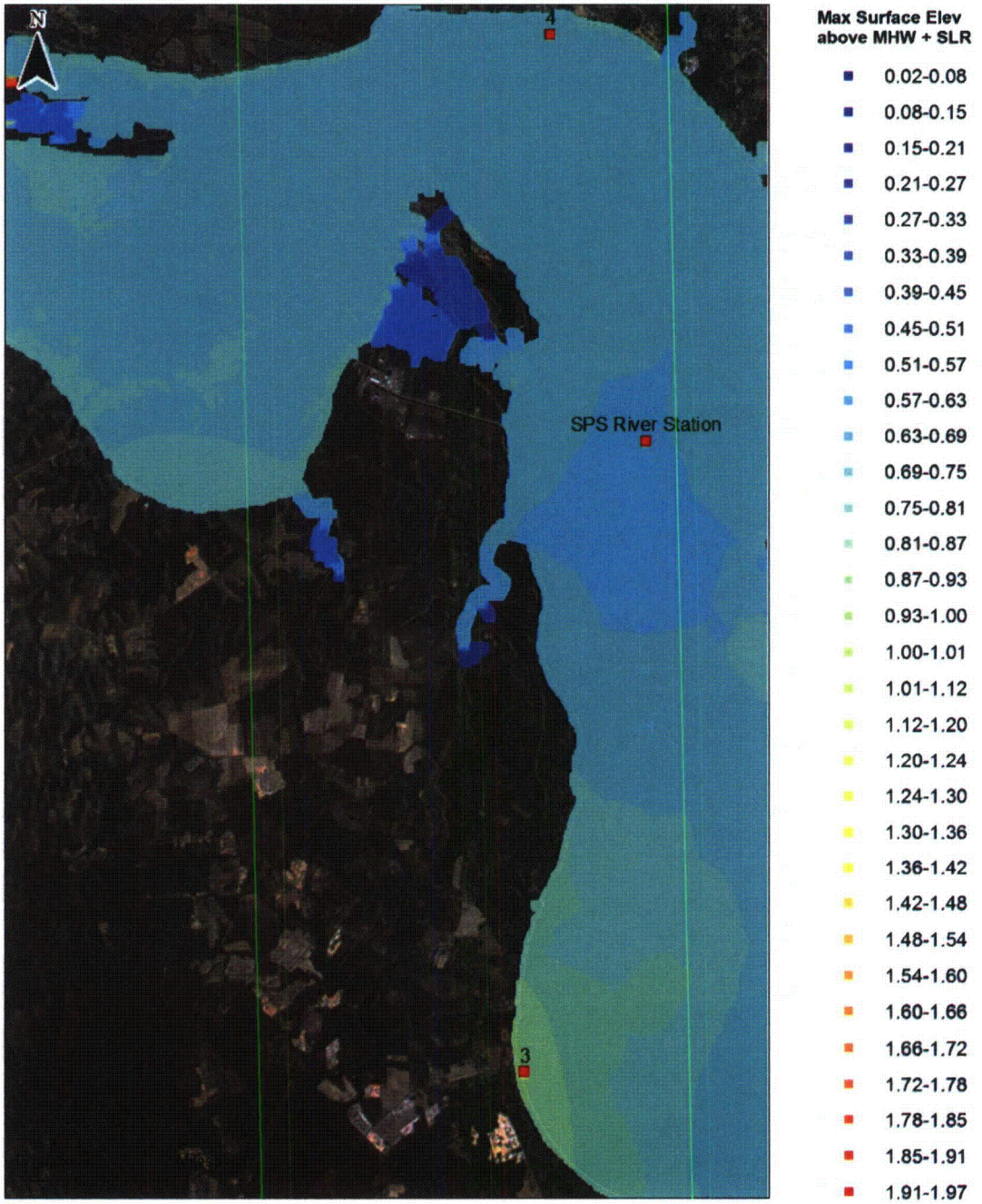

Figure 2.6-17: Maximum surface elevation (color scale in meters) for the scaled M2 tide plus CVV tsunami (Case TT2) in the 10 m grid, in the immediate vicinity of the plant.
Reference water level "0" is equal to the mean high water (MHW) at Sewells Point plus the SLR component of the AWL (0.586 meters NAVD88).

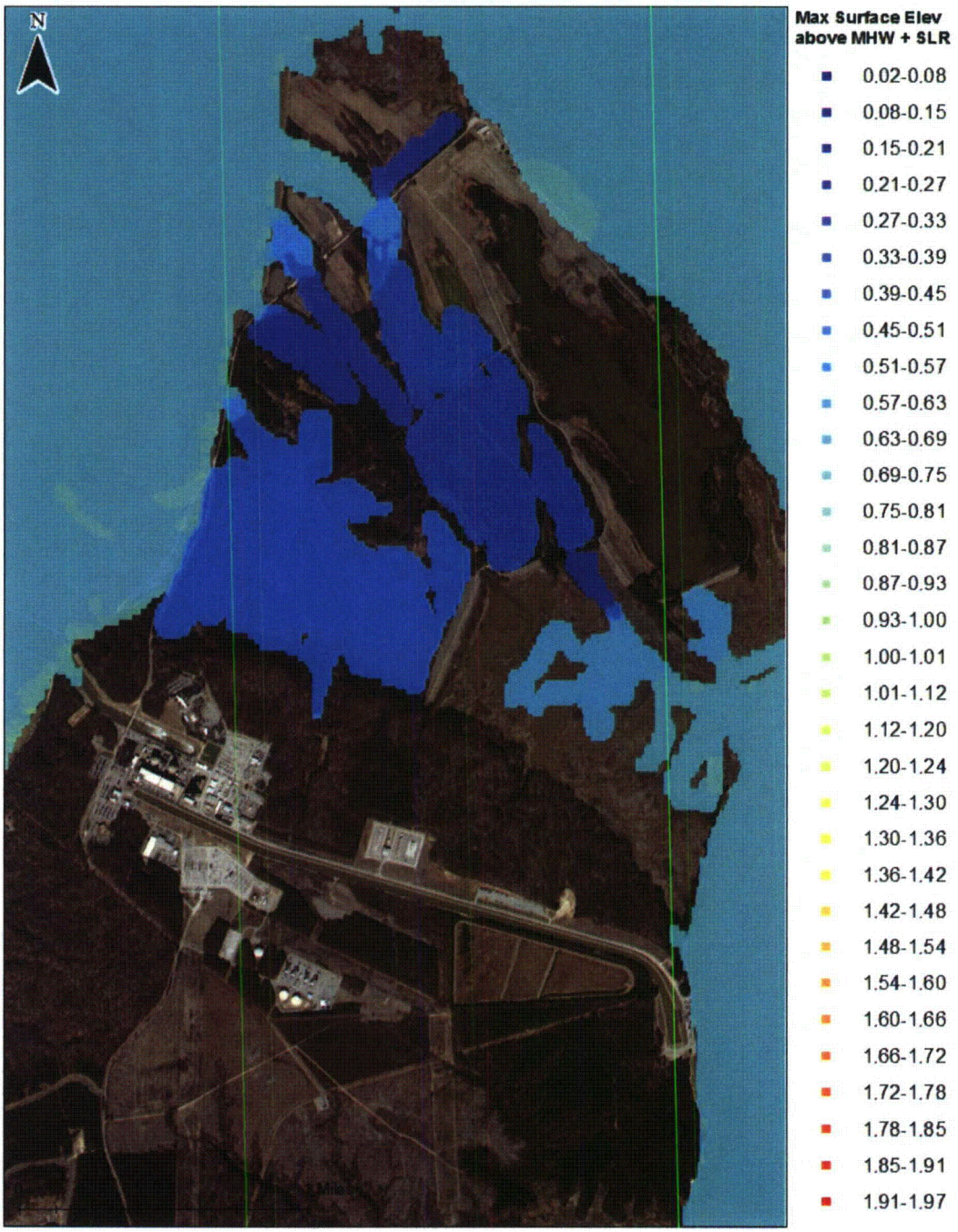

Figure 2.6-18: Time series of surface elevation for the scaled M2 tide plus SMF Currituck proxy tsunami (Case TT2). Reference water level "0" is equal to the mean high water (MHW) at Sewells Point plus the SLR component of the AWL (0.586 meters NAVD88). Station 3 (thick dashed), Station 4 (thick chained), and the SPS river station (thick solid) in the 10 m grid. Thin red lines in show the tide only results at Stations 3 and 4. Time axis indicates time since the start of the SMF event.

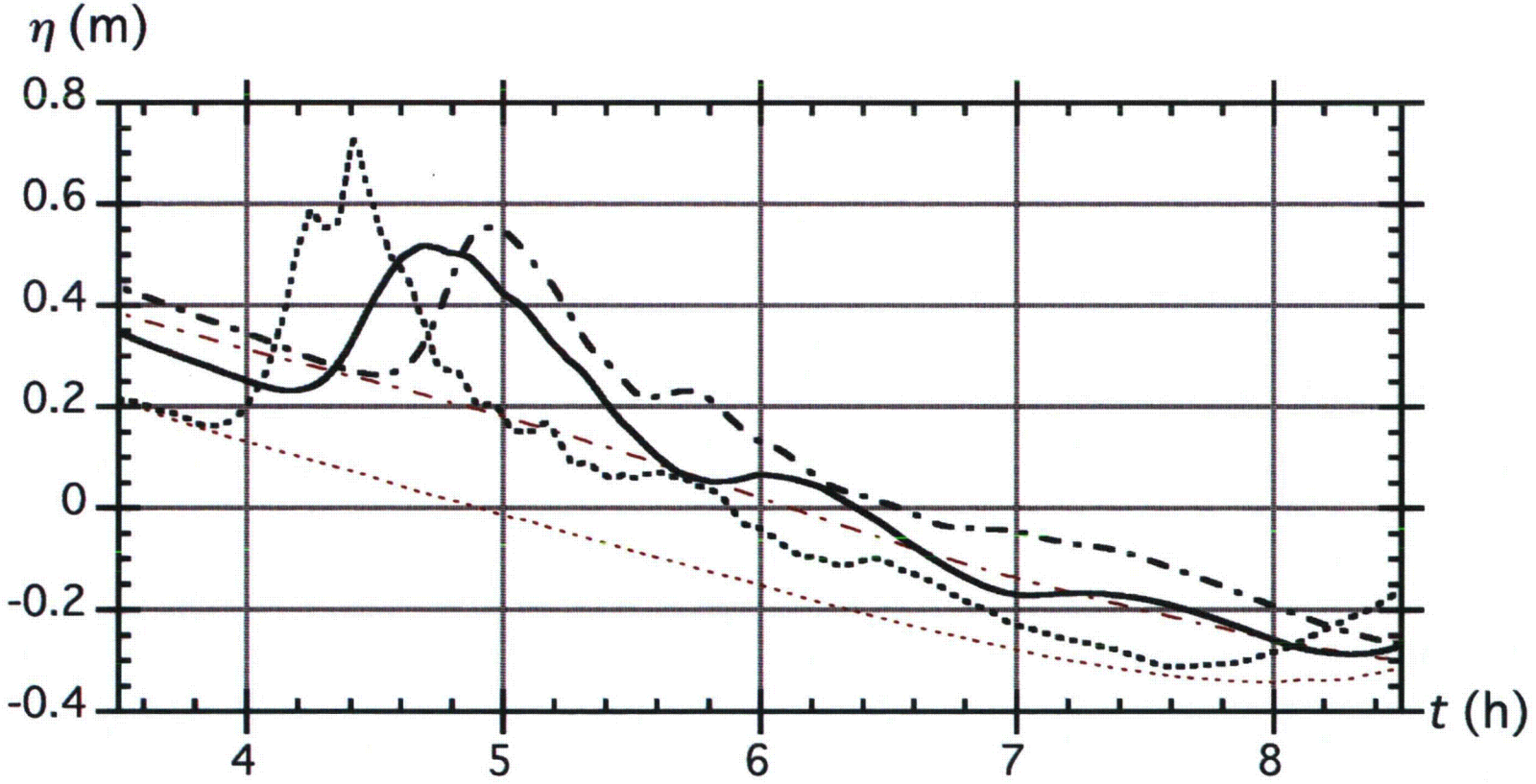

Figure 2.6-19: Maximum surface elevation (color scale in meters) for the scaled M2 tide plus SMF Currituck proxy tsunami (Case TT2) in the 10 m grid. Reference water level "0" is equal to the mean high water (MHW) at Sewells Point plus the SLR component of the AWL (0.586 meters NAVD88). The black triangle marks the SPS site and the red squares mark the locations of Station 3, Station 4 and the SPS river station.

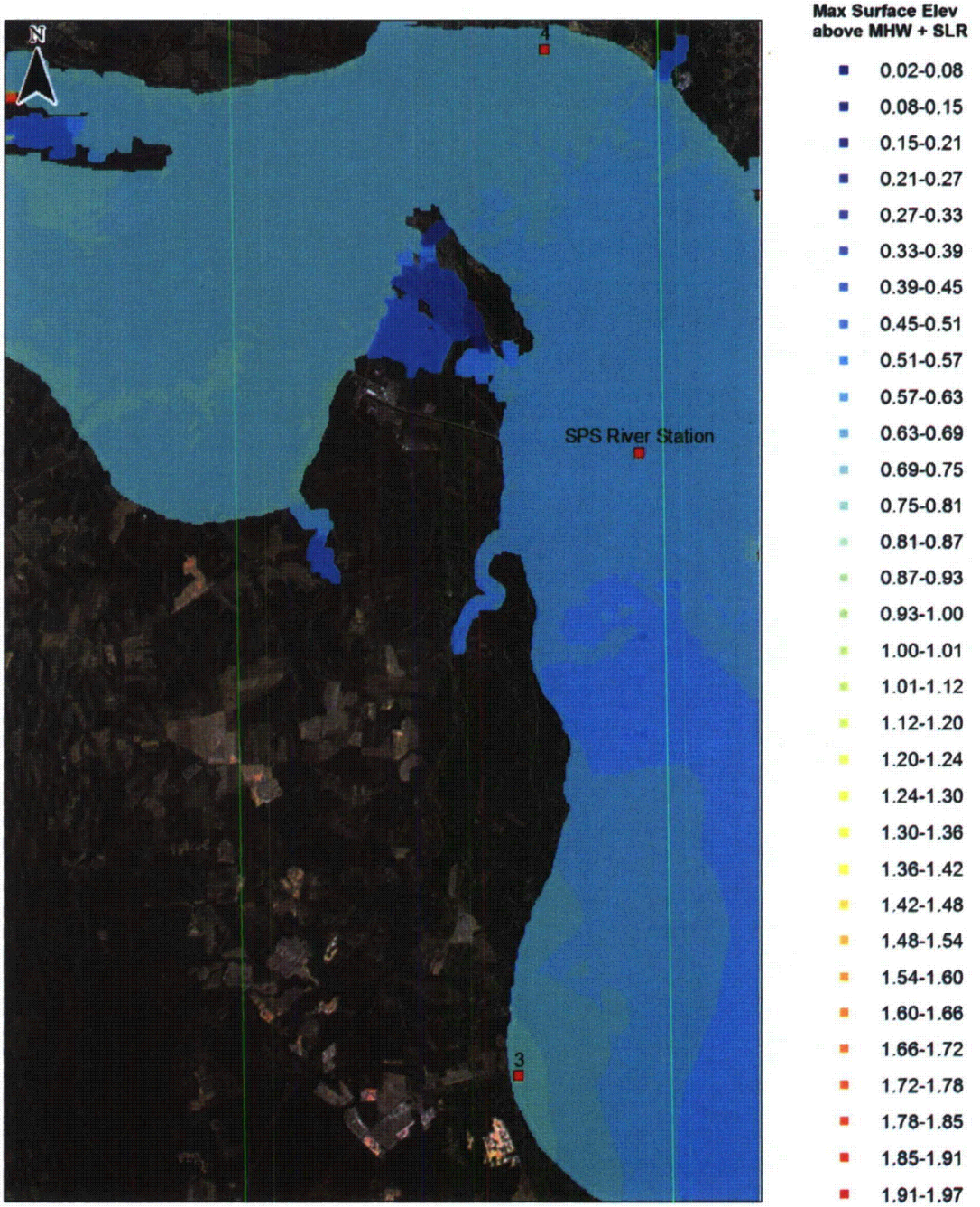

Figure 2.6-20: Maximum surface elevation (color scale in meters) for the scaled M2 tide plus SMF Currituck proxy tsunami (Case TT2) in the 10 m grid in the immediate vicinity of the plant. Reference water level "0" is equal to the mean high water (MHW) at Sewells Point plus the SLR component of the AWL (0.586 meters NAVD88).

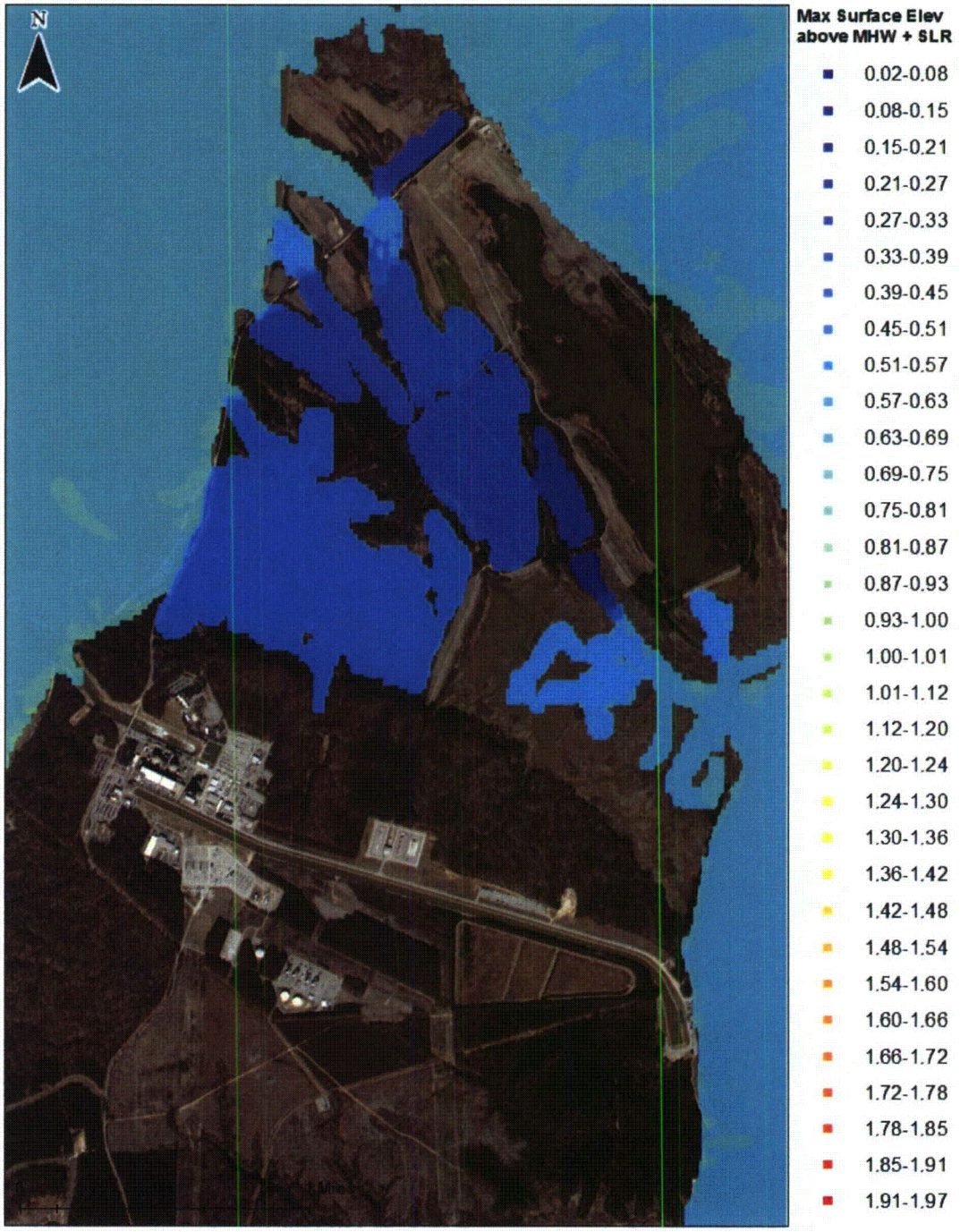

Figure 2.6-21: Time series of surface elevation for the scaled M2 tide plus SMF Currituck proxy tsunami (Case TT1) at (a) Station 2, (Sewells Point, VA), in the 154 m grid (solid) and in the 39 m grid (dashed) and (b) Station 3 (thick dashed), Station 4 (thick chained), and the SPS river station (thick solid) in the 10 m grid. *Reference water level "0" is equal to the mean high* water (MHW) at Sewells Point plus the SLR component of the AWL (0.586 meters NAVD88).